

ผลของวิธีการทำให้ปราศจากเชื้อต่อคุณสมบัติทางเคมีกายภาพของแผ่นไฮโดรเจลปิดแผลจีซีเอสเอฟ
ที่เตรียมจากพอลิแซ็กคาไรด์เจลของเปลือกผลทุเรียนและพอลิไวนิลแอลกอฮอล์



นางสาวฉันทนา นัยนรินทร์

จุฬาลงกรณ์มหาวิทยาลัย
CHULALONGKORN UNIVERSITY

บทคัดย่อและแฟ้มข้อมูลฉบับเต็มของวิทยานิพนธ์ตั้งแต่ปีการศึกษา 2554 ที่ให้บริการในคลังปัญญาจุฬาฯ (CUIR)
เป็นแฟ้มข้อมูลของนิสิตเจ้าของวิทยานิพนธ์ ที่ส่งผ่านทางบัณฑิตวิทยาลัย

The abstract and full text of theses from the academic year 2011 in Chulalongkorn University Intellectual Repository (CUIR)
are the thesis authors' files submitted through the University Graduate School.

วิทยานิพนธ์นี้เป็นส่วนหนึ่งของการศึกษาตามหลักสูตรปริญญาเภสัชศาสตรมหาบัณฑิต

สาขาวิชาเภสัชอุตสาหกรรม ภาควิชาวิทยาการเภสัชกรรมและเภสัชอุตสาหกรรม

คณะเภสัชศาสตร์ จุฬาลงกรณ์มหาวิทยาลัย

ปีการศึกษา 2557

ลิขสิทธิ์ของจุฬาลงกรณ์มหาวิทยาลัย

EFFECT OF STERILIZATION METHODS ON PHYSICOCHEMICAL PROPERTIES OF
G-CSF HYDROGEL DRESSING PREPARED FROM DURIAN FRUIT-HULLS
POLYSACCHARIDE GEL AND POLYVINYL ALCOHOL

Miss Chanthana Nainiran



A Thesis Submitted in Partial Fulfillment of the Requirements
for the Degree of Master of Science in Pharmacy Program in Industrial Pharmacy
Department of Pharmaceutics and Industrial Pharmacy
Faculty of Pharmaceutical Sciences
Chulalongkorn University
Academic Year 2014
Copyright of Chulalongkorn University

ฉันทนา นัยนรินทร์ : ผลของวิธีการทำให้ปราศจากเชื้อต่อคุณสมบัติทางเคมีกายภาพของแผ่นไฮโดรเจลปิดแผลจีซีเอสเอฟที่เตรียมจากพอลิแซ็กคาไรด์เจลของเปลือกผลทุเรียนและพอลิไวนิลแอลกอฮอล์ (EFFECT OF STERILIZATION METHODS ON PHYSICOCHEMICAL PROPERTIES OF G-CSF HYDROGEL DRESSING PREPARED FROM DURIAN FRUIT-HULLS POLYSACCHARIDE GEL AND POLYVINYL ALCOHOL) อ.ที่ปรึกษาวิทยานิพนธ์หลัก: อ. ภญ. ดร.พรรณเพ็ญ วัฒนาอาษากิจ, อ.ที่ปรึกษาวิทยานิพนธ์ร่วม: ดร.พิริยาร สุวรรณมาลา, 101 หน้า.

การศึกษานี้มีวัตถุประสงค์เพื่อศึกษาผลของวิธีทำให้ปราศจากเชื้อต่อคุณสมบัติทางเคมีกายภาพของแผ่นไฮโดรเจลปิดแผลที่เตรียมจากพอลิแซ็กคาไรด์เจลของเปลือกผลทุเรียน (ดีจี) และพอลิไวนิลแอลกอฮอล์ (พีวีเอ) ซึ่งมีหรือไม่มีสารจีซีเอสเอฟทั้งแบบแผ่นเปียกและแผ่นแห้ง ดีจีพีวีเอไฮโดรเจลแบบแผ่นเปียกเตรียมด้วยเทคนิคเยือกแข็งอ่อนละลาย และแบบแผ่นแห้งเตรียมโดยนำไฮโดรเจลแผ่นเปียกที่ได้ทำแห้งด้วยวิธีทำแห้งแบบเยือกแข็ง เตรียมใส่บรรจุภัณฑ์ชนิดพอลิเอทิลีนความหนาแน่นต่ำเชิงเส้นประสานกับไนลอน วิธีทำให้ปราศจากเชื้อ 3 วิธี ได้แก่ การฉายรังสีแกมมา 15 และ 25 กิโลเกรย์ การอบแก๊สเอทิลีนออกไซด์ และการอบแก๊สไฮโดรเจนเปอร์ออกไซด์พลาสมา โดยที่การฉายรังสีแกมมาสามารถทำได้ทั้งแผ่นเปียกและแผ่นแห้ง ขณะที่การอบแก๊สเอทิลีนออกไซด์และการอบแก๊สไฮโดรเจนเปอร์ออกไซด์พลาสมาทำเฉพาะกับตัวอย่างที่เป็นแผ่นแห้ง ศึกษาคุณสมบัติของแผ่นไฮโดรเจล ปริมาณน้ำในแผ่น สัดส่วนเจล ความสามารถในการดูดซับน้ำ คุณสมบัติทางเชิงกล คุณสมบัติเชิงความร้อน การดูดกลืนแสงอินฟราเรด และความปราศจากเชื้อของแผ่น ดีจีพีวีเอไฮโดรเจลทั้งชนิดที่มีและไม่มีจีซีเอสเอฟแบบแผ่นเปียกมีลักษณะภายนอกใส สีน้ำตาลอ่อน ยืดหยุ่น ขณะที่แบบแผ่นแห้งมีลักษณะภายนอกทึบแสง แห้งและเหนียว แผ่นไฮโดรเจลแบบเปียกมีปริมาณน้ำในแผ่นสูงประมาณ 90 เปอร์เซ็นต์ โดยที่แผ่นแห้งมีปริมาณน้ำต่ำกว่า 10 เปอร์เซ็นต์ ความสามารถในการดูดซับน้ำ ค่ามอดูลัสของยังและความทนต่อแรงดึงของไฮโดรเจลแบบแผ่นแห้งมีค่าสูงกว่าแบบแผ่นเปียก ภาพเอซซีเอ็มของไฮโดรเจลแบบแผ่นเปียกแสดงโครงสร้างที่เป็นลักษณะร่างแหขนาดใหญ่ ขณะที่แผ่นแห้งมีร่างแหที่มีความพรุนมากกว่า แผ่นไฮโดรเจลที่ทำให้ปราศจากเชื้อในทุกวิธีผ่านการทดสอบความปราศจากเชื้อ การฉายรังสีแกมมาเพิ่มเพิ่มความทนต่อแรงดึงของแผ่นไฮโดรเจลทั้งแบบแผ่นเปียกและแผ่นแห้ง ปริมาณรังสีที่เพิ่มขึ้นมีผลเพิ่มสัดส่วนเจล ส่งผลให้ปริมาณน้ำในแผ่นและความสามารถในการดูดซับน้ำของไฮโดรเจลแบบแผ่นเปียกลดลง การทำให้ปราศจากเชื้อทั้ง 3 วิธีมีผลลดสัดส่วนเจลของแผ่นแบบแห้งและส่งผลให้ความสามารถในการดูดซับน้ำเพิ่มขึ้น นอกจากนี้การฉายรังสีและการอบแก๊สไฮโดรเจนเปอร์ออกไซด์พลาสมามีผลเพิ่มค่ามอดูลัสของยังและความทนต่อแรงดึง การศึกษาเบื้องต้นของการปลดปล่อยจีซีเอสเอฟจากแผ่นไฮโดรเจลพบว่า การทำให้ปราศจากเชื้อทั้ง 3 วิธีมีผลให้การปลดปล่อยจีซีเอสเอฟมีค่าลดลงโดยเฉพาะวิธีการอบแก๊สไฮโดรเจนเปอร์ออกไซด์พลาสมาและปริมาณรังสีแกมมาที่เพิ่มขึ้นมีผลลดการปลดปล่อยเช่นกัน

ภาควิชา วิทยาการเภสัชกรรมและเภสัชอุตสาหกรรม ลายมือชื่อนิสิต

สาขาวิชา เภสัชอุตสาหกรรม ลายมือชื่อ อ.ที่ปรึกษาหลัก

ปีการศึกษา 2557 ลายมือชื่อ อ.ที่ปรึกษาร่วม

5476204033 : MAJOR INDUSTRIAL PHARMACY

KEYWORDS: POLYSACCHARIDE GEL FROM DURIAN FRUIT-HULLS / POLYVINYL ALCOHOL / STERILIZATION METHODS / G-CSF / HYDROGEL DRESSING

CHANTHANA NAINIRAN: EFFECT OF STERILIZATION METHODS ON PHYSICOCHEMICAL PROPERTIES OF G-CSF HYDROGEL DRESSING PREPARED FROM DURIAN FRUIT-HULLS POLYSACCHARIDE GEL AND POLYVINYL ALCOHOL. ADVISOR: PHANPHEN WATTANAARSAKIT, Ph.D., CO-ADVISOR: PHIRIYATORN SUWANMALA, Ph.D., 101 pp.

The purpose of this study was to evaluate effects of sterilization methods on physicochemical properties of hydrogel dressing prepared from Durian fruit-hulls polysaccharide gel (DG) and polyvinyl alcohol (PVA) with and without granulocyte-colony stimulating factor (G-CSF) loaded in wet and dried-form hydrogels. DG/PVA wet-form hydrogels were prepared by freeze-thaw technique and the dried-form hydrogels were prepared by freeze drying of the wet-form hydrogel. Hydrogel dressings were packed in linear low density polyethylene laminated nylon (LLDPE/Nylon) packaging using three sterilization methods: gamma irradiation 15 and 25 kGy, ethylene oxide gas and hydrogen peroxide gas plasma. Gamma irradiation could be processed in both wet and dried-form hydrogels. Ethylene oxide gas and hydrogen peroxide gas plasma processed only for the dried-form. The hydrogels were characterized for water content, gel fraction, water absorption capacity, mechanical properties, differential scanning calorimetry, fourier transform infrared spectroscopy and sterility test. The findings showed that the wet-form DG/PVA and G-CSF loaded hydrogels had light brown colour, transparency and elasticity while the dried-forms had opaque and stiffness. Water content of the wet and dried-form hydrogels were about 90 percent and less than 10 percent, respectively. Water absorption capacity, Young's modulus and tensile strength of the dried-form hydrogels were higher than the wet-form. Scanning electron microscope (SEM) of the wet-form hydrogels had network structure with large pores, whereas the dried-form had more porosities. Sterility test of all sterilized hydrogels are acceptable. Gamma irradiation had increased tensile strength of both wet and dried-forms. Higher of radiation dose increased gel fraction resulted in the decrease of water content and water absorption capacity of wet-form hydrogels. Sterilization by gamma radiation, ethylene oxide gas or hydrogen peroxide gas plasma decreased gel fraction resulted in the increase of water absorption capacity of dried-form hydrogels. In addition, gamma irradiation or hydrogen peroxide gas plasma increased properties of Young's modulus and tensile strength. Preliminary study of G-CSF release from hydrogels implied that all three sterilization methods could decreased G-CSF release especially hydrogen peroxide gas plasma sterilization.

Department: Pharmaceutics and Industrial
 Pharmacy

Field of Study: Industrial Pharmacy

Academic Year: 2014

Student's Signature

Advisor's Signature

Co-Advisor's Signature

ACKNOWLEDGEMENTS

Firstly, I wish to express my sincere gratitude and deep appreciation to my thesis advisor, Dr. Phanphen Wattanaarsakit for her precious guidance, continuous support, attention and encouragement throughout my study. In addition, I wish to express my grateful thank to Dr. Phiriyatorn Suwannamala, my thesis co-advisor, and Thailand Institute of Nuclear Technology (public organization) for helpful advice and supported for gamma sterilization technique and equipment.

Besides my advisor and co-advisor, I would like to thank to all of my thesis committee: Assoc.Prof.Parkpoom Tengamnuay, Ph.D., Assoc.Prof.Sunanta Pongsamart, Ph.D. and Dr.Narueporn Sutanthavibul for their valuable suggestions and comments. Once again thank you to Assoc.Prof.Sunanta Pongsamart, Ph.D. for her advice of polysaccharide gel from Durian fruit-hulls extraction process and techniques.

I would like to acknowledge Pol.Lt.Col Ngamsin Wanishpongpan and Police General hospital for supporting in ethylene oxide gas and hydrogen peroxide gas plasma sterilization of the product and helpful advice. I am thankful to Dr.Kasinee Hemvichian from Thailand Institute of Nuclear Technology(public organization) for numerous discussions that helped me improve my knowledge in the area and also grateful to lovely staffs, Ms.Pattra Lertsarawut and Ms.Theeranan Tangthong for accomplished a main part of my research. Many thank also goes to The Thai Red Cross Society for supporting the packaging material for sterilization.

Moreover, my heartfelt thanks to Ms.Apirom Laocharoenkeat, head of sterile pharmaceutical manufacturing division, and great colleagues at Siriraj hospital for their sympathy and encouragement. I am also grateful to classmates, scientist and staffs in the Department of Pharmaceutics and Industrial Pharmacy, Faculty of Pharmaceutical Sciences, Chulalongkorn University, for their assistance and support.

I appreciate the financial support from the 90th anniversary of Chulalongkorn University fund for this research project and Siriraj development scholarship for master degree's tuition fee. I am also thankful to the Scientific and Technological Research Equipment Center, Chulalongkorn University for providing equipments and services.

Finally, I would like to dedicate this thesis to my parents especially my passed away mom who have shown me unconditional love and support. My infinite thanks goes to my loving husband for sticking with me through all the good times and bad and helping to keep me sane.

CONTENTS

	Page
THAI ABSTRACT	iv
ENGLISH ABSTRACT	v
ACKNOWLEDGEMENTS	vi
CONTENTS	vii
CONTENT OF FIGURE.....	1
CONTENT OF TABLE	4
ABBREVIATIONS.....	1
CHAPTER I INTRODUCTION.....	2
CHAPTER II LITERATURE REVIEW	5
2.1 Wound dressing	5
2.1.1 Wound healing processes	5
2.1.2 Types of wound dressing.....	8
2.2 Hydrogels	10
2.2.1 Hydrogel-based materials	11
2.2.1.1 Polysaccharide gel from durian fruit-hulls	11
2.2.1.2 Polyvinyl alcohol.....	12
2.2.2 Hydrogel preparation methods.....	13
2.2.3 Hydrogel characterization methods.....	15
2.3 Growth factors	18
2.3.1 Granulocyte-macrophage colony-stimulating factor	19
2.3.2 Granulocyte colony-stimulating factor	22
2.4 Sterilization methods	22

	Page
2.4.1 Ionizing radiation	22
2.4.2 Ethylene oxide gas.....	25
2.4.3 Hydrogen peroxide gas plasma.....	26
CHAPTER III MATERIALS AND METHODS	28
Materials.....	28
Methods.....	29
3.1 Preparation of polysaccharide gel extract from durian fruit-hulls.....	29
3.2 Preparation of polysaccharide gel from durian fruit-hulls and polyvinyl alcohol hydrogel dressing.....	29
3.2.1 Preparation of DG/PVA hydrogels.....	29
3.2.1.1 Preparation of wet-form DG/PVA hydrogels (DG/PVA-W).....	29
3.2.1.2 Preparation of dried-form DG/PVA hydrogels (DG/PVA-F).....	30
3.2.2 Preparation of G-CSF loaded polysaccharide gel from durian fruit-hulls and polyvinyl alcohol hydrogel dressing	30
3.3 Physicochemical characterization.....	31
3.4 Selection of hydrogel packaging materials	33
3.5 Sterilization methods for hydrogel dressings	34
3.5.1 Gamma irradiation	34
3.5.2 Ethylene oxide gas sterilization	34
3.5.3 Hydrogen peroxide gas plasma sterilization.....	34
3.6 Sterility testing	35
3.7 Preliminary study of G-CSF release from hydrogel dressings.....	35
3.8 Statistical analysis.....	35
CHAPTER IV RESULT AND DISCUSSION	36

	Page
4.1 Properties of powder extract polysaccharide gel from durian fruit-hulls.....	36
4.2 Physicochemical properties of DG/PVA hydrogels.....	38
4.3 Selection of hydrogel packaging	47
4.4 Sterility test	48
4.5 Effect of sterilization methods on physicochemical properties of DG/PVA hydrogels	49
4.5.1 Gamma irradiation	49
4.5.2 Ethylene oxide gas sterilization	63
4.5.3 Hydrogen peroxide gas plasma.....	68
4.6 Effect of sterilization methods on G-CSF release from DG/PVA hydrogel	79
CHAPTER V CONCLUSION.....	81
REFERENCES	82
APPENDIX.....	89
Appendix 1 Biological indicators.....	89
Appendix 2 Packaging materials for hydrogel.....	90
Appendix 3 Sterility testing.....	96
Appendix 4 ELISA assay	99
VITA.....	101

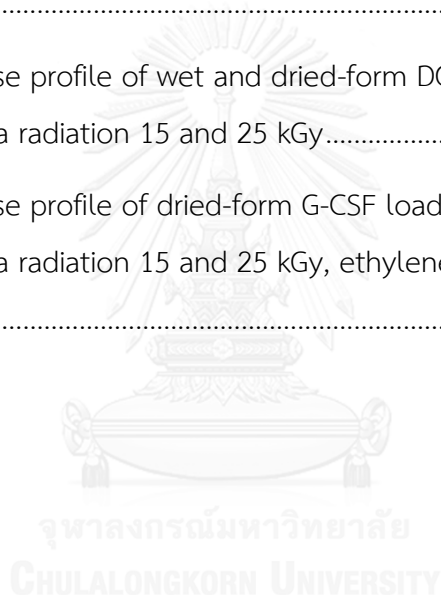
CONTENT OF FIGURE

Figure 1 Normal wound healing processes	6
Figure 2 Chemical structure of polygalacturonic acid	12
Figure 3 Chemical structure of polyvinyl alcohol.....	12
Figure 4 Molecular structure of granulocyte-macrophage colony-stimulating factor..	19
Figure 5 Actions of GM-CSF on components of the wound healing process	19
Figure 6 Structure of granulocyte colony-stimulating factor.....	22
Figure 7 Effect of gamma radiation on water molecules.....	24
Figure 8 Gamma Irradiator (GC-5000).....	24
Figure 9 Ethylene oxide gas sterilizer (3M-Sterivac).....	25
Figure 10 Hydrogen peroxide gas plasma sterilizer (Sterrad 100s).....	27
Figure 11 FTIR spectra of DG powder lot M81 (lot L-II in the previous study) and lot N-01.....	37
Figure 12 DSC thermograms of DG powder lot M81 (lot L-II in the previous study) and lot N-01.....	37
Figure 13 Water content of wet and dried-form DG/PVA hydrogels.....	39
Figure 14 Water absorption capacity of wet and dried-form DG/PVA hydrogels.....	39
Figure 15 Gel fraction of wet and dried-form DG/PVA hydrogels.....	40
Figure 16 Mechanical properties of wet and dried-form DG/PVA hydrogels (A) Young's Modulus (B) % Elongation (C) Tensile strength	41
Figure 17 FTIR spectra of DG and PVA raw materials and PVA and DG/PVA hydrogels.....	42
Figure 18 FTIR spectra of wet and dried-form DG/PVA hydrogels.....	43
Figure 19 DSC thermograms of wet and dried-form DG/PVA hydrogels	43

Figure 20 FTIR spectra of wet-form DG/PVA with G-CSF loaded and unloaded hydrogels.....	44
Figure 21 FTIR spectra of dried-form DG/PVA with G-CSF loaded and unloaded hydrogels.....	45
Figure 22 FTIR spectra of G-CSF loaded wet and dried-form DG/PVA hydrogels.....	46
Figure 23 Water content of wet-form DG/PVA hydrogels after gamma irradiation.....	50
Figure 24 Water absorption capacity of wet-form DG/PVA hydrogels after gamma irradiation.....	51
Figure 25 Gel fraction of wet-form DG/PVA hydrogels after gamma irradiation.....	52
Figure 26 Mechanical properties of wet-form DG/PVA hydrogels after gamma irradiation.....	53
Figure 27 FTIR spectra of wet-form DG/PVA hydrogels after gamma irradiation.....	54
Figure 28 DSC thermograms of wet-form DG/PVA hydrogels after gamma irradiation.....	55
Figure 29 FTIR spectra of G-CSF loaded wet-form hydrogels after gamma irradiation.....	57
Figure 30 Water content of dried-form DG/PVA hydrogels after gamma irradiation	59
Figure 31 Water absorption capacity of dried-form DG/PVA hydrogels after gamma irradiation.....	59
Figure 32 Gel fraction of dried-form DG/PVA hydrogels after gamma irradiation	60
Figure 33 FTIR spectra of dried-form DG/PVA hydrogels after gamma irradiation	61
Figure 34 FTIR spectra of dried-form G-CSF loaded hydrogels after gamma irradiation.....	61
Figure 35 Mechanical properties of dried-form DG/PVA hydrogels after gamma irradiation (A) Young's Modulus (B) % Elongation (C) Tensile strength.....	62

Figure 36 Water content of dried-form DG/PVA hydrogels after ethylene oxide gas sterilization.....	64
Figure 37 Water absorption capacity of dried-form DG/PVA hydrogels after ethylene oxide gas sterilization	64
Figure 38 Gel fraction of dried-form DG/PVA hydrogels after ethylene oxide gas sterilization.....	65
Figure 39 Mechanical properties of dried-form DG/PVA hydrogels after ethylene oxide gas sterilization (A) Young's Modulus (B) % Elongation (C) Tensile strength	66
Figure 40 FTIR spectra of dried-form G-CSF loaded and unloaded DG/PVA hydrogels after ethylene oxide gas sterilization	67
Figure 41 Water content of dried-form DG/PVA hydrogels after hydrogen peroxide gas plasma sterilization	69
Figure 42 Water absorption capacity of dried-form DG/PVA hydrogels after hydrogen peroxide gas plasma sterilization.....	69
Figure 43 Gel fraction of dried-form DG/PVA hydrogels after hydrogen peroxide gas plasma sterilization	70
Figure 44 Mechanical properties of dried-form DG/PVA hydrogels after hydrogen peroxide gas plasma sterilization (A) Young's Modulus (B) % Elongation (C) Tensile strength.....	71
Figure 45 FTIR spectra of dried-form G-CSF loaded and unloaded DG/PVA hydrogels after hydrogen peroxide gas plasma sterilization.....	72
Figure 46 Mechanical properties of dried-form DG/PVA hydrogels after sterilization by gamma radiation 25 kGy, ethylene oxide and hydrogen peroxide gas plasma (A) Young's Modulus (B) % Elongation (C) Tensile strength	75
Figure 47 Water absorption capacity of dried-form DG/PVA hydrogels after sterilization by gamma radiation 25 kGy, ethylene oxide and hydrogen peroxide gas plasma	76

Figure 48 FTIR spectra of dried-form DG/PVA hydrogels after sterilization by gamma radiation 25 kGy, ethylene oxide and hydrogen peroxide gas plasma	77
Figure 49 FTIR spectra of dried-form G-CSF loaded hydrogels after sterilization by gamma radiation 25 kGy, ethylene oxide and hydrogen peroxide gas plasma	77
Figure 50 DSC thermograms of dried-form DG/PVA hydrogels after sterilization by gamma radiation 25 kGy, ethylene oxide and hydrogen peroxide gas plasma.....	78
Figure 51 DSC thermograms of dried-form G-CSF loaded DG/PVA hydrogels after sterilization by gamma radiation 25 kGy, ethylene oxide and hydrogen peroxide gas plasma	78
Figure 52 G-CSF release profile of wet and dried-form DG/PVA hydrogels after sterilization by gamma radiation 15 and 25 kGy.....	79
Figure 53 G-CSF release profile of dried-form G-CSF loaded hydrogels after sterilization by gamma radiation 15 and 25 kGy, ethylene oxide gas and hydrogen peroxide gas plasma	80



CONTENT OF TABLE

Table 1 The clinical study of topically applied rhGM-CSF in patients with different type of wound.....	21
Table 2 Properties of DG powder extract.....	36

Table 3 Morphology of DG/PVA hydrogels.....	38
Table 4 Mechanical properties of wet and dried-form DG/PVA hydrogels	40
Table 5 Selection of packaging materials for sterilization	47
Table 6 Morphology of wet-form DG/PVA hydrogels after gamma irradiation.....	49
Table 7 Mechanical properties of wet-form DG/PVA hydrogels after gamma irradiation.....	53
Table 8 Morphology of G-CSF loaded wet-form hydrogels after gamma irradiation...	56
Table 9 Morphology of G-CSF loaded and unloaded dried-form hydrogels after gamma irradiation.....	58
Table 10 Mechanical properties of dried-form DG/PVA hydrogels after gamma irradiation.....	62
Table 11 Morphology of G-CSF loaded and unloaded dried-form hydrogel after ethylene oxide gas sterilization	63
Table 12 Mechanical properties of dried-form DG/PVA hydrogels after ethylene oxide gas sterilization.....	66
Table 13 Morphology of dried-form G-CSF loaded and unloaded DG/PVA hydrogels after hydrogen peroxide gas plasma sterilization	68
Table 14 Mechanical properties of dried-form DG/PVA hydrogels after hydrogen peroxide gas plasma sterilization	71
Table 15 Morphology of dried-form hydrogels after sterilization by gamma radiation 25 kGy, ethylene oxide and hydrogen peroxide gas plasma	73
Table 16 Morphology of G-CSF loaded dried-form hydrogels after sterilization by gamma radiation 25 kGy, ethylene oxide and hydrogen peroxide gas plasma.....	74
Table 17 Mechanical properties of dried-form DG/PVA hydrogels after sterilization by gamma radiation 25 kGy, ethylene oxide and hydrogen peroxide gas plasma.....	75



ABBREVIATIONS

DG	Durian fruit-hulls polysaccharide gel
PVA	Polyvinyl alcohol
DG/PVA	Hydrogel containing DG 2% w/w and PVA 5% w/w
DG/PVA-W	Wet-form of DG/PVA hydrogel
DG/PVA-F	Dried-form of DG/PVA hydrogel
G-CSF	Granulocyte Colony Stimulating Factor
GM-CSF	Granulocyte-Macrophage Colony Stimulating Factor

G-DG/PVA	G-CSF loaded DG/PVA hydrogel
G-DG/PVA-W	Wet -form of G-CSF loaded DG/PVA hydrogel
G-DG/PVA-F	Dried-form of G-CSF loaded DG/PVA hydrogel
kGy	KiloGray
EO	Ethylene Oxide gas
HO	Hydrogen Peroxide gas plasma
FTIR	Fourier Transform Infrared spectroscopy
DSC	Differential Scanning Calorimetry
TSB	Tryptic Soy Broth
SCDB	Soybean Casein Digest Broth



CHAPTER I

INTRODUCTION

The hydrogels consist of a three-dimensional networks of cross-linked hydrophilic polymers that are insoluble in water and interact with aqueous solutions by swelling (Peppas, et al., 2009). Hydrogels can absorb an excess of wound exudates, protect the wound from external mechanical stress, provide a barriers to secondary infection and they are able to keep granulation and epithelial tissue moist so hydrogels are indicated for wound dressing by their properties (Kickhöfen, et al.,

1986). Polyvinyl alcohol (PVA) is one of the most popular synthetic polymer hydrogels due to its good biocompatibility, biodegradable, non-carcinogenic and able to absorb water or biological fluid efficiently (Varshney, 2007). PVA hydrogels can be obtained in various ways such as freezing and thawing (Hassan and Peppas, 2000), chemical cross-linking (Reis, et al., 2006), gamma irradiation (Dutta, 2012) and ultra violet (Xu, et al., 2010) etc. PVA has blended with some natural polymer to obtain the desirable properties of polymeric material. The polysaccharide gel from durian fruit-hulls (DG) is a natural polymer, that first isolated by Pongsamart and Panmaung in 1998, showed inhibitory activity against various bacterial strains such as *Staphylococcus aureus*, *Staphylococcus epidermidis*, *Lactobacillus pentosus*, *Micrococcus luteus*, *Bacillus subtilis* and *Escherichia coli* except *Lactobacillus plantarum* (Pongsamart, et al., 2005) and did not produce inhibitory activity against *Candida albicans* and *Saccharomyces cerevisiae* (Lipipun, et al., 2002). Furthermore, DG could help rapid wound closure in pig and dog model (Chansiripornchai, et al., 2005; Siripokasupkul, 2004). In 2009, Eakwaropas and colleague developed the hydrogel wound dressing from DG and PVA that resulted in better membrane properties than PVA hydrogel and suitable for further development in biomedical application (Eakwaropas, 2009).

Growth factors are soluble secreted proteins that are important for coordinating cell-cell and cell-matrix interactions during normal injury repair. Therefore, exogenous growth factors delivered to non-healing wounds may facilitate cellular responses and resulted in wound closure (Koria, 2012). Hydrogel dressings are interesting medical device that could be used as growth factors delivery system.

The sterilization of hydrogel dressings is very important to ensure the patient's safety. Method of sterilization must be carefully selected because the physical, mechanical and biological properties of biomaterial are affected during the

process (Marreco, et al., 2004). Typical methods used to sterilize wound dressing are ethylene oxide gas sterilization, steam sterilization, gamma irradiation and gas plasma sterilization. Some natural polymers are sensitive to high temperature sterilization so steam sterilization method should be avoided. Each sterilization method has their advantage and disadvantage, i.e., ethylene oxide and gas plasma sterilization methods require a gas to penetrate into the packaged product and contact the wound dressing thus the packaging must be permeable to the sterilizing gas. Application of gamma irradiation can cause crosslinking or degradation to occur in the polymer of dressing. The effect of sterilization methods on properties of polymeric material and growth factors should be evaluated.

The purpose of this study is to evaluate the effect of sterilization methods on physicochemical properties of G-CSF loaded and unloaded hydrogel dressing prepared from DG and PVA.

CHAPTER II

LITERATURE REVIEW

2.1 Wound dressing

The role of a wound dressing is to provide the right environment to enhance and promote wound healing. A moist healing environment stimulates cell proliferation and encourages epithelial cells to migrate. Wound dressings that create and maintain a moist environment are considered to provide the optimal conditions for wound healing (Jones, et al., 2006).

An ideal wound dressing should maintain humidity at the wound site while removing excess exudate, protect wound from further trauma, allow gaseous exchange, can be removed without causing trauma to the wound, should be impermeable to bacteria, thermally insulating, non-toxic and non-allergenic, free of toxic wound contaminants, require infrequently changes, comfortable and cost effective.

2.1.1 Wound healing processes

Wound healing is a dynamic process consisting of four continuous, overlapping and precisely programmed phases: haemostasis, inflammation, proliferation and remodeling. Interruptions or prolongation in the process can lead to delayed wound healing or a non-healing chronic wound (Guo and DiPietro, 2010).

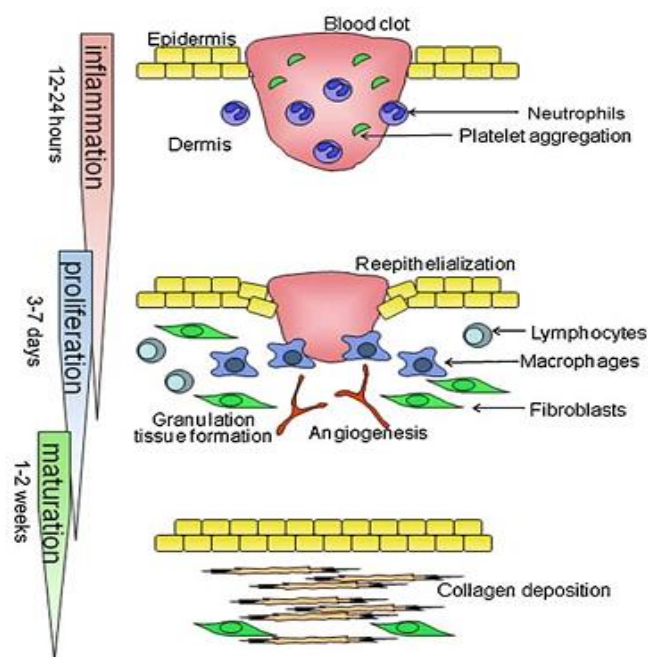


Figure 1 Normal wound healing processes

(Kondo and Ishida, 2010)

2.1.1.1 Haemostasis phase

Haemostasis phase occur immediately after injury. Essentially there are three different stages of hemostasis. Vascular constriction stage is the stage that blood vessels constrict to stop bleeding and reduce exposure to bacteria. The second state is platelet aggregation and the third stage is blood coagulation.

2.1.1.2 Inflammatory phase

Occur 12 to 24 hours after injury. Once blood vessels in the wound bed have contracted and haemostasis has been successfully achieved, it soon dissipates and the blood vessels open up (vasodilation) to increase blood flow to the injury site. This increased blood flow bringing inflammatory cells to fight infection and other cells to clean up the damaged tissue. The result is redness and swelling around the injured site for 2-3 days. In the image to the right, the redness surrounding the wound can be seen.

2.1.1.3 Proliferative phase

Occur within day 3 to day 7. There are three important stages of the proliferative phase in wound healing processes : epithelialization, fibroplasia and angiogenesis stage.

Epithelialization is the process of new skin formation over the injured area. The process begins almost immediately after the injury as the skin cells (epidermal cells), undergo a change allowing them to detach and migrate across the wound bed. The skin cells have enzymes designed to break up the scab (eschar) which forms on the wound surface. A moist environment promotes wound healing by encouraging epithelialization.

Fibroplasia is the process of fibroblasts forming and laying down new collagen. Collagen is the main component of skin and critical for structure, strength and support. Collagen is formed approximately 3 days after injury and collagen formation continues for about 6 weeks. Collagen is laid down in a random, cross-linked fashion to increase strength over the injured surface. Elastin is another important structural protein which is present in small amounts and provides elasticity to skin.

Angiogenesis is the process of forming new blood vessels. An ample blood supply is necessary to sustain new skin growth. The small blood vessels which form cause a redness to form around the scar tissue. Macrophages, one of the key cells designed to clean up the tissue debris also secretes growth factors to stimulate the growth of new blood vessels.

2.1.1.4 Remodeling phase

Occur within 2 weeks to 1 year. In this phase, there is an attempt to recover normal tissue structure. It is a phase marked by maturation of elements and affections of the extracellular matrix, leading to proteoglycan and collagen deposits. In a later phase, fibroblasts of granulation tissue are transformed into myofibroblasts and behave as contractile tissue that responds to agonists that stimulate smooth muscles. At the same time, there is an extracellular matrix reorganization.

Choosing the wound dressing are based on types of wounds, size , wound site, amount of drainage and presence of infection.

2.1.2 Types of wound dressing

2.1.2.1 Gauze dressings

Gauze dressings are made of woven or non-woven materials and available in a variety of shapes and sizes. They are used for infected wounds which require packing, draining and requiring very frequent dressing changes.

Advantages of gauze dressings are available in many sizes and forms also gauze can be used for infected wounds and can be combined with other topical products. It's effective for packing wounds with tunnels, tracts, or undermining.

Disadvantages of gauze dressings are gauze must be held in place by a secondary dressing. The dressings have to change frequently. Gauze may adhere to the wound and not recommended for effective moist wound healing.

Example of gauze dressing is Bactigras[®] medicated paraffin gauze dressing.

2.1.2.2 Transparent film dressings

Transparent film dressings allow oxygen and water vapor pass through but prevent bacterial contamination. This dressing type usually composed of polyurethane polymer. They are used for partial-thickness wounds, pressure ulcers and minor burns stage I and stage II

Advantage of this dressing is having transparency property which the wound can be visualized, preventing bacterial contamination and its film conform to the wound well. It's promotes autolytic debridement, prevent and reduces friction.

Disadvantage of the dressing are stick to the wound bed. Most transparent dressings do not absorb moisture and are not indicated for draining wounds.

Example of transparent dressings are Opsite[®] , Tegaderm[®] film

2.1.2.3 Hydrocolloid dressings

Hydrocolloid dressings are adhesive patches containing colloidal particles such as methylcellulose, gelatin or pectin that swell to gel-like mass when contact with the wound exudate. These dressings are used for burn wounds, pressure ulcers and venous ulcers.

Advantage of this dressings is to prevent the skin surrounding of the wound from losing of moisture also donating moisture to the wound and encourage autolytic debridement. It's provide wound cushion and can absorb moderate exudate.

Disadvantage of the dressings can leave a residue present in the wound and cannot be used in wound with infection.

Example of hydrocolloid dressings are Tegaserb[®], Duoderm[®]

2.1.2.4 Foam dressings

Foam dressings are non-adhesive patches which composed of a film coated gel or polyurethane polymer. This dressings are suitable for pressure ulcers, skin graft, venous ulcers and diabetic ulcers

Advantage of foam dressing is having high absorption capacity of wound exudate, non-adhesive to the wound bed and available in many shape and size. Foam is conformable, easy to apply and remove because it's nonadherent. The frequency of dressing changes depends on the amount of wound drainage.

Disadvantage of this dressing is needed secondary dressing or tape to secure some of the first foam dressing. A may be Foam dressings can allow excess moisture accumulate, macerating periwound skin. They cannot be used on wounds with eschar or no exudates.

Example of foam dressings are Allevyn[®] and Polyderm[®]

2.1.2.5 Hydrogel dressings

Hydrogels consist of a matrix of insoluble polymers with up to 96% water content enabling them to donate moisture to the wound surface and

maintain a moist environment at wound bed. The polymers are partially hydrated so hydrogels have the ability to absorb a degree of wound exudate. The hydrogels transmit moisture vapour and oxygen. Hydrogels promote wound debridement by rehydration of non-viable tissue, thus facilitating the process of natural autolysis. The moisture in the wound is also essential in pain management for the patient and these dressings are very soothing and cooling. The most common types of hydrogel dressings are amorphous gels, sheet dressings, filler or fiber types of material and gauze types of dressings. These dressings are suitable for diabetic ulcers, pressure ulcers, surgical wounds, burns and skin tears.

Advantage of the hydrogel dressings are non-adhesive to the wound or the tissue and high water content that suitable for dry and necrotic wounds to help hydration with skin moisture retention and promote effective healing. Hydrogel dressings are available in different types of hydrogel dressing.

Disadvantage of the dressing is not indicated for wound producing high levels of exudate or gangrenous tissue which should kept dry to reduce risk of infection.

Example of hydrogel dressings are Aquasite[®], Intrasite[®] gel and Flexigel[®]

2.2 Hydrogels

Hydrogels are three-dimensional networks formed from hydrophilic homopolymers, copolymers or macromers cross-linked to form insoluble polymer matrices. These polymers are typically soft and elastic due to their thermodynamic compatibility with water and have used in many biomedical applications (Peppas, et al., 2009). The hydrogels can respond to the fluctuations of the environmental stimuli such as pH, temperature, ionic strength, electric field or presence of enzyme. In the swollen state, they are soft and rubbery that resembling the living tissue (Das, 2013).

The water absorption capacity and permeability are the most important characteristic features of the hydrogel. The polar hydrophilic groups are the first to

be hydrated upon contact with water which leads to the formation of ‘primary bound water’. Therefore, the network swells and exposes the hydrophobic groups which are capable of interacting with molecules of water leading to the formation of ‘secondary bound water’, also called hydrophobically-bound water. Primary and secondary bound water are often combined to total bound water. The network will absorb additional water by covalent or physical cross-links. The additional absorbed water is called ‘free water’ or ‘bulk water’ and assumed to fill the space between the network chains, and/or the center of larger pores.

Hydrogels are classified into two categories, chemical hydrogel and physical hydrogel. Chemical hydrogel is a hydrogel that the crosslinking process is formed by chemical covalent bonds which is replacing hydrogen bond by stronger and stable covalent bonds. The chemical hydrogels are permanent and irreversible. Physical hydrogel is the hydrogel prepared by physical process. The methods to achieve physical hydrogels are association, aggregation, crystallization (freeze-thaw technique), complexation and hydrogen bonding are The physical hydrogels are reversible due to the conformational change. (Omidian and Park, 2012)

2.2.1 Hydrogel-based materials

2.2.1.1 Polysaccharide gel from durian fruit-hulls

Polysaccharide gel from durian fruit-hulls (DG) was first extracted by Pongsamart and Panmuang in 1998. The elemental compositions are carbon(C), hydrogen(H) and oxygen(O) in molar ratio closed to 3:6:3. Polysaccharide gel has an average molecular weight of 500-1,400 kDa (Pongsamart, 2003). DG is a water soluble polysaccharide. Compose of long chain polygalacturonic acid, which was more than fifty percent of total sugar, with branch chain neutral sugars such as arabinose, rhamnose, fructose, glucose and galactose. The viscosity of 3% (w/v) DG was 405.2 ± 7.4 cps and pH was 2.4 ± 0.2 (Hokputsaa, et al., 2004)

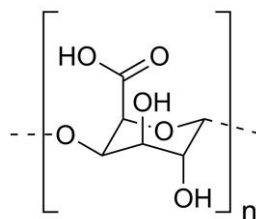


Figure 2 Chemical structure of polygalacturonic acid

DG showed inhibitory activity against six bacterial strains such as *Staphylococcus aureus*, *Staphylococcus epidermidis*, *Lactobacillus pentosus*, *Micrococcus luteus*, *Bacillus subtilis* and *Escherichia coli* except *Lactobacillus plantarum* (Pongsamart, et al., 2005) and did not produce inhibitory activity against *Candida albicans* and *Saccharomyces cerevisiae* (Lipipun, et al., 2002). DG was used to form several type of preparation improved wound healing. For instance, dressing film prepared by casting solvent evaporation method presented swelling and bioadhesive properties that dressing film can absorb water to provide moist environment for wound healing (Chansiripornchai, et al., 2005) and fiber dressing patch prepared by freeze-drying method that also absorbed moisture from environment and providing moist to the wound were evaluated the efficacy in dog skin (Siripokasupkul, 2004). DG can be used as bactericidal agent and excipient in pharmaceutical and cosmetics.

2.2.1.2 Polyvinyl alcohol

Polyvinyl alcohol (PVA) is a hydrophilic polymer interesting in biomaterial research due to its excellent biocompatibility and mechanical properties (Kobayashi and Hyu, 2010), non-toxic and physical properties like soft tissue (Stasko, et al., 2009). PVA hydrogel has been proposed as tissue mimicking, vascular cell culturing and vascular implanting (Jiang, et al., 2011).

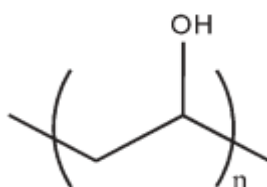


Figure 3 Chemical structure of polyvinyl alcohol

There are various methods to fabricate the PVA hydrogel, for example, chemical crosslinking (Reis, et al., 2006), gamma irradiation (Dutta, 2012), freezing and thawing (Hassan, et al., 2000). Freezing and thawing technique is physical crosslinking due to crystallite formation. This method does not require the presence of a crosslinking agent. The freezing and thawing technique has been a popular method for synthesis PVA hydrogel because of non-toxic, easy to operate and PVA hydrogels showed increased mechanical strength over other methods because the crystalline regions are better distributing the mechanical load or stress.

2.2.2 Hydrogel preparation methods

2.2.2.1 Chemical cross-linking

The cross-linking of natural and synthetic polymers can be achieved through the reaction of their functional groups (such as OH, COOH, and NH₂) with cross-linkers such as aldehyde (e.g. glutaraldehyde). There are a number of methods reported in literature to obtain chemically cross-linked permanent hydrogels.

Chemical cross-linkers: cross-linking agent such as glutaraldehyde (Hennink and Nostrum, 2002) has been used to obtain the cross-linked hydrogel network of various synthetic and natural polymers.

Grafting: Grafting involves the polymerization of a monomer on the backbone of a preformed polymer. The polymer chains are activated by the action of chemical reagents, or high energy radiation treatment. The growth of functional monomers on activated radicals leads to branching and further to cross-linking. Grafting technique can be divided into two types such as chemical grafting, macromolecular backbones are activated by the action of a chemical reagent (Tripathi and Mishra, 2012), and radiation grafting, grafting can be initiated by the use of high energy radiation (Neri, et al., 2011).

2.2.2.2 Radiation cross-linking

Radiation cross-linking does not involve the use of chemical additives and therefore retaining the biocompatibility of the biopolymer. The modification and sterilisation can be achieved in single step and hence it is a cost effective process to modify biopolymers having their end-use specifically in biomedical application (Aiji, et al., 2005). The mechanism of this technique mainly on producing free radicals in the polymer following the exposure to the high energy source such as gamma ray or electron beam. The action of radiation will depend on the polymer environment (i.e. dilute solution, concentrated solution, solid state).

2.2.2.3 Physical cross-linking

There has been an increased interest in physical or reversible gels due to relative ease of production and the advantage of not using cross-linking agents. The physical hydrogels are formed by various methods such as

Heating/cooling a polymer solution: the gel formation is due to helix-formation, association of helices and forming junction zones (Noda, et al., 2008).

Ionic interaction: ionic polymers can be cross-linked by the addition of di- or tri-valent counterions. This method underlies the principle of gelling a polyelectrolyte solution (e.g. Na^+ alginate $^-$) with a multivalent ion of opposite charges (e.g. $\text{Ca}^{2+} + 2\text{Cl}^-$) (Fan, et al., 2012).

Complex coacervation: the hydrogels can be formed by mixing of a polyanion with a polycation. The underlying principle of this method is that polymers with opposite charges stick together and form soluble and insoluble complexes depending on the concentration and pH of the respective solutions (Yin and Stöver, 2003).

Hydrogen bonding: H-bonded hydrogel can be obtained by lowering the pH of aqueous solution of polymers carrying carboxyl groups (Kharlampieva, et al., 2007).

Maturation (heat induced aggregation): maturation process demonstrate that a hydrogel can be produced with precisely structured molecular dimensions. The controlling feature is the agglomeration of the protein components within the molecularly disperse system that is present in of the naturally occurring gum. Maturing of the gum leads to transfer of the protein associated with the lower molecular weight components to give larger concentrations of high molecular weight fraction (Al-Assaf, et al., 2007).

Freeze-thawing: The mechanism involves the formation of microcrystals in the structure due to freeze-thawing (Mc Gann, et al., 2009). In addition to their nontoxic process, the hydrogels from freeze-thawing technique were interested in many pharmaceutical and biomedical applications.

2.2.3 Hydrogel characterization methods

2.2.3.1 Water content

The bound water is then obtained by difference of the measured total water content of the hydrogel test specimen, and the calculated free water content (Kaplan and Güner, 2000).

2.2.3.2 Swelling measurement (Water absorption capacity)

Method A, according to the Japanese Industrial Standard K8150 method, the dry hydrogel is immersed in deionized water for 48 hours at room temperature on a roller mixer. After swelling, the hydrogel is filtered by a stainless steel net of 30 meshes (681 μm). The swelling is calculated as follows

$$\text{Swelling} = (W_s - W_d) / W_d$$

Where, W_s is the weight of hydrogel in swollen state and W_d is the weight of hydrogel in dry state.

Method B, measuring the swelling of hydrogel, in a volumetric vial the dry hydrogel (0.05-0.1g) was dispersed into sufficiently high quantity of water (25-30 ml) for 48 hrs at room temperature. The mixture is then centrifuged to obtain the layers of water-bound material and free unabsorbed water.

Method C, according to the Japanese Industrial Standard (JIS) K7223, the dry gel is immersed in deionized water for 16 h at room temperature. After swelling, the hydrogel was filtered using a stainless-steel net of 100-mesh (149 μ m). Swelling is calculated as follows

$$\text{Swelling} = \frac{C}{B} * 100$$

Where C is the weight of hydrogel obtained after drying and B is the weight of the insoluble portion after extraction with water.

2.2.3.3 Gel fraction

Method A, The hydrogel content of a given material is estimated by measuring its insoluble part in dried sample after immersion in deionized water. The sample should be prepared at a dilute concentration (typically about 1%) to ensure that hydrogel is fully dispersed in water (Gulrez and Al-Assaf, 2011). The gel fraction is calculated as follow:

$$\text{Gel Fraction (\%hydrogel)} = \left(\frac{W_d}{W_i} \right) * 100$$

Where, W_i is the initial weight of dried sample and W_d is the weight of the dried insoluble part of sample after extraction with water.

Method B, a more accurate measure of the insoluble fraction for hydrocolloids which modified by changing the solvent from mild alkaline to water. The weight (W_1) of a 70 mm glass fiber paper (pore size 1.2 micron) is determined following drying in an oven at 105 °C for 1 hour and subsequently cooled in a desiccator containing silica gel. Depending on the test material, 1-2 wt%

(S) dispersion can be prepared in distilled water followed by overnight hydration at room temperature. The hydrated dispersion is then centrifuged for 2-5 minutes at 2500 rpm prior to filtration. Drying of the filter paper is carried out in an oven at 105 °C followed by cooling to a constant weight (W_2). % Insoluble can then be calculated:

$$\text{Gel Fraction (\%Hydrogel)} = (W_2 - W_1 / S) * 100$$

2.2.3.4 Scanning Electron Microscopy

SEM can be used to provide information about the sample's morphology. This technique used to capture the characteristic network structure in hydrogels (Kim and Chu, 2000).

2.2.3.5 Fourier Transform Infrared Spectroscopy

This technique is used for identifying chemical structure of a substance. It is based on the principle that the basic components of a substance can be excited and absorb infrared light at frequencies that are typical of the types of the chemical bonds. The resulting IR absorption spectrum represents a fingerprint of measured sample. (Yang, et al., 2008)

2.2.3.6 Differential scanning calorimetry

The main methods used to characterize and quantify the amount of free and bound water in hydrogels (Pinho, et al., 2014).

2.2.3.7 Mechanical properties

Mechanical tests were conducted to assess the hydrogel properties. To establish a library of mechanical properties of hydrogels and to determine the range of application (Oliveira, et al., 2014). Tensile tests are used to determine the mechanical properties of material such as the modulus of elasticity, tensile strength, elongation, elastic limit, yield point, yield strength and other tensile properties. Mechanical properties are governed by the basic concepts of elasticity, plasticity and toughness. Elasticity is the capacity of a material to undergo temporary deformation. When the caused this deformation is removed, the material returns to its original shape. Plasticity or ductility is the ability to undergo permanent

deformation without failure. Toughness is the ability of material to deform plastically and to absorb energy in the process before fracture.

2.2.3.8 Other techniques

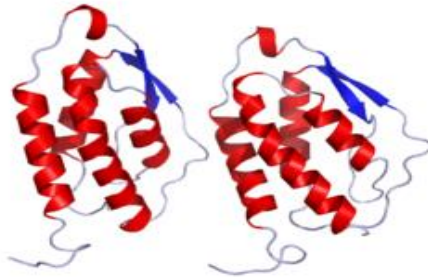
Sol-gel analysis (Rosiak, 1998), Thermo-gravimetric analysis (TGA) (Rusu, et al., 2015), Nuclear magnetic resonance (NMR) (Mathur and Scranton, 1996), X-ray powder diffraction (XRD) (Mishra, et al., 2008), etc.

2.3 Growth factors

Growth factors are multifunctional peptides that play fundamental roles in wound healing process. Several growth factors that are released at the wound site are presumed to be necessary for wound healing. These include epidermal growth factor (EGF), fibroblast growth factor (FGF), insulin-like growth factor (IGF), keratinocyte growth factor (KGF), platelet-derived growth factor (PDGF), transforming growth factor (TGF) and vascular endothelial growth factor (VEGF). Growth factor is generally used in a broad sense, to indicate substances which increase cell proliferation, mitogenic activity, and extracellular matrix formation. However, the action of growth factors does not end with wound closure and tissue remodelling (Grazul-Bilska, et al., 2003).

Recent advances in many of the wound dressing used delivery system of growth factors that are relevant to the wound healing process, i.e., PDGF-BB (Li, et al., 2009), FGF-2 (Obara, et al., 2003), bFGF (Liu, et al., 2007), rhEGF (G, et al., Mar-Apr 2012), SDF-1 (PW, et al., 2011), rhGM-CSF (RW and JA., 2000). Several growth factors, including PDGF, FGF-2, IGF and KGF, have been used in clinical trials, and PDGF is currently approved for use in human medicine (Pierce, et al., 1991).

2.3.1 Granulocyte-macrophage colony-stimulating factor



MW. 14434.5 g/mol

Figure 4 Molecular structure of granulocyte-macrophage colony-stimulating factor

Granulocyte-macrophage colony-stimulating factor (GM-CSF) is a protein secreted by macrophages, T cells, mast cells, NK cells, endothelial cells and fibroblast. GM-CSF has been shown to enhance the number of mechanisms essential to wound healing (RW, et al., 2000) (Figure 4).

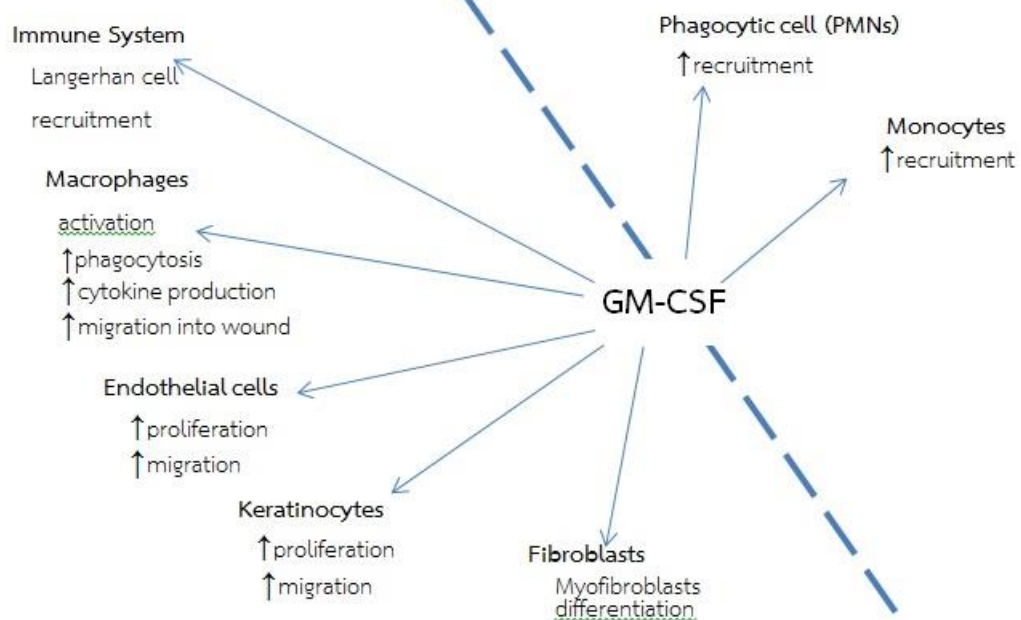


Figure 5 Actions of GM-CSF on components of the wound healing process

In vivo studies, GM-CSF stimulates α -SM actin synthesis in myofibroblasts (Rubbia-Brandt, et al., 1991), thereby facilitating wound contraction. Enhancement of keratinocytes growth, the selective recruitment of Langerhans cells into the dermis (Kaplan, et al., June 1992), causes local recruitment of inflammatory cells, activated mononuclear phagocytes, promote migration of epithelial cells and regulated cytokine production (Smith, et al., 1998).

The systematic review of topically applied rhGM-CSF in clinical study has reported to successfully treat wounds with diverse etiology (Hu, et al., 2011)(Table 1)

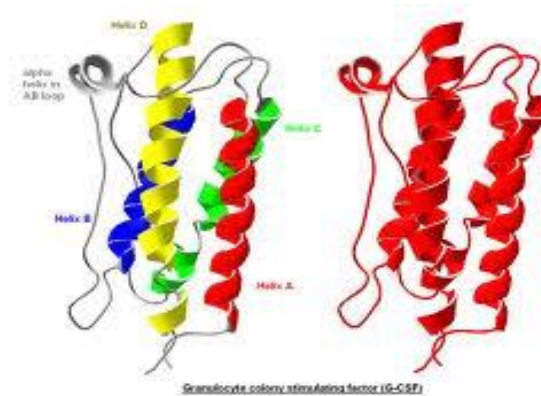


Studies	Sample ^a age gender	Primary study aim	Wound category	Dosage of GM-CSF and administration	Key finding
Robson et al. [44]	15 + 15* Total 61 28-70 years	To compare the healing response of sequential, topically applied GM-CSF bFGF to that of each cytokine alone and to a placebo in pressure ulcers	Pressure ulcer on the truncal area (grade III/IV); ulcer duration >8 weeks; initial ulcer volume 10-200 cm ²	2.0 µg/cm ² GM-CSF topically applied daily for 35 days; 5.0 µg/cm ² bFGF topically applied daily for 35 days; 2.0 µg/cm ² GM-CSF applied for 10 days, followed sequentially by 25 days of topically applied 5.0 µg/cm ² bFGF; or the comparative placebo, applied daily for 35 days Ditto	Ulcers treated with cytokines had greater closure than those in placebo-treated patients. Patients treated with bFGF alone did the best, followed by the GM-CSF/bFGF group. But the GM-CSF alone had no effect in terms of ulcer volume wound closure compared to placebo on day 36 No differences were seen among the four treatment groups during the follow-up phase of the trial
Payne et al. [45] The successive study of Robson et al. [44]	14 + 14 (Original size = [54] [51]) 28-70 years	Long term outcome of the pressure ulcer treated by cytokines	Ditto	Ditto	
Santos et al. [54]	10 + 10 28 vs 29 years	To assess topically applied GM-CSF as an adjunct to antimicrobial therapy for cutaneous Leishmaniasis ulcers	Cutaneous Leishmaniasis ulcers	GM-CSF was diluted for topical use and was applied 3 times weekly for 3 weeks (1-2 µg/cm ² /lesion)	The mean healing time was 43 days in the GM-CSF group and was 104 days in the placebo group. Ten (100%) of 10 patients in the GM-CSF group healed within 60 days, compared with 5 (50%) of 10 patients in the placebo group The median wound healing time was 17 days in GM-CSF group, which was obviously shorter than that in placebo group (20 days). The mean wound healing rate in GM-CSF group was 24.5%, 70.5%, 95.3%, 99.5% respectively on 8th, 14th, 20th, 28th day after treatment, which were obviously higher than that in placebo group (15.1%, 51.4%, 84.6%, and 97.1%, respectively)
Wang et al. [48]	200 (214) + 102 (107) 18-65 years	To evaluate the efficacy and safety of recombinant rhGM-CSF hydrogel in wound healing in patients with deep partial thickness burn	Deep second degree burn with total body surface area burn <50%	rhGM-CSF hydrogel 100 µg/100 cm ² /day, topically applied	Time for complete healing day in GM-CSF group 14.71 vs control group 20.48; the total healing reached 100% in first group as compare to 96.67 in control group at 28-day point
Zhang et al. [35]	56(50) + 27(30) 33 67 vs 36 9 years m/f 54/6 vs 21/9	To evaluate the efficacy and safety of recombinant rhGM-CSF hydrogel in wound healing in patients with deep partial thickness burn	Deep second degree burn with total body surface area burn <50%	rhGM-CSF hydrogel 100 µg/100 cm ² /day, topically applied	Time for complete healing day in GM-CSF group 14.71 vs control group 20.48; the total healing reached 100% in first group as compare to 96.67 in control group at 28-day point

* Data are presented as final events of experiment (original events) + final events of control (original events); m: male; f: female.

Table 1 The clinical study of topically applied rhGM-CSF in patients with different type of wound

2.3.2 Granulocyte colony-stimulating factor



MW. 19,600 g/mol

Figure 6 Structure of granulocyte colony-stimulating factor

Granulocyte colony-stimulating factor (G-CSF), a 19.6 kDa glycoprotein consisting of 174 amino acid residue, is an antiparallel four- α -helix bundle (Lieschke and Burgess, 1992). It is subgroup in hematopoietin family as GM-CSF. In this study, G-CSF was used as a model growth factor instead of GM-CSF because it has similar structure with GM-CSF and commercially available in Thailand.

2.4 Sterilization methods

Typical methods used to sterilize wound dressing are ethylene oxide gas sterilization, gas plasma technology, steam sterilization and ionizing radiation. Many of biomaterials are made from natural polymers and the active substances incorporated that are all thermal sensitive, choosing the low temperature sterilization methods would be a reason.

2.4.1 Ionizing radiation

Sterilization by ionizing radiation is a low-temperature sterilization method that has been used for many kinds of medical products. Gamma radiation and electron beams are used to effect ionization of the molecules in organisms. Gamma rays are formed with the self disintegration of Cobalt-60 or Cesium-137

sources. Mutations are thus formed in the DNA and these reactions alter replication. These processes are very dangerous and only well-trained and experienced staff should decide upon the desirability of their use and should ensure monitoring of the processes. Specially designed and purpose-built installations and equipment must be used. It is usual to select an absorbed radiation level of 25 kiloGray (kGy) or 2.5 megarad (Mrad), although other levels may be employed provided that they have been validated. The bio-indicator strains proposed for validation of this sterilization process are: spores of *Bacillus pumilus* (e.g. ATCC 27142 or CIP 77.25) with 25 kGy (2.5 Mrad) for which the D-value is about 3 kGy (0.3 Mrad) using 10^7 - 10^8 spores per indicator; for higher doses, spores of *Bacillus cereus* (e.g. SSI C 1/1) or *Bacillus sphaericus* (e.g. SSI C₁A) are used .

The action of radiation on microorganisms can be divided into direct and indirect effects. The indirect effects occur as an important part of the total action of radiation. The mainly formed radiolytic products of water molecules yielding radicals $\text{OH}\cdot$, e^-_{aq} and $\text{H}\cdot$ (Figure 6). The action of hydroxyl radical responsible for an important part of the indirect effect. Drying or freezing of living organisms can reduce these indirect effects. The gamma radiation interacts with water, leading to the formation of free radicals that can diffuse far enough to reach and damage DNA. These radicals formed in the hydration layer around DNA molecule are responsible for 90% of DNA damage. The direct effect is a consequence of the ionizing action of the high energy radiation. It is estimated that the irradiation of a living cell at one gray induces 1000 single strand breaks, 40 double strand breaks, 150 cross-links between DNA and proteins and 250 oxidations of thymine

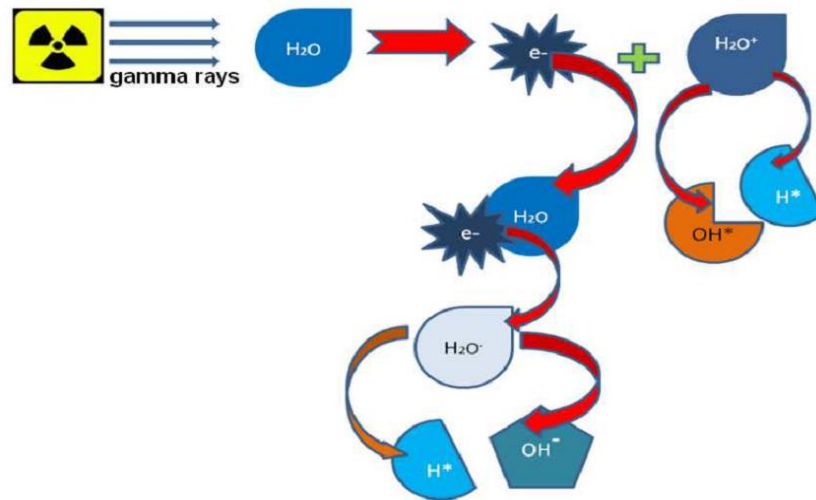


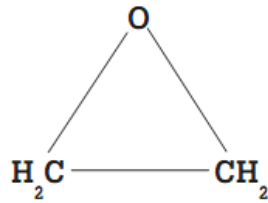
Figure 7 Effect of gamma radiation on water molecules

The gamma irradiation process does not create residuals. Complete penetration can be achieved depending on the thickness of material. It supplies energy saving and needs no chemical or heat dependence. Radiation doses should be monitored with specific dosimeters during the entire process. Dosimeters should be calibrated against a standard source on receipt from the supplier and at appropriate intervals thereafter. The radiation system should be reviewed and validated whenever the source material is changed and, in any case, at least once a year.



Figure 8 Gamma Irradiator (GC-5000)

2.4.2 Ethylene oxide gas



Ethylene oxide (EO) has been widely used as a low-temperature sterilant since the 1950s. EO is a colourless gas that is flammable and explosive. The operating ranges are gas concentration (450 to 1200 mg/l), temperature (37 to 63 °C), relative humidity (40 to 80%) and exposure time (1 to 6 hours). Within certain limitations, an increase in gas concentration and temperature may shorten the time necessary for achieving sterilization. The basic EO sterilization cycles consists of five stages ; preconditioning, gas introduction, exposure, evacuation and air washes. Mechanical aeration for 8 to 12 hours at 50 to 60 °C allows desorption of the toxic EO residual contained in exposed absorbent materials. Ambient room aeration also will achieve desorption of the toxic EO but requires 7 days at 20 °C



Figure 9 Ethylene oxide gas sterilizer (3M-Sterivac)

The microbicidal activity of EO is considered to be the result of alkylation of protein, DNA and RNA. Alkylation within cell prevents normal cellular metabolism and replication. EO inactivates all microorganisms although bacterial spores especially *Bacillus atrophaeus* are more resistant than other microorganisms. For this reason *Bacillus atrophaeus* is the recommended biological indicator.

The main advantage is that it can sterilize heat or moisture sensitive medical equipment without deleterious effects on the material used in the medical devices. However, long term used may subject to cumulative toxic substances, ethylene chlorohydrins and ethylene glycol, and ethylene oxide can deposit in the porous devices (Mendes, et al., 2007).

2.4.3 Hydrogen peroxide gas plasma

Hydrogen peroxide gas plasma sterilization technology was patented in 1987 and marketed in the United States in 1993. Gas plasmas have been referred to as the fourth state of matter; liquids, solids, gases and gas plasma. Gas plasmas are generated in an enclosed chamber under deep vacuum using radio frequency or microwave energy to excite the gas molecules and produce charged particles, many of which are in the form of free radicals.

The hydrogen peroxide vapor diffuses through the chamber (50 minutes) and initiates the inactivation of microorganisms. An electrical field created by a radio frequency is applied to the chamber to create gas plasma. Microbicidal free radicals (e.g., hydroxyl and hydroperoxyl) are generated in the plasma. The excess gas is removed and in the final stage of process the sterilization chamber is returned to atmospheric pressure by introduction of high-efficiency filtered air. The by-products of the cycle, water vapor and oxygen, are nontoxic and no need for aeration period (Calvet, et al., 2008). Materials and devices that cannot tolerate high temperatures and humidity, such as some plastics, electrical devices, and corrosion-susceptible metal alloys, can be sterilized by hydrogen peroxide gas plasma. This method has been compatible with most (>95%) medical devices and materials.

Production of free radicals within a plasma field that are capable of interacting with essential cell component and thereby disrupt the metabolism of microorganisms.



Figure 10 Hydrogen peroxide gas plasma sterilizer (Sterrad 100s)

The main advantage is the process produce nontoxic by product that comprise of water vapor and oxygen therefore no need for aeration period. However, disadvantage of this method are high cost of operation cycle and hydrogen peroxide gas plasma must be used with porous packaging and the choice is usually Tyvek, spunbonded polyethylene. It is not advisable to use paper in gas plasma sterilization because cellulose can absorbed the sterilant.

CHAPTER III

MATERIALS AND METHODS

Materials

1. Polysaccharide Gel Extract from Durian Fruit-Hulls
2. Polyvinyl Alcohol MW. 89,000-98,000 and degree of hydrolysis 99+% (Lot no. MKBC4420, Sigma-aldrich, USA)
3. G-CSF (Lot no. A5A1B, Granocyte, Chugai Pharmaceutical, Japan)
4. G-CSF Human ELISA kit (ab100524, abcam, USA)

Equipments

1. Ethylene oxide sterilizer (3M Steri-Vac, USA)
2. Gamma Irradiator (GC 5000, BRIT, India)
3. Hydrogen peroxide gas plasma sterilizer (Sterrad 100S, USA)
4. Analytical balance (AG204, Mettler Toledo, Switzerland)
5. Analytical balance (PB3002, Mettler Toledo, Switzerland)
6. Critical point dryer (Balzers Union CPD 020, Liechtenstein)
7. Differential scanning calorimetry (DSC) (DSC822^e, Mettler Toledo, Switzerland)
8. Freezer (FC-27, Sharp, Thailand)
9. Fourier transform infrared spectrometer (Spectrum one, Perkin-Elmer)
10. Hot air oven (Memmert, Germany)
11. Hotplate stirrer (HTS-1003, LMS, Japan)

12. Lyophilizer (Lyolab. USA)
13. pH meter (Model 210A+, Thermo Orion, Germany)
14. Refrigerator (Hitachi, Japan)
15. Rotary evaporator (R-220, Buchi, Switzerland)
16. Scanning electron microscope (JSM-5410 LV, JEOL, Japan)
17. Viscometer (DV-I, Brookfield, USA)

Methods

3.1 Preparation of polysaccharide gel extract from durian fruit-hulls

Polysaccharide gel extract from durian fruit-hulls (Lot N01) were prepared as described previously (Pongsamart and Panmaung, 1998). Briefly, ground fresh fruit rinds were dried in hot air oven at 50 °C. The dried material was extracted with water pH 4.5 (adjusted with citric acid) and heated at 90-100 °C for 20 minutes. The water extract was concentrated under reduced pressure at 70 °C and the gel-like precipitate was obtained by addition of acidified aqueous ethanol at room temperature. The precipitate was washed twice with 75% ethanol and 95% ethanol, then dried successively by hot air oven at 50 °C , grounded and sieved. The DG lot N01 was studied for pH and viscosity in 3% solution and the powder for FTIR and DSC compared to previous lot of M81.

3.2 Preparation of polysaccharide gel from durian fruit-hulls and polyvinyl alcohol hydrogel dressing

3.2.1 Preparation of DG/PVA hydrogels

3.2.1.1 Preparation of wet-form DG/PVA hydrogels (DG/PVA-W)

In this study, hydrogels were made from 2 %w/w DG and 5 %w/w PVA (DG/PVA, 2 : 5) in water using following freeze-thaw conditions: freezing at -20°C for 24 hours and thawing at 30°C for 24 hours (Eakwaropas, 2009). PVA powder was dissolved in deionized water and heated up to 90°C for 60 min to achieve complete dissolution. DG powder was completely swollen in deionized water at room temperature (RT). The PVA 10% w/w and the DG 4% w/w solutions were mixed with a ratio of 50 : 50. The mixing solution was poured into a plastic mold at the thickness of 3.5 mm and sealed. The viscous solution was frozen at -20°C for 24 hours followed by thawing at 30°C for 24 hours and repeated the freezing-thawing until 3 cycles to form a hydrogel dressing.

3.2.1.2 Preparation of dried-form DG/PVA hydrogels (DG/PVA-F)

Dried-form DG/PVA hydrogels were prepared using wet-form hydrogel and dried by freeze-drying technique. The freeze-drying condition comprising of extra freeze at -20°C for 2 hours vacuum 1,000 MT, primary drying; from -20°C to 30°C increased 10°C for each step in 180 minutes vacuum 1,000 MT and secondary drying at 20°C for 2 hours vacuum 900 MT. Both wet-form and dried-form hydrogels were characterized for physical properties in 3.4.

3.2.2 Preparation of G-CSF loaded polysaccharide gel from durian fruit-hulls and polyvinyl alcohol hydrogel dressing

G-CSF loaded hydrogels were prepared both wet (G-DG/PVA-W) and dried-form (G-DG/PVA-F) hydrogels. Prepared the mixing solution of DG and PVA as described in 3.2.1.1 and added G-CSF to the mixture (amount of $2\ \mu\text{g}/\text{cm}^2$ of hydrogel) before adjust the weight of mixed hydrogel. Continue stirred the mixing solution for 1 hour. The mixing solution was poured into a plastic mold at the thickness of 3.5 mm and sealed. The viscous solution was frozen at -20°C for 24 hours followed by thawing at 30°C for 24 hours and repeated the freezing-thawing

until 3 cycles to form a G-CSF loaded hydrogel dressing. Dried-form of G-CSF loaded hydrogels were prepared as 3.2.1.2.

Both of wet and dried forms of G-DG/PVA hydrogels were characterized physicochemical properties of SEM, FTIR and DSC as described in 3.4 and were studied protein conformation determination and protein release assay as described in 3.7.

3.3 Physicochemical characterization

3.3.1 Scanning Electron Microscopy (SEM)

The morphology study of the DG/PVA hydrogel were studied by Scanning Electron Microscope JEOL model JSM-5410W. The wet hydrogel was cut into small pieces and dehydrated before testing by using Critical Point Dryer (CPD). In brief, each piece of hydrogel was soaked and swirled in 30% ethanol for 30 minutes, then soaked and swirled in 50% , 70% and 95% ethanol for 30 minutes, respectively. Finally soaked in absolute ethanol for 10 minutes in triplicate. The sample was put in CPD to remove absolute ethanol by liquid carbon dioxide under critical point. Then liquid carbon dioxide changed into gaseous state under ambient condition, the sample was immediately dried with no collapsed in surface or its structure. The hydrogels were sputter coated with gold prior examination. Micrographs were recorded at magnifications 200X. The hydrogel surface and its cross-section were determined at 15 kV.

3.3.2 Water content

DG/PVA hydrogel in identical size (round shape diameter 2.82 cm, area 6.243 cm²) was dried in hot air oven at 50 °C until having constant weight (W_d). Water content in the hydrogel was calculated by equation (1) (Kaplan, et al., 2000).

$$\text{Water content (\%)} = \frac{W_o - W_d}{W_o} \times 100 \quad (1)$$

3.3.3 Gel fraction

Dried hydrogel from 3.4.2 was soaked in excess of deionized water for 4 days (Sirousazar, et al., 2011) then swollen hydrogel was dried until having constant weight as 3.4.2. Gel fraction was calculated by equation (2).

$$\text{Gel fraction (\%)} = \frac{W_e}{W_o} \times 100 \quad (2)$$

Where :

W_e is the dried weight correlated to one gram of initial hydrogel after soaking in deionized water.

W_o is the dried weight correlated to one gram of initial hydrogel before soaking in deionized water.

3.3.4 Water absorption capacity

DG/PVA hydrogel in identical size (round shape diameter 2.82 cm, area 6.243 cm²) was soaked in excess of deionized water at room temperature for 4 days. The swollen hydrogel was wiped gently to remove excess surface water using filter paper and weighed at various time points. The water absorption capacity was calculated by equation (3) (Francis, et al., 2009).

$$\text{Water absorption (\%)} = \frac{W_s - W_o}{W_o} \times 100 \quad (3)$$

Where :

W_s is the weight of the swollen hydrogels.

W_o is the initial weight of hydrogels (before soaking in water).

3.3.5 Fourier transform infrared spectroscopy (FTIR)

FTIR of DG, PVA and DG/PVA hydrogel were examined using a Perkin Elmer Spectrum One fitted with a universal ATR sampling accessory. All data were recorded at 25 °C, in the spectral range of 4000-515 cm⁻¹, utilizing a 16 scan per sample cycle.

3.3.6 Differential Scanning Calorimetry (DSC)

The DSC analysis was performed using Mettler Toledo DSC822^e. Dry hydrogels 1-3 mg were heated from 25 to 400 °C under N₂ atmosphere (60 mL/min) with a heating rate of 10 °C/min.

3.3.7 Mechanical properties

For wet-form hydrogel, the membrane was cut into specific shape (2 cm wide at the end and 1 cm wide in the middle). The mechanical data were measured using Universal tensile testing machine (Shimadzu) 500 N with a constant crosshead speed of 20 mm/min at room temperature (Oliveira, et al., 2014).

For dried-form hydrogel, the hydrogel was immersed in deionized water for 12 hrs. Then the membrane sample was cut into the specific shape and measured by the same instrument and conditions as previously described.

3.4 Selection of hydrogel packaging materials

Four plastic packaging materials were studied for all sterilization methods and selected for experiment. Specific type of Spunbonded polyethylene (Tyvex[®]) for each gaseous sterilization methods was used as control packaging. The studied was done by inserting specialized biological indicator in the pouches of different packaging materials following guidance for industry and FDA staff-biological indicator (510(k)).

3.4.1 Low density polyethylene (LDPE)

Two types of LDPE were studied, Thin type (LDPE-Thn) with thickness 0.05 mm and thick type (LDPE-Thk) with thickness 0.11 mm.

3.4.2 High density polyethylene (HDPE)

Two types of HDPE were studied, Thin type (LDPE-Thn) with thickness 0.03 mm and thick type (LDPE-Thk) with thickness 0.09 mm.

3.4.3 Linear low density polyethylene laminated Nylon (LLDPE/Nylon) with thickness 0.11 mm.

3.4.4 Polyethylene terephthalate laminated Nylon and Metallite (PET/Nylon/Metallite) with thickness 0.09 mm.

3.5 Sterilization methods for hydrogel dressings

3.5.1 Gamma irradiation

The hydrogel dressings were packed in the selected packaging and studied for gamma irradiation sterilization. Wet-form hydrogels were studied with gamma radiation dose of 10, 15, 20 and 25 kGy. Dried-form hydrogels were studied with gamma radiation dose of 15 and 25 kGy. The condition was operated at room temperature and a dose rate of 4.4 kGy/hr.

3.5.2 Ethylene oxide gas sterilization

Ethylene oxide gas sterilization was studied only for the dried-form hydrogels. The condition was operated at 55 °C for 2 hours and aeration time for vacuum of the ethylene oxide gas residual for 24 hours. For wet-form hydrogels this sterilization method was not suitable due to the residual of ethylene oxide gas was much deposited in moisture hydrogel.

3.5.3 Hydrogen peroxide gas plasma sterilization

Hydrogen peroxide gas plasma sterilization was studied only for the dried-form hydrogels. The condition was operated at temperature less than 55 °C for 54 minutes. This sterilization method was limited using only for dried samples.

Both unloaded and loaded G-CSF hydrogels were sterilized as described above. After passing each sterilization process, DG/PVA hydrogels were characterized physicochemical properties as described in 3.3 but G-CSF loaded hydrogels were characterized for SEM, FTIR and DSC. Both unloaded and loaded G-CSF hydrogels were tested for sterility in 3.6.

3.6 Sterility testing

The hydrogels were immediately tested for sterility after each sterilization methods. Samples were immersed in a soybean casein digest broth for cultivation of microorganism and incubated at 37°C for 5 days. Non-sterilized samples were used as positive controls and the media were used as negative control. Clouding of broth after 5 days indicated contamination and inefficient sterilization.

3.7 Preliminary study of G-CSF release from hydrogel dressings

A piece of hydrogel dressing incorporated G-CSF in identical size (round shape diameter 2.82 cm, area 6.243 cm²) (before and after sterilization) and DG/PVA hydrogel using as control were immersed in 10 ml PBS buffer pH 7.4 in conical tube and shaking 100 rpm at 37°C. Aliquots of 1 ml solution medium were withdrawn and replaced with fresh PBS 1 ml at predetermined time intervals. The aliquot solutions were subjected to centrifuge at 7500g for 10 min and determined the amount of G-CSF by enzyme-linked immunosorbent assay (see Appendix).

3.8 Statistical analysis



The results were analyzed by Independent-sample T-Test and One-way ANOVA . Test of normality and homogeneity of variances were performed.

CHAPTER IV

RESULT AND DISCUSSION

4.1 Properties of powder extract polysaccharide gel from durian fruit-hulls

Table 2 Properties of DG powder extract

Lot number	Appearance	pH	Viscosity (cps)
M81 (L-II)		2.38	292 (S18 ; 10.0 RPM , 96.8%)
N01		2.32	421 (S18 ; 6.0 RPM , 84.0%)

CHULALONGKORN UNIVERSITY

The powder extract of durian fruit-hulls polysaccharide gel (Lot N01) was characterized its viscosity, pH, FTIR and DSC compared to previous lot (M81, L-II). It was found that the appearance of DG powder lot N01 was fine powder with brown color as similar to lot M81. The viscosity of 3% DG solution was 421 cps whereas M81 was 292 cps, it might be due to polysaccharide chain hydrolysis after long time storage (Chen, et al., 2014). The pH of DG lot N01 was 2.32 similar to lot M81 which was 2.38.

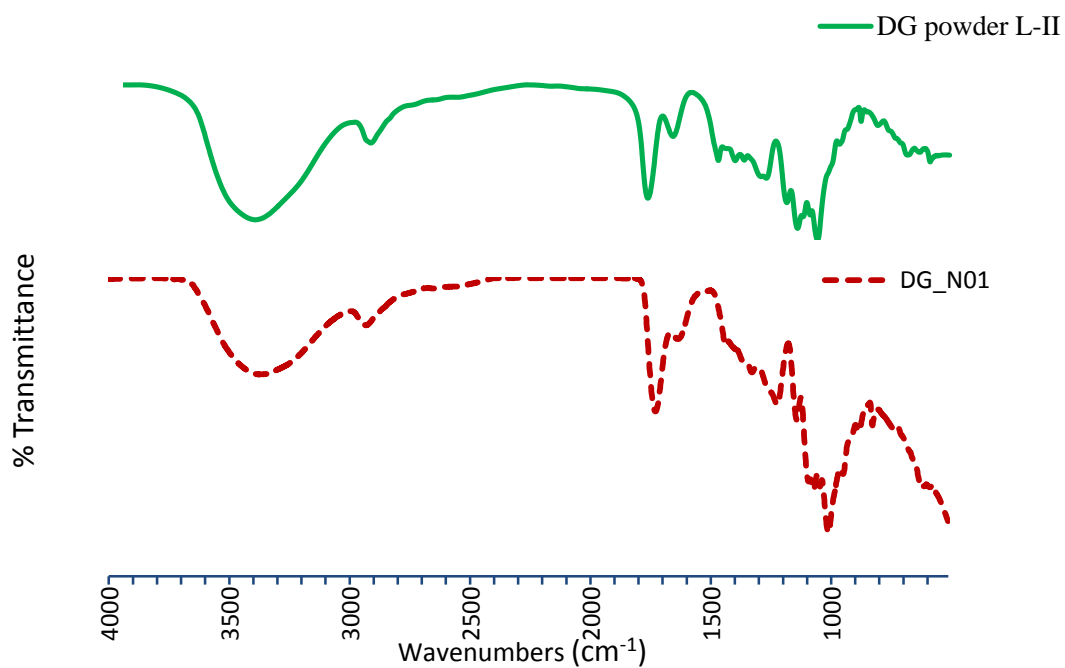


Figure 11 FTIR spectra of DG powder lot M81 (lot L-II in the previous study) and lot N-01

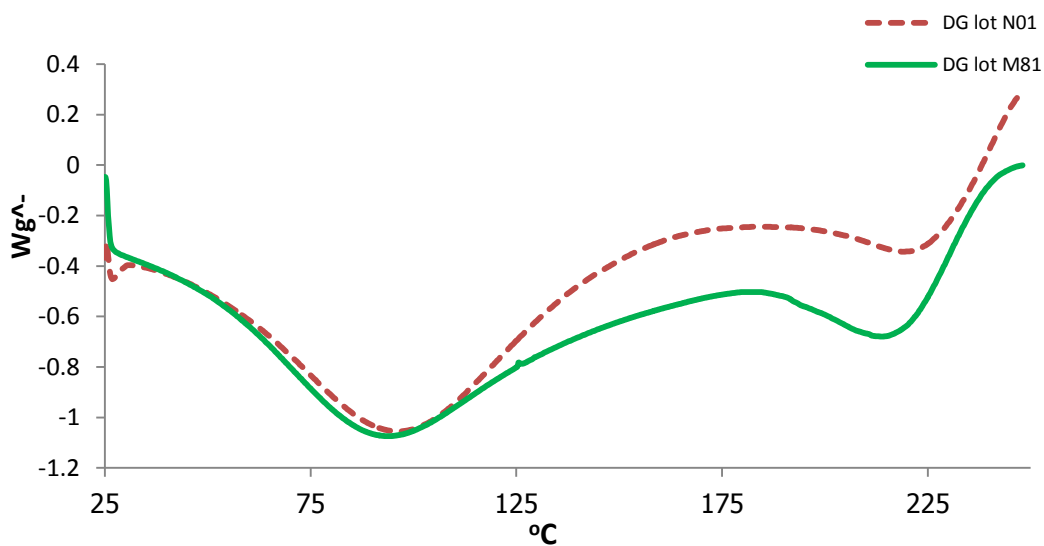

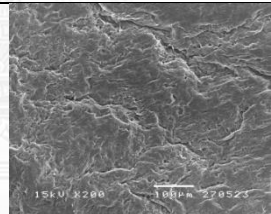
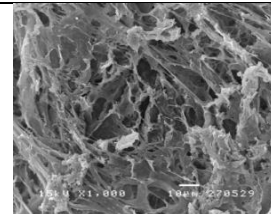

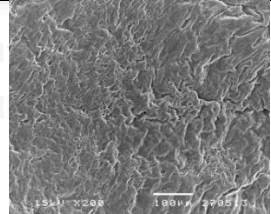
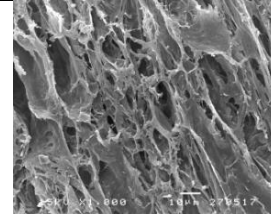

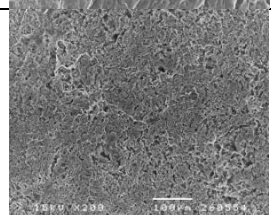
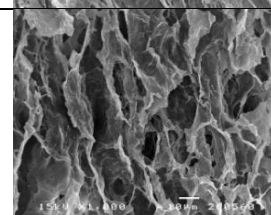

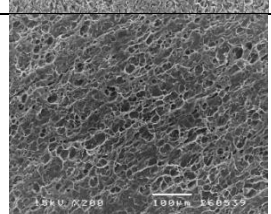
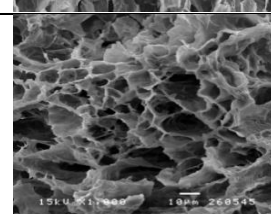


Figure 12 DSC thermograms of DG powder lot M81 (lot L-II in the previous study) and lot N-01

FTIR was used to characterize the functional group in both two lots of DG powder, lot M81 and lot N01. FTIR spectrum in Figure 11 showed the important absorption bands, broad peak at wavenumber $3477\text{--}3328\text{ cm}^{-1}$ indicated OH stretching, alkyl stretching (R-CH_2) peak was founded at 2966 cm^{-1} and strong sharp peak of carbonyl group (C=O) associated with aldehyde group was appeared at 1743 cm^{-1} . Thermal analysis of DG powder in Figure 12 showed similar curves. Therefore both lot of DG powder are chemically identical.

4.2 Physicochemical properties of DG/PVA hydrogels

Table 3 Morphology of DG/PVA hydrogels

Hydrogel	Appearance	Surface (x200)	Cross-section (x1000)
DG/PVA-W			
G-DG/PVA-W			
DG/PVA-F			
G-DG/PVA-F			

The morphology of wet and dried-form DG/PVA hydrogels with G-CSF loaded and unloaded before sterilization were studied as showed in Table 3. The wet-form G-CSF loaded and unloaded hydrogel had similar appearance that light brown color and flexibility. SEM photographs of the hydrogels showed similar appearance of surface and internal structure. The appearance of dried-form hydrogel showed opaque, light brown color and stiffness. SEM of dried-form hydrogel both loaded and unloaded G-CSF had pores on the surface and cross-section had more porosity than wet-form hydrogel.

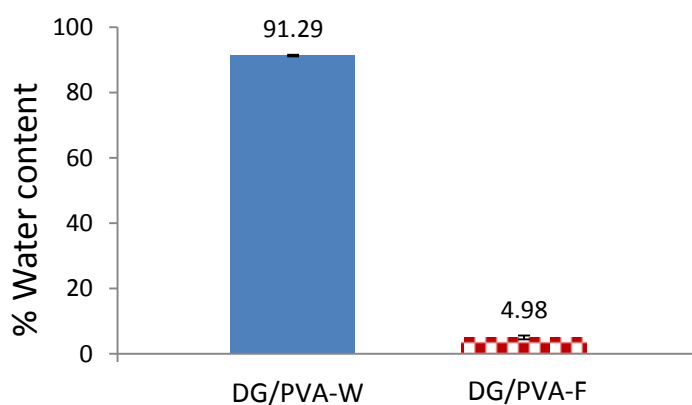


Figure 13 Water content of wet and dried-form DG/PVA hydrogels

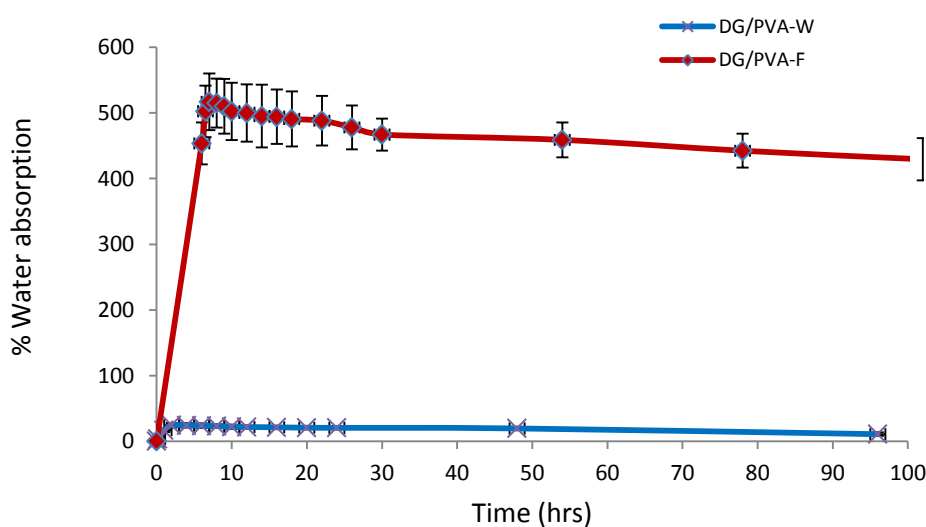


Figure 14 Water absorption capacity of wet and dried-form DG/PVA hydrogels

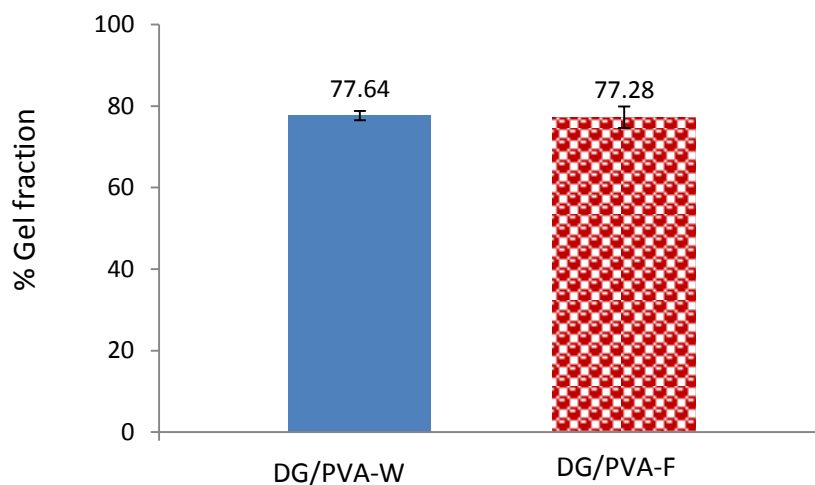


Figure 15 Gel fraction of wet and dried-form DG/PVA hydrogels

The water content, water absorption capacity and gel fraction of wet and dried-form DG/PVA hydrogels were studied as showed in Figure 13-15, respectively. Water content of wet-form hydrogel was $91.29 \pm 0.22\%$ and dried-form hydrogel was $4.98 \pm 0.61\%$. Water absorption capacity of the dried-form hydrogel was $516.91 \pm 43.19\%$ within 7 hours which was much higher than the wet form hydrogel, $24.36 \pm 3.35\%$ in 2 hours (Figure 14). Due to dried-form hydrogel had very low water content (less than 5%) and could reswelled and retained water more than 500% of dried weight while the wet-form had more water content. From Figure 15, Gel fraction of wet and dried-from hydrogels were $77.64 \pm 1.15\%$ and $77.28 \pm 2.61\%$, respectively. There was different between the gel fraction of wet and dried-form DG/PVA hydrogels.

Table 4 Mechanical properties of wet and dried-form DG/PVA hydrogels

Hydrogel	Young's Modulus (N/mm ²)	% Elongation	Tensile strength (MPa)
DG/PVA-W	0.033 ± 0.004	580.997 ± 85.056	0.143 ± 0.039
DG/PVA-F	0.051 ± 0.005	577.574 ± 42.934	0.261 ± 0.045

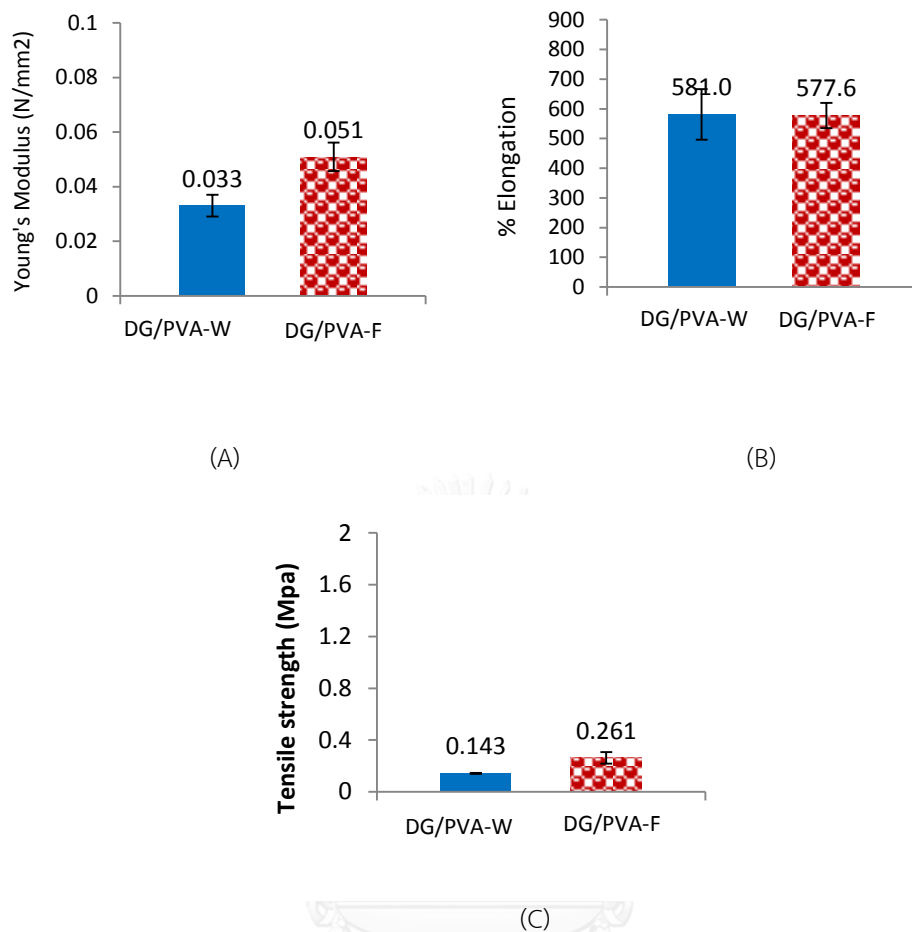


Figure 16 Mechanical properties of wet and dried-form DG/PVA hydrogels (A) Young's Modulus (B) % Elongation (C) Tensile strength

The mechanical properties of wet and dried-form hydrogels were studied as showed in Figure 16. Young's modulus and Tensile strength of dried-form hydrogel were increased significantly compared to the wet-form [$t(9) = -3.09$, $p = 0.013$ and $t(9) = -2.48$, $p = 0.035$] whereas percent of elongation was not different. The result implied that freeze drying method for preparing the dried-form hydrogel increased stiffness and hydrogel strength while was not affected elongation property of the hydrogel.

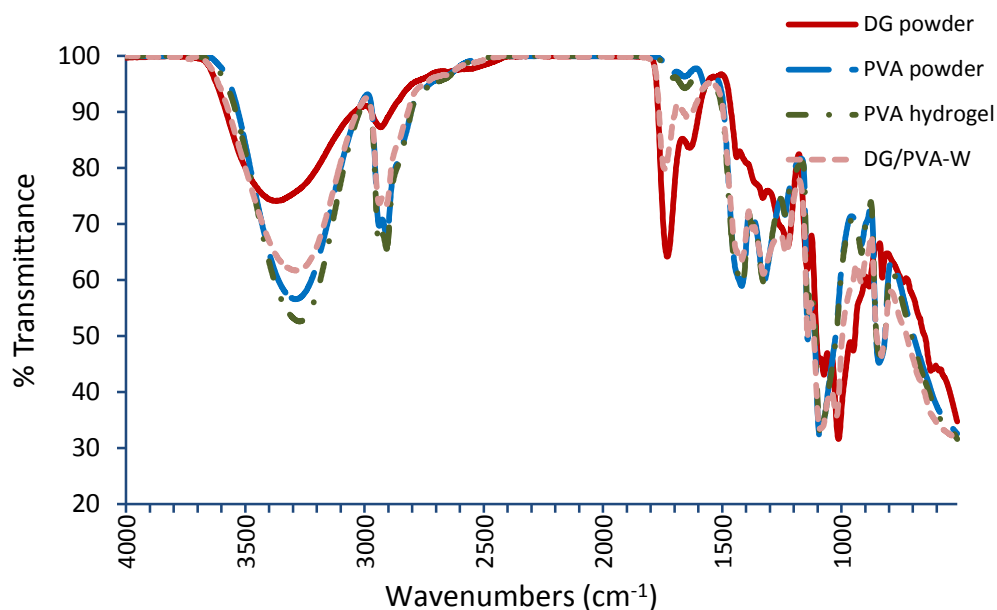
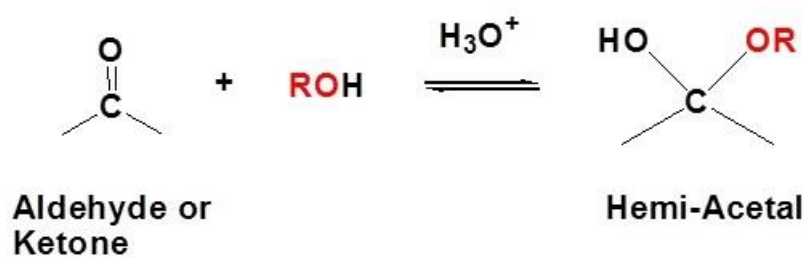


Figure 17 FTIR spectra of DG and PVA raw materials and PVA and DG/PVA hydrogels

From FTIR spectrum of PVA powder depicted in Figure 17 showed a peak of OH stretching at about 3324 cm^{-1} indicating the presence of the hydroxyl group that was the functional group of PVA. The hydrogel of PVA gave the FTIR spectrum pattern as same as the PVA powder. However, mixing DG with PVA to form a DG/PVA hydrogel changed the pattern of FTIR spectrum. It could be observed that the peak intensity of carbonyl group (1752 cm^{-1}) was decreased while the intensity of OH stretching (3351 cm^{-1}) and C-H stretching (2947 and 2938 cm^{-1}) were increased when compared to the FTIR spectrum of DG powder. According to this observation, it could be proposed that the hydroxyl group of PVA undergo the nucleophilic addition with the aldehyde group of DG to form the corresponding hemiacetal especially in acid catalysts condition as shown in the reaction below (Azofra, et al., 2012).



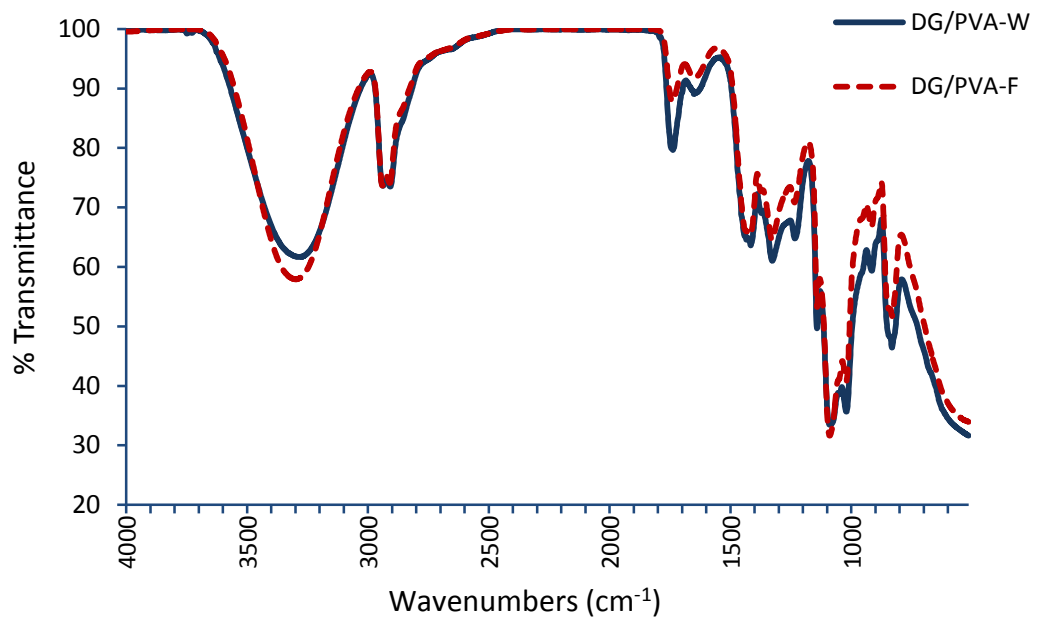


Figure 18 FTIR spectra of wet and dried-form DG/PVA hydrogels

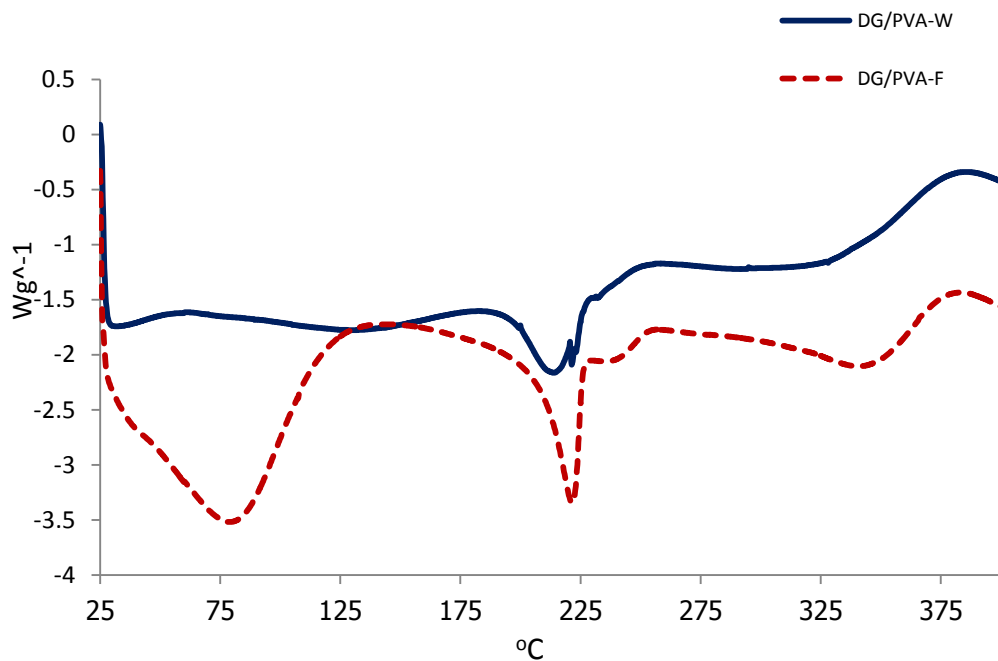


Figure 19 DSC thermograms of wet and dried-form DG/PVA hydrogels

FTIR and DSC studied of wet and dried-form hydrogels were showed in Figure 18 and 19. FTIR spectrum of dried-form hydrogel showed decreasing the peak

intensity of carbonyl group at 1751 cm^{-1} and increasing peak intensity of hydroxyl group at 3351 cm^{-1} . It might be the result of dehydration from the hydrogel then affected the equilibrium of hemiacetal reaction as discussed above. Dehydration referred to loss of hydroxyl group from equilibrium reaction therefore in acid catalysts condition hemiacetal decomposing to maintain equilibrium constant. The reverse of acetal formation was shown below. From DSC curves showed the endothermic peak of PVA were at the same region (Huang, et al., 2009).

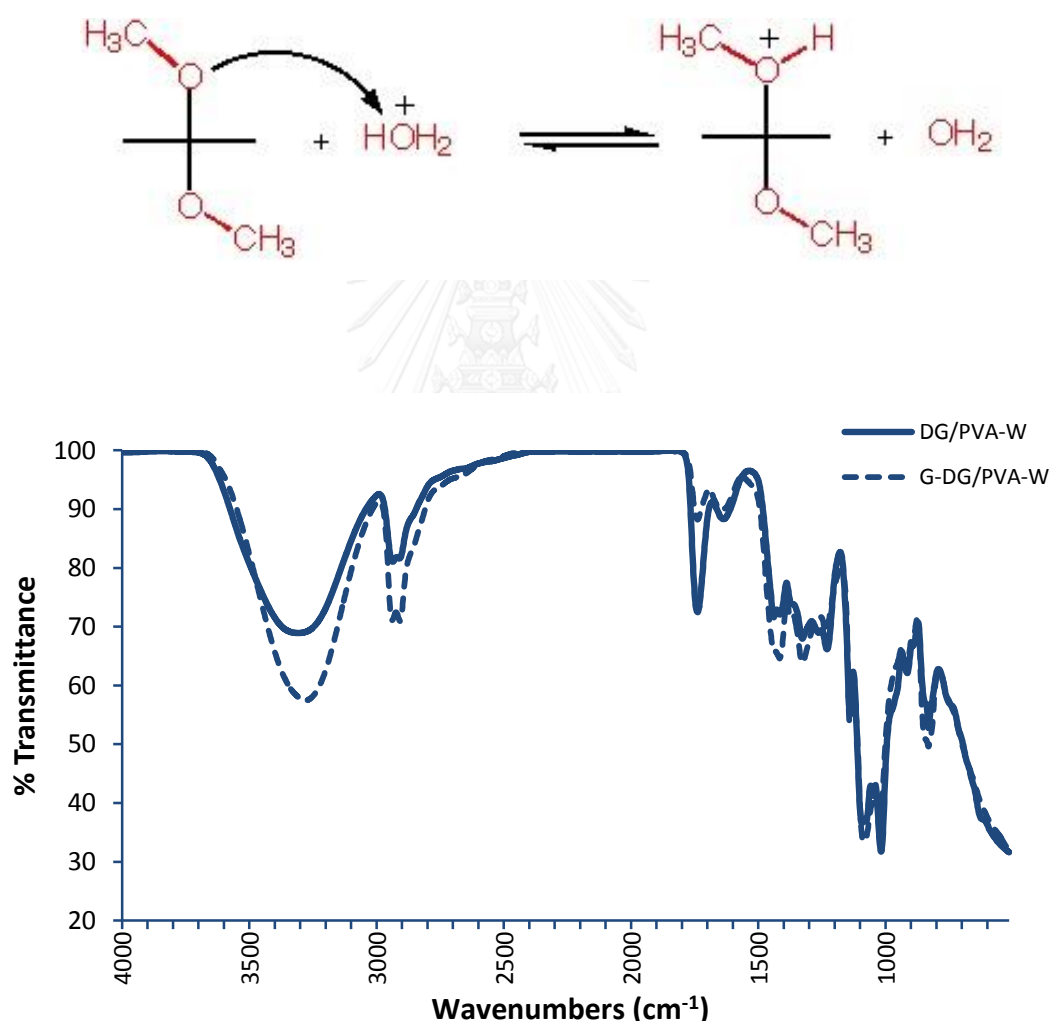


Figure 20 FTIR spectra of wet-form DG/PVA with G-CSF loaded and unloaded hydrogels

The wet-form hydrogels with G-CSF loaded and unloaded were studied for FTIR as showed in Figure 20. There were the decreasing in the peak intensity of carbonyl groups (at 1749 cm^{-1}) and the increasing in the band intensity of hydroxyl

group (at 3312 cm^{-1}) and alkyl groups (at 2948 and 2943 cm^{-1}) in the FTIR spectrum of G-CSF loaded hydrogel compared to the solely DG/PVA hydrogel. This phenomenon might take place due to the additional reaction between DG aldehyde group and PVA OH group or the reaction between the OH containing amino acid residues in G-CSF and the aldehyde group of DG to form the additional hemiacetal.

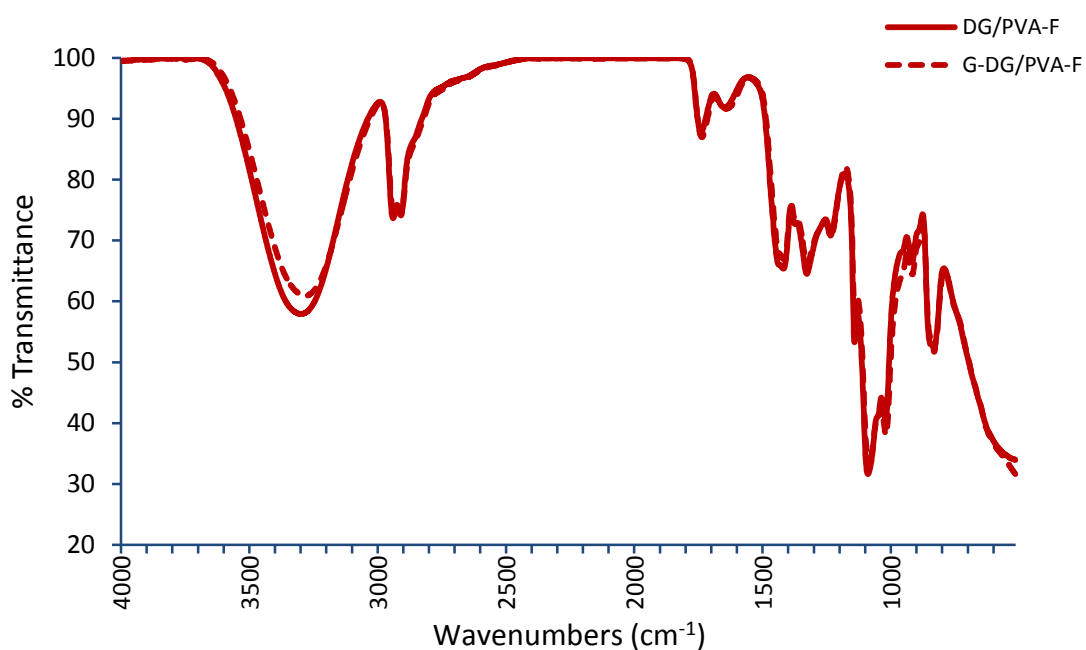


Figure 21 FTIR spectra of dried-form DG/PVA with G-CSF loaded and unloaded hydrogels

Dried-form hydrogels with G-CSF loaded and unloaded were studied for FTIR as showed in Figure 21. There was no different of FTIR spectrum between dried-form DG/PVA hydrogel and G-CSF loaded DG/PVA hydrogel.

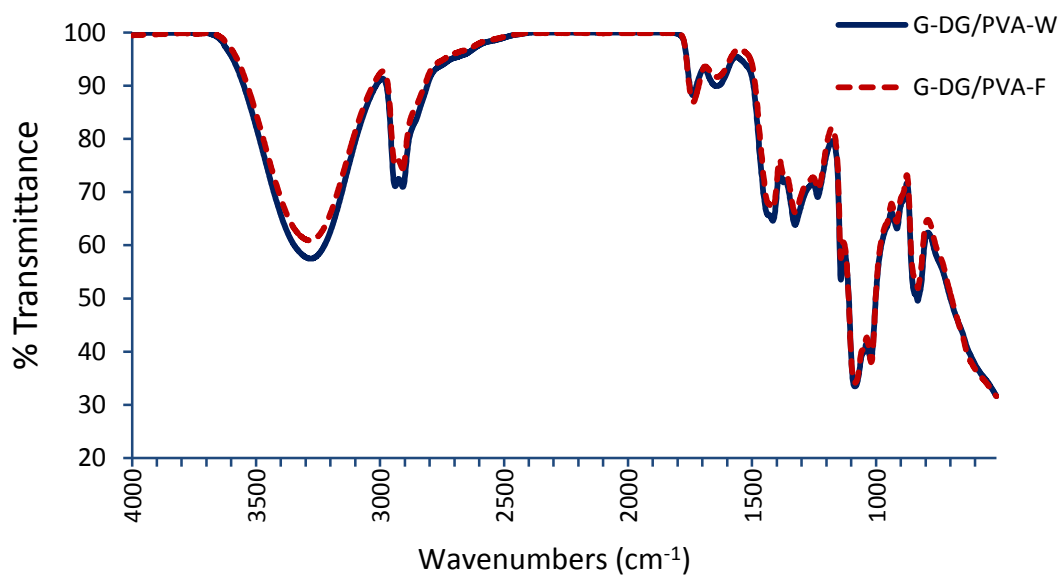


Figure 22 FTIR spectra of G-CSF loaded wet and dried-form DG/PVA hydrogels

FTIR spectra of both G-CSF loaded wet and dried-form hydrogels were compared as showed in Figure 22. The spectra showed the same pattern. FTIR spectrum of G-CSF loaded dried-form hydrogel was slightly decreased intensity of the peak at 3318 cm⁻¹ (OH-stretching) and 2948 cm⁻¹ (C-H stretching) that might be the lesser chemical reaction in dried-form than in wet-form.

4.3 Selection of hydrogel packaging

Table 5 Selection of packaging materials for sterilization

Packaging materials		Sterilization methods		
		Gamma irradiation (25kGy)	Ethylene Oxide gas (EO)	H ₂ O ₂ gas plasma (HO)
Low density polyethylene (LDPE)	Thin type	√	√	X
	Thick type	√	√	X
High density polyethylene (HDPE)	Thin type	√	√	X
	Thick type	√	√	X
Linear low density polyethylene laminated Nylon (LLDPE/Nylon)		√	√	√
Polyethylene terephthalate laminated Nylon and Metallite (PET/Nylon/Metallite)		√	X	X

√ = sterilant could pass packaging material (Biological indicator was sterilized)

X = sterilant could not pass packaging material (Biological indicator was not sterilized)

All four different types of packaging materials can be used for gamma radiation sterilization. Whereas two types of LDPE and HDPE and LLDPE/Nylon can be used for ethylene oxide gas sterilization. LLDPE/Nylon can be used for hydrogen peroxide gas plasma. Therefore, LLDPE/Nylon was selected to be used as packaging material for three sterilization methods.

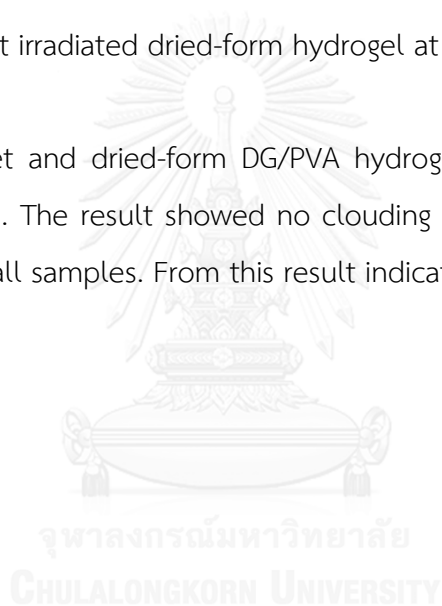
4.4 Sterility test

Hydrogel	Sterilization method					
	Gamma irradiation				Ethylene oxide gas	Hydrogen peroxide gas plasma
	10 kGy	15 kGy	20 kGy	25 kGy		
DG/PVA-W	√	√	√	√	√	√
DG/PVA-F	N/A	√	N/A	√	√	√

√ = TSB media is clear after incubate 37°C for 5 days (n=3)

N/A = Not irradiated dried-form hydrogel at radiation dose 10 and 20 kGy


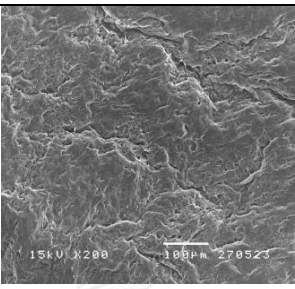
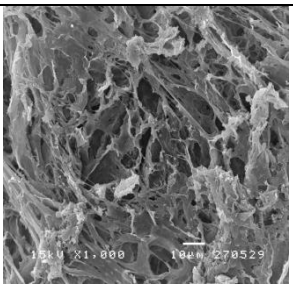

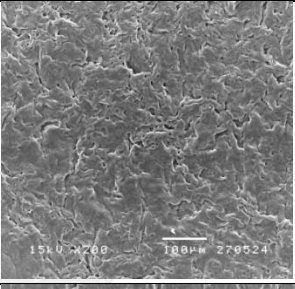
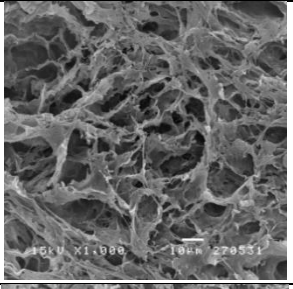

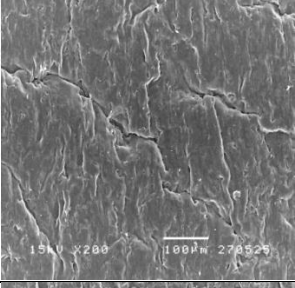
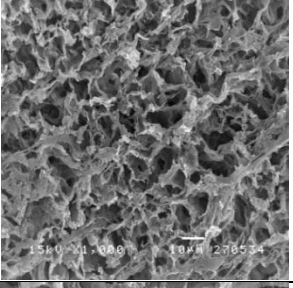

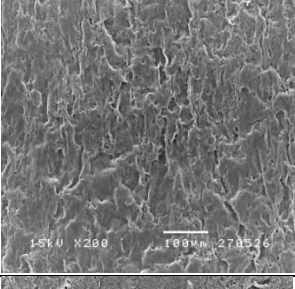
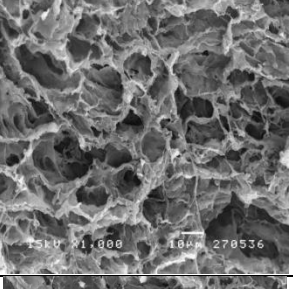

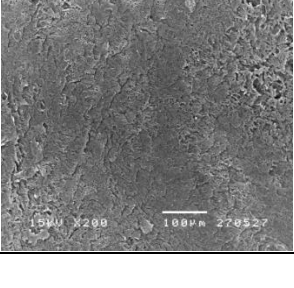
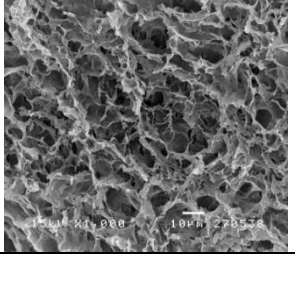
Sterility of wet and dried-form DG/PVA hydrogels which sterilized by three methods were tested. The result showed no clouding of the media after incubated for 5 days at 37°C in all samples. From this result indicated that all hydrogels sterile.



4.5 Effect of sterilization methods on physicochemical properties of DG/PVA hydrogels

4.5.1 Gamma irradiation

Table 6 Morphology of wet-form DG/PVA hydrogels after gamma irradiation

Hydrogel	Appearance	Surface (x200)	Cross-section (x1000)
DG/PVA-W			
DG/PVA-W 10kGy			
DG/PVA-W 15kGy			
DG/PVA-W 20kGy			
DG/PVA-W 25kGy			

The morphology of wet-form DG/PVA hydrogels sterilized by gamma irradiation at different dose were showed in Table 6. Increasing dose of radiation from 10 to 25 kGy, all hydrogels showed similar in appearance but the hydrogels patches had strengthen. SEM photographs supported the observation of hydrogels strengthen as can be seen a dense surface and higher porosity with increasing in radiation dose.

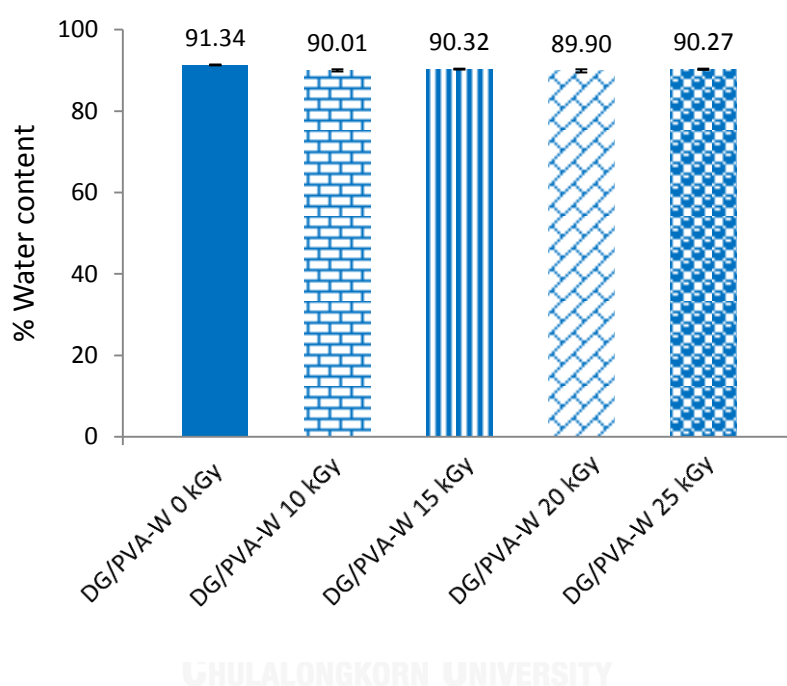


Figure 23 Water content of wet-form DG/PVA hydrogels after gamma irradiation

The water content of wet-form DG/PVA hydrogels after gamma irradiation were studied as showed in Figure 23. After gamma irradiation, the water content of hydrogels were decreased [$F(4, 20) = 24.95, p = 0.000$]. This dues to gamma radiation initiated free radicals on PVA polymer chains then chemical cross-linking between PVA polymer chains has occurred resulting in decrease of percentage of water content.

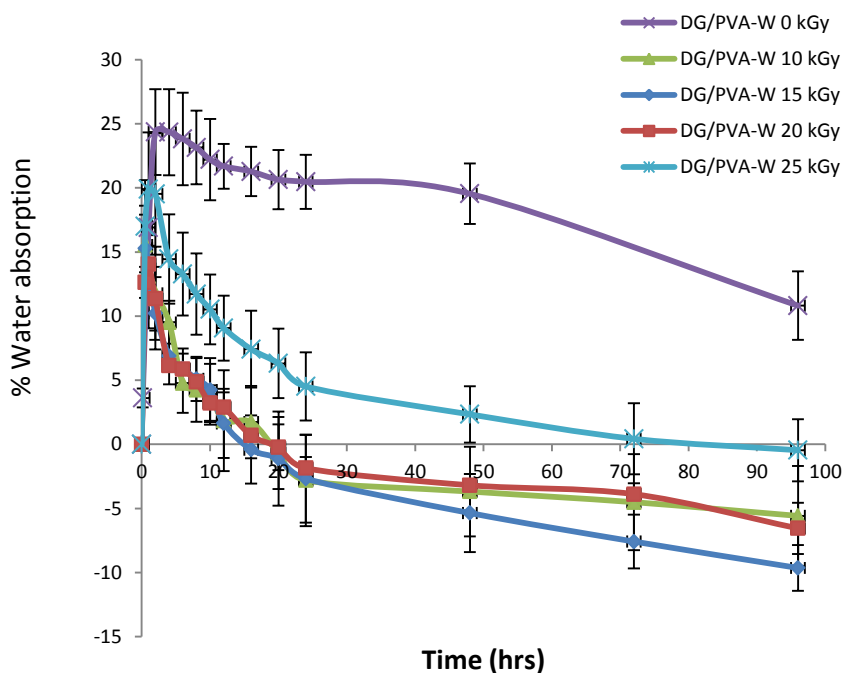


Figure 24 Water absorption capacity of wet-form DG/PVA hydrogels after gamma irradiation

The water absorption capacity of the wet-form hydrogels after gamma irradiation at 10, 15, 20 and 25 kGy were studied as showed in Figure 24. Non-irradiated hydrogel had maximum water absorption capacity $24.36 \pm 3.35\%$ (2 hours) whereas irradiated hydrogels at gamma radiation dose of 10, 15, 20 and 25 kGy had maximum water absorption capacity $15.56 \pm 3.05\%$ (30 minutes), $15.29 \pm 2.62\%$ (30 minutes), $13.08 \pm 2.28\%$ (1 hour) and $19.90 \pm 4.44\%$ (1 hour), respectively. Gamma irradiation decreased water absorption capacity of the hydrogels, statistically significant at dose 10, 15 and 20 kGy [$F(4,15)=8.53$, $p=0.001$]. This observation can be explained by the fact that an increase in irradiated dose enhances the formation of radicals on PVA polymer chains, resulting in high cross-linking between PVA polymer chains. The degree of cross-linking has a direct effect on the level of swelling of the

polymer. Increased cross-linking density decreased swelling capacity of polymers. Moreover, the irradiated hydrogels had lower water absorption capacity than its original weights after 20 hours, it might be the reason of DG polymer dissolved in water and hydrogel erosion.

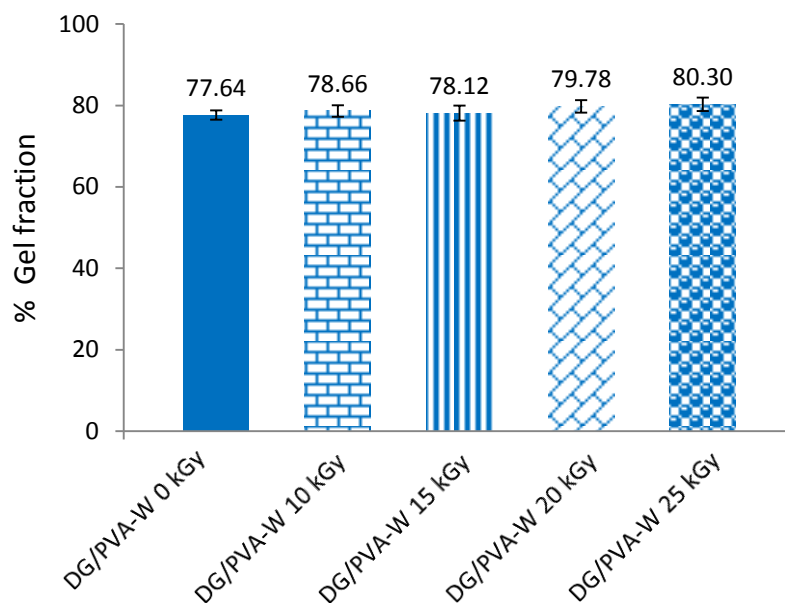


Figure 25 Gel fraction of wet-form DG/PVA hydrogels after gamma irradiation

Gel fraction of the wet-form hydrogels after gamma irradiation were studied in Figure 25. The gel fraction of irradiated wet-form hydrogels trended to increase with the radiation dose, from $77.64 \pm 1.15\%$ to $80.30 \pm 1.62\%$.

Table 7 Mechanical properties of wet-form DG/PVA hydrogels after gamma irradiation

Hydrogel	Young's Modulus (N/mm ²)	% Elongation	Tensile strength (MPa)
DG/PVA-W	0.030±0.003	534.947±41.778	0.123±0.005
DG/PVA-W 10kGy	0.027±0.002	694.840±14.823	0.150±0.015
DG/PVA-W 15kGy	0.024±0.002	548.985±36.888	0.115±0.013
DG/PVA-W 20kGy	0.026±0.003	707.716±38.440	0.154±0.025
DG/PVA-W 25kGy	0.031±0.001	755.720±76.325	0.199±0.041

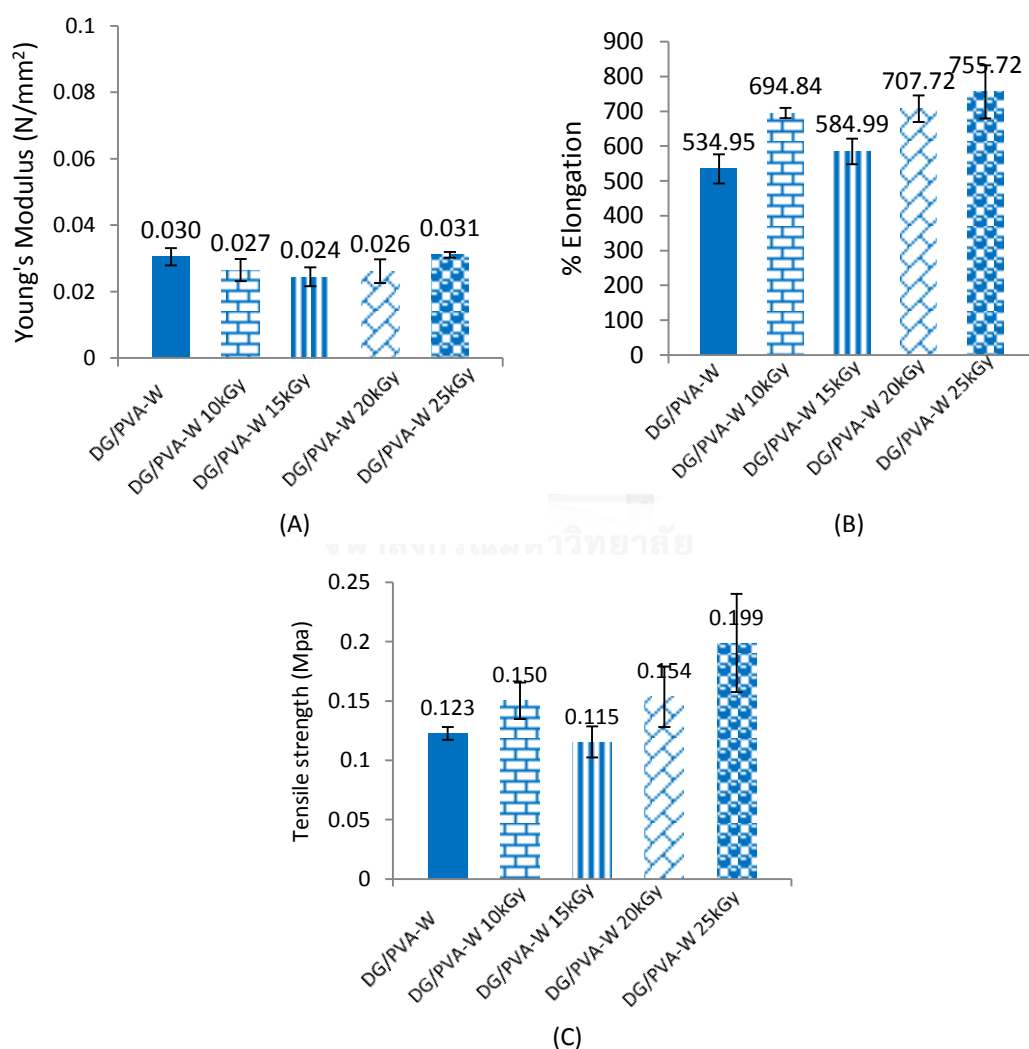


Figure 26 Mechanical properties of wet-form DG/PVA hydrogels after gamma irradiation

(A) Young's Modulus (B) % Elongation (C) Tensile strength

The mechanical properties of wet-form DG/PVA hydrogels after gamma irradiation were studied compare to non-irradiated hydrogel as showed in Table 7 and Figure 26. Young's modulus of irradiated hydrogels were not difference from non-irradiated hydrogel. Percentage of elongation of hydrogels gamma irradiated at dose 10, 20 and 25 kGy were significantly higher than non-irradiated hydrogels [F(4,10)=9.795, $p=0.002$] and tensile strength of the hydrogel irradiated at dose 25 kGy was significantly higher than non-irradiated and irradiated 15 kGy [F(4,12)=6.503, $p=0.005$]. The mechanical properties data form irradiated hydrogel at dose 15 kGy were deviated from the radiation dose 10 20 and 25 kGy. It might be the defect from characterized process. From the result of mechanical strength, gamma irradiation affected on the wet-form hydrogels in strength and flexibility whereas the stiffness of the wet-form hydrogels after gamma irradiation were not changed.

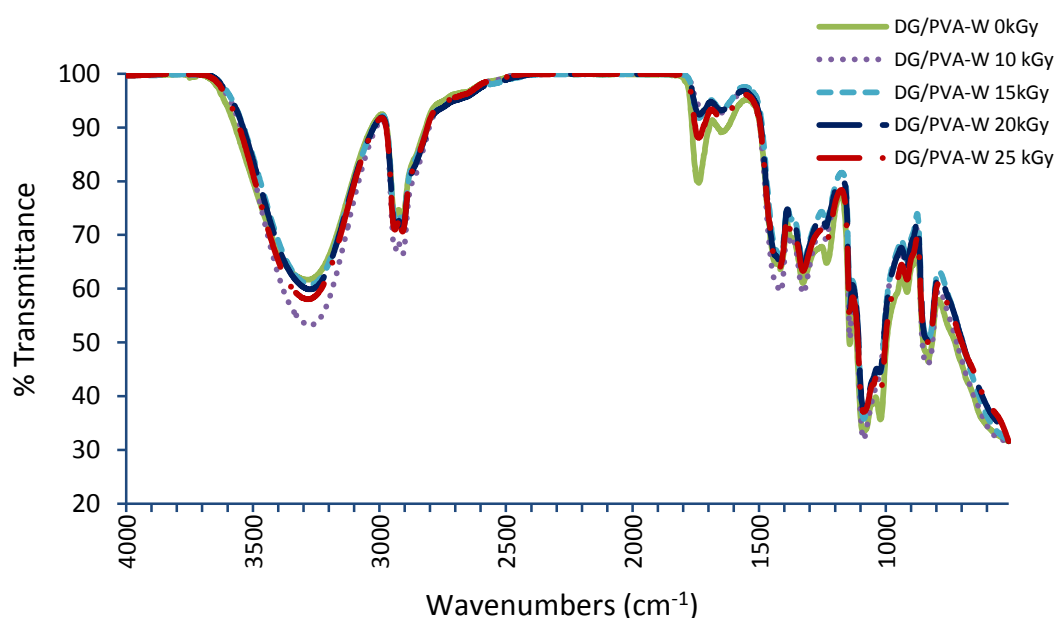


Figure 27 FTIR spectra of wet-form DG/PVA hydrogels after gamma irradiation

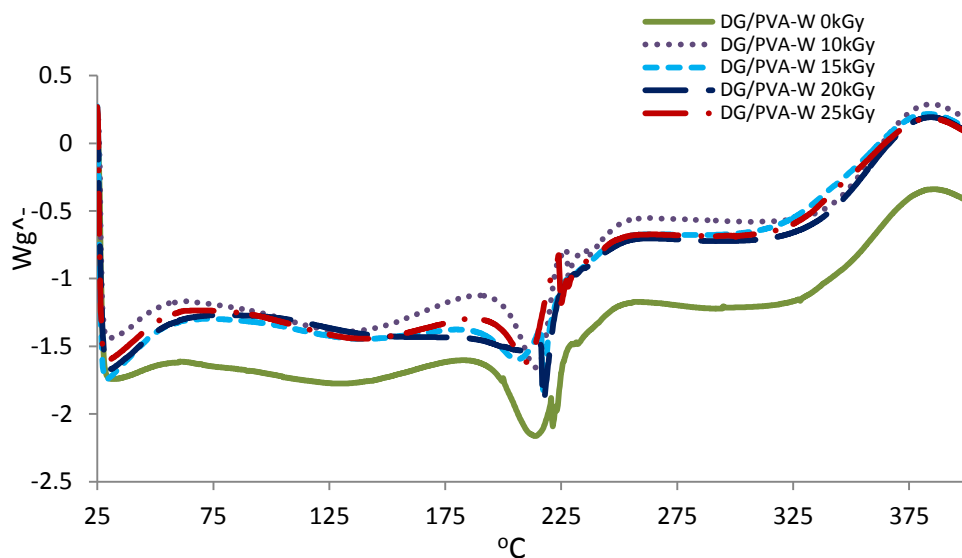

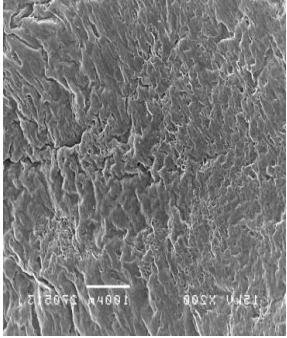
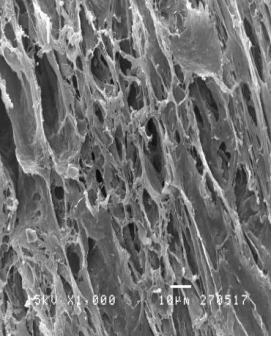

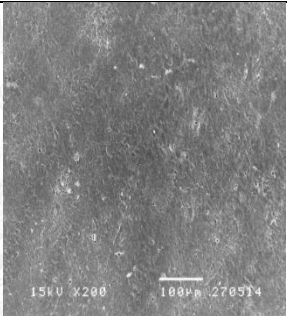
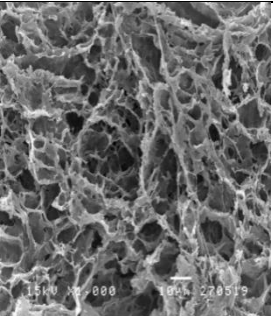

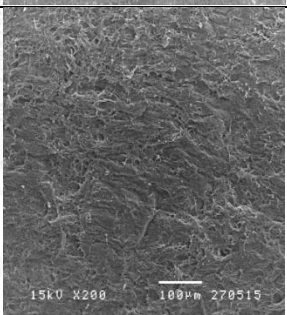
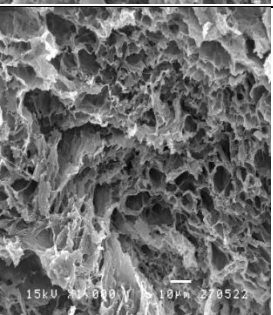


Figure 28 DSC thermograms of wet-form DG/PVA hydrogels after gamma irradiation

From figure 27, FTIR spectrum showed less intensity peak of carbonyl group ($C=O$ at 1750 cm^{-1}) but then increasing of hydroxyl group intensity peak (OH stretching about $3279\text{-}3342\text{ cm}^{-1}$). From this incident, it could be the consequence of free radical generated by gamma energy deposited on the polymer chains then polymer cross-linked occur and when hydrogel obtained more energy from gamma ray the PVA polymer chain were effected (Bhat, et al., 2005). The main chain scission of PVA polymer will take place therefore increasing intensity of OH -stretching and CH_2 -stretching in hydrogel irradiated 10 kGy and decreased in higher dose of radiation. From this reason, we could explained that the elongation and tensile strength of wet-form DG/PVA hydrogel irradiated at dose 10 kGy from mechanical properties testing and drop in dose 15 kGy after that increasing with radiation dose were consequence from high energy free radical of gamma ray enhanced the PVA chemical cross-link and affected on main chain PVA polymer scission. DSC curves showed endothermic peak of hydrogel still at the same position. DSC curves shown in Figure 28 were presented the endothermic peak of PVA in hydrogel but the peak were not sharp and intense as non-irradiated hydrogel.

Table 8 Morphology of G-CSF loaded wet-form hydrogels after gamma irradiation

Hydrogel	Appearance	Surface (x200)	Cross-section (x1000)
G-DG/PVA-W 0 kGy			
G-DG/PVA-W 15 kGy			
G-DG/PVA-W 25 kGy			

The morphology of wet-form of G-CSF loaded hydrogels after gamma irradiation had similar appearance to non-sterilized hydrogel. However, SEM photographs of the irradiated hydrogels presented dense surface and more porosities as same as unloaded G-CSF wet-form hydrogels.

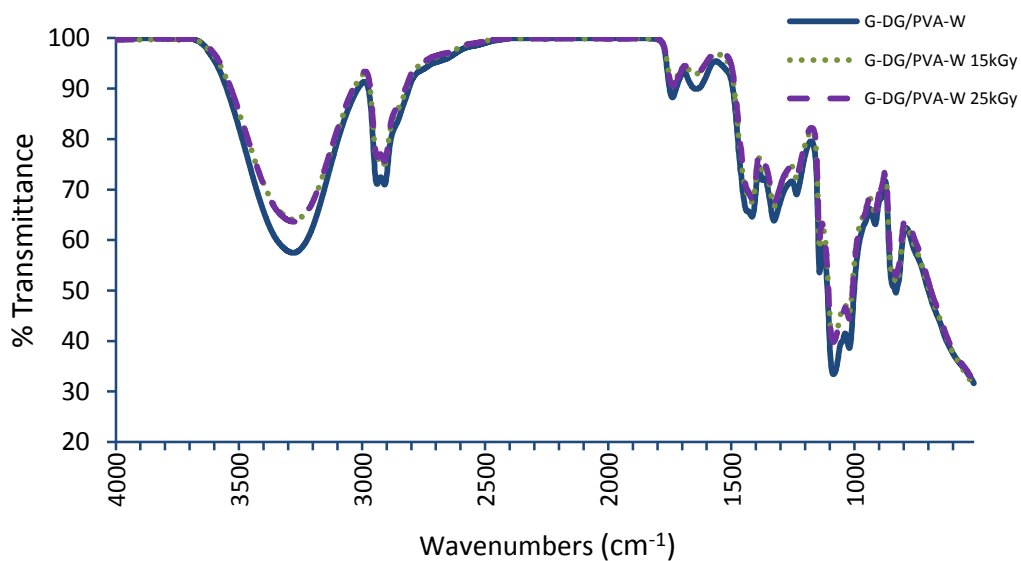

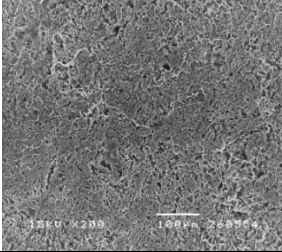
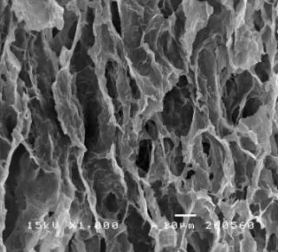

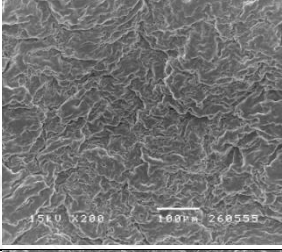
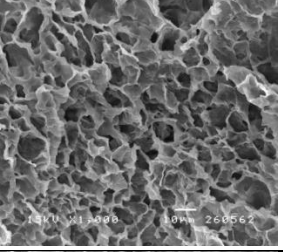

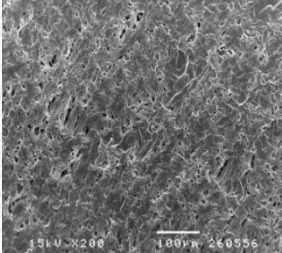
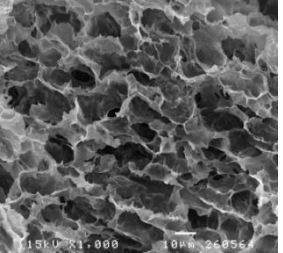

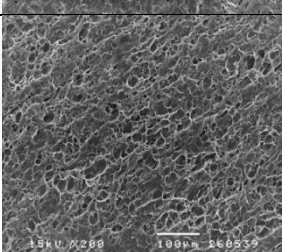
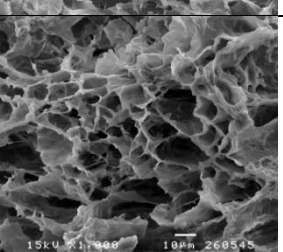

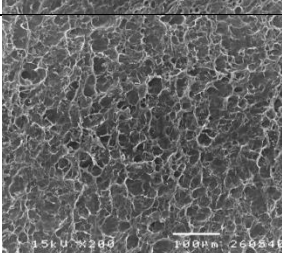
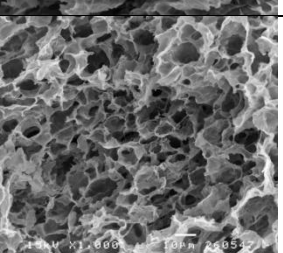

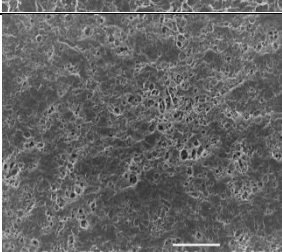
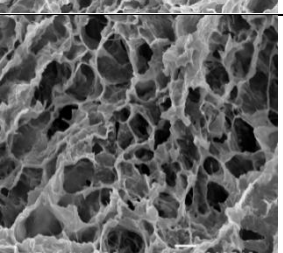


Figure 29 FTIR spectra of G-CSF loaded wet-form hydrogels after gamma irradiation

G-CSF loaded wet-form hydrogels after gamma irradiation were studied for FTIR as showed in Figure 29. The intensity of OH-stretching peak from FTIR spectrum of G-CSF loaded hydrogels was decreased after gamma irradiation at dose 15 and 25 kGy. Due to gamma radiation could broke a main chain of PVA polymer as discussed above.

Table 9 Morphology of G-CSF loaded and unloaded dried-form hydrogels after gamma irradiation

Hydrogel	Appearance	Surface (x200)	Cross-section (x1000)
DG/PVA-F 0 kGy			
DG/PVA-F 15kGy			
DG/PVA-F 25kGy			
G-DG/PVA-F 0 kGy			
G-DG/PVA-F 15kGy			
G-DG/PVA-F 25kGy			

From Table 9, the morphology of G-CSF loaded and unloaded dried-form hydrogels sterilized by gamma radiation were darkened in colour and SEM photographs showed smaller pore sizes in irradiated hydrogels.

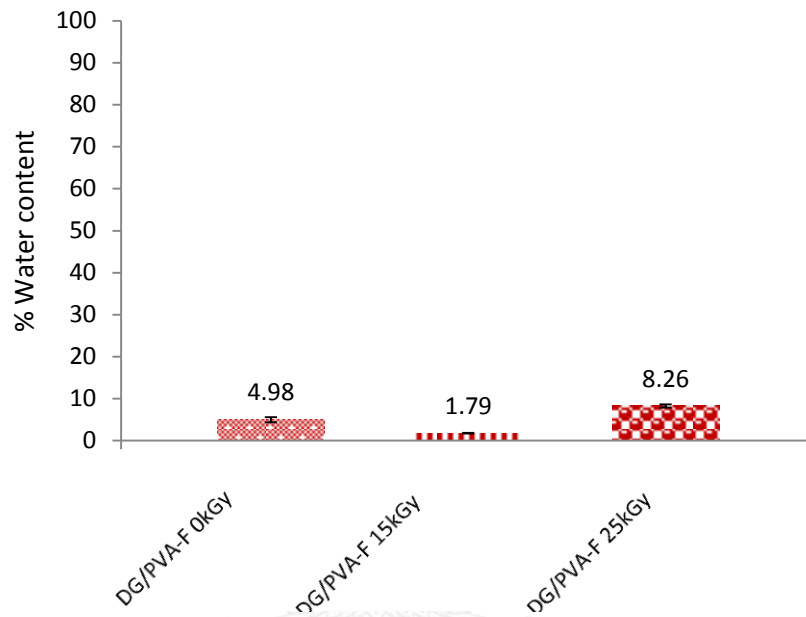


Figure 30 Water content of dried-form DG/PVA hydrogels after gamma irradiation

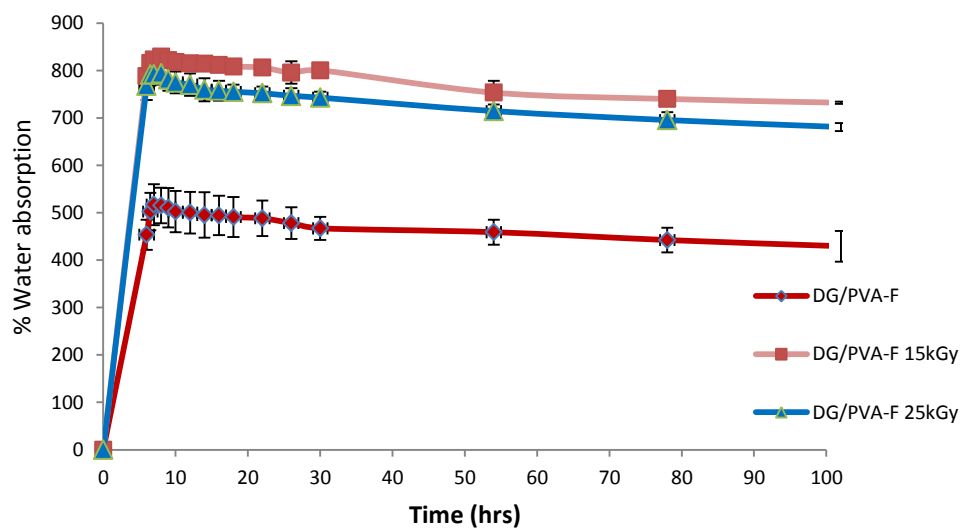


Figure 31 Water absorption capacity of dried-form DG/PVA hydrogels after gamma irradiation

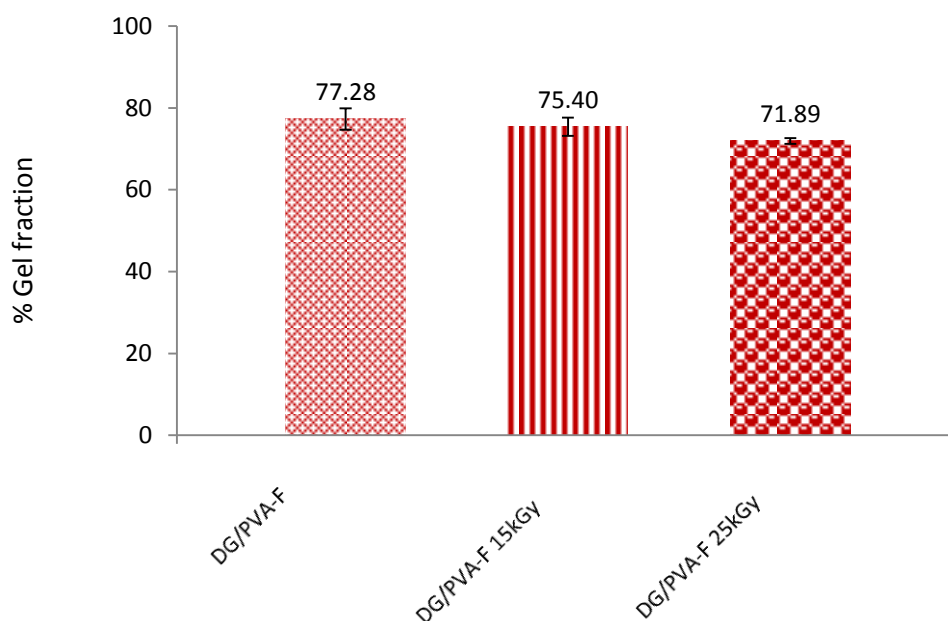


Figure 32 Gel fraction of dried-form DG/PVA hydrogels after gamma irradiation

From Figure 30, the water content of dried-form DG/PVA hydrogel were not different between non-irradiated and irradiated hydrogels. As well as gel fraction in Figure 32, There were no effected of gamma radiation on gel fraction properties. The water absorption capacity of dried-form hydrogels were studied as showed in Figure 34 showed that dried-form hydrogels after gamma irradiation at 15 and 25 kGy were $829 \pm 4.99\%$ and $794.35 \pm 24.41\%$, respectively. There were increasing in water absorption capacity from non-irradiated significantly [$F(2,5) = 81.190$, $p=0.000$]. From this result, gamma irradiation could enhanced the water absorption capacity of dried-form DG/PVA hydrogel whereas no effected on water content and gel fraction.

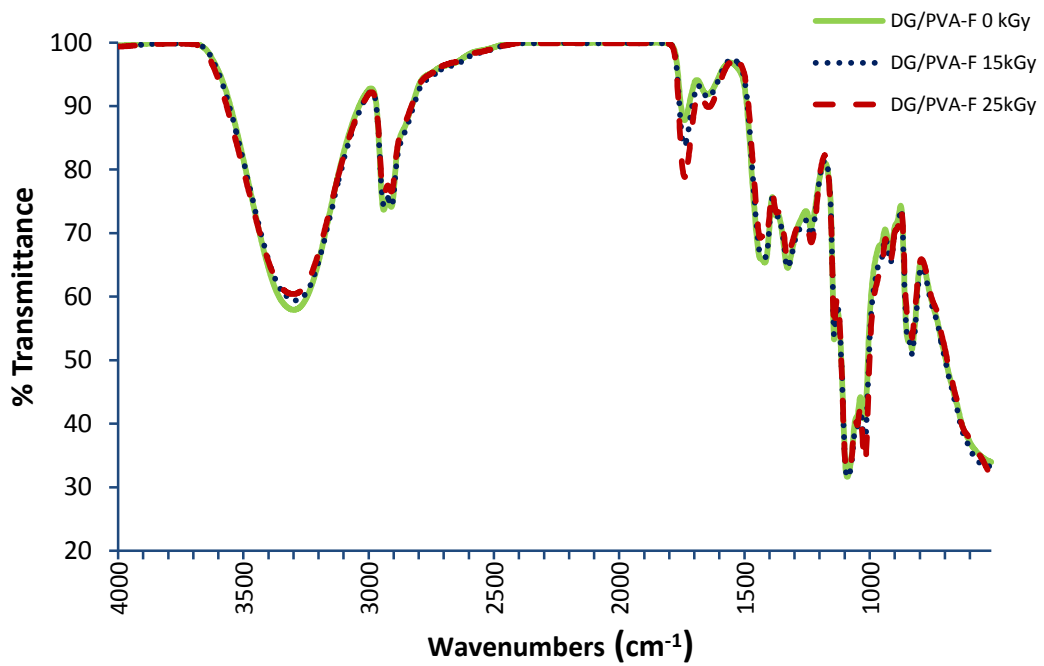


Figure 33 FTIR spectra of dried-form DG/PVA hydrogels after gamma irradiation

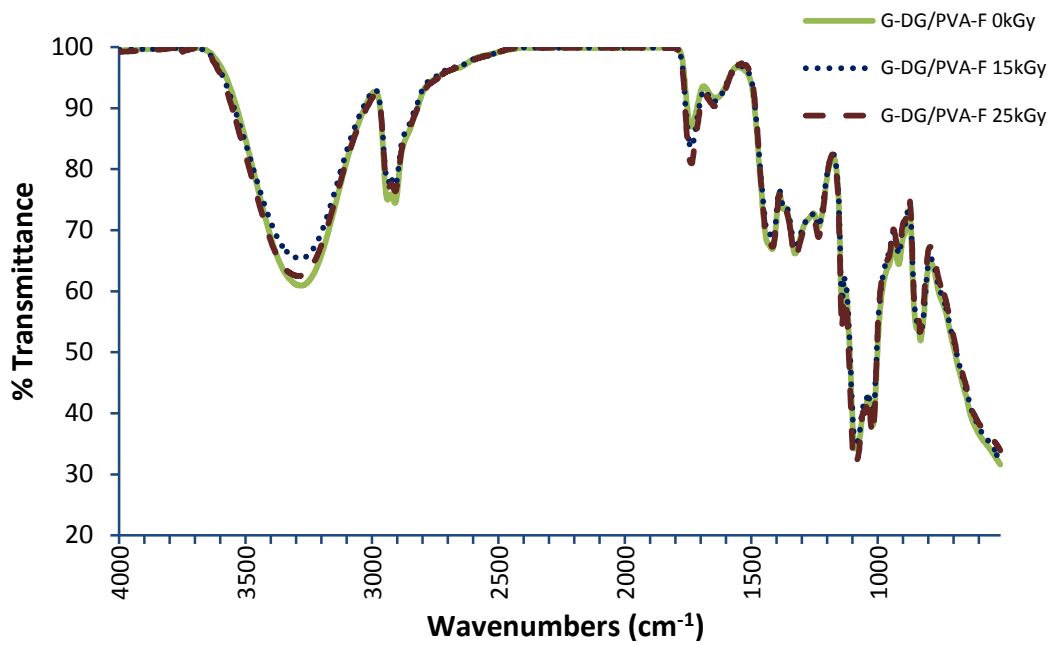


Figure 34 FTIR spectra of dried-form G-CSF loaded hydrogels after gamma irradiation

The dried-form G-CSF loaded and unloaded DG/PVA hydrogels after gamma irradiation were studied for FTIR as showed in Figure 33 and 34. There were increasing intensity of C=O stretching associated to aldehyde at 1755 cm^{-1} . It could be the result of hemiacetal formation in hydrogel as described above. By the way the chemical reaction in dried-form hydrogel may hardly occur than wet-form.

Table 10 Mechanical properties of dried-form DG/PVA hydrogels after gamma irradiation

Hydrogel	Young's Modulus (N/mm ²)	% Elongation	Tensile strength (MPa)
DG/PVA-F	0.051±0.005	577.574±42.934	0.261±0.045
DG/PVA-F 15kGy	0.082±0.009	571.659±47.712	0.423±0.048
DG/PVA-F 25kGy	0.095±0.012	651.613±43.045	0.590±0.072

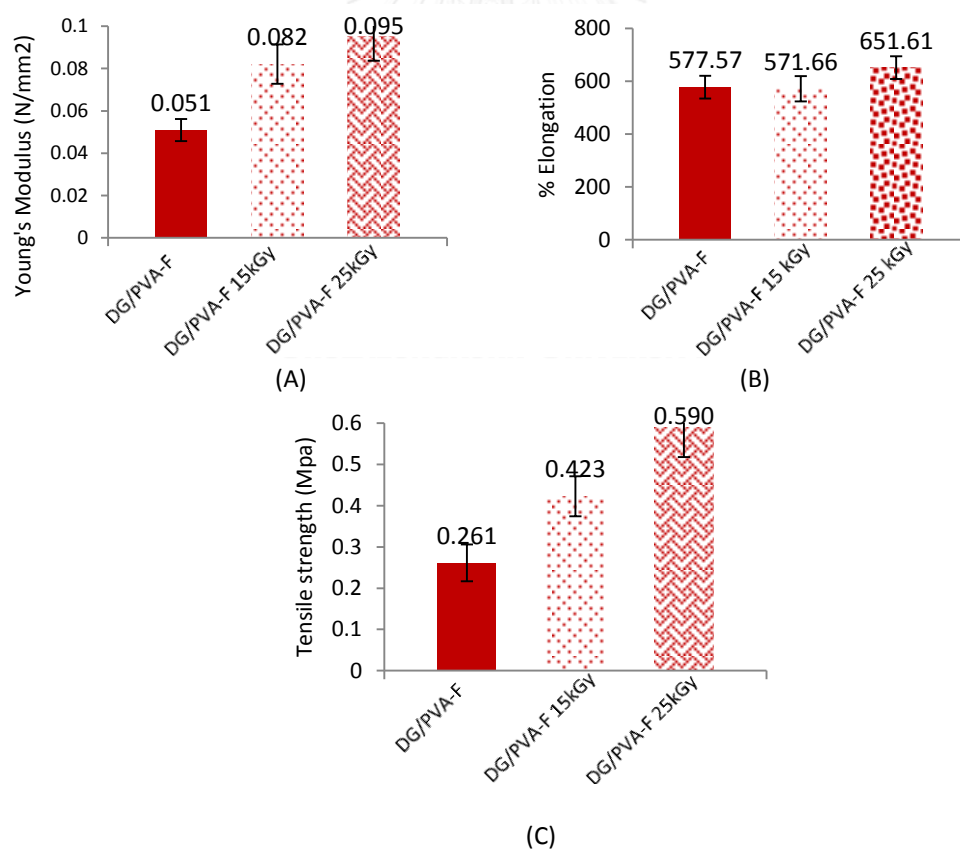



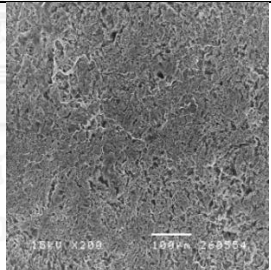
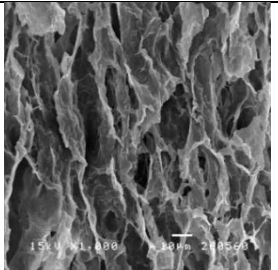

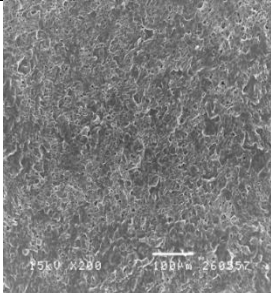
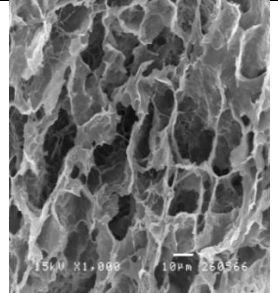

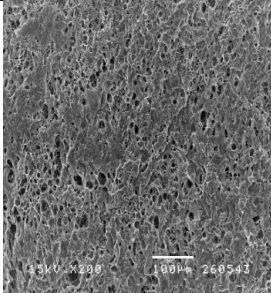
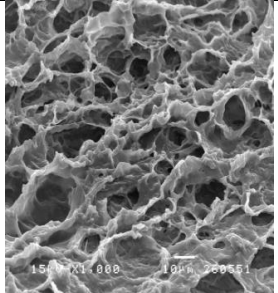
Figure 35 Mechanical properties of dried-form DG/PVA hydrogels after gamma irradiation

(A) Young's Modulus (B) % Elongation (C) Tensile strength

The mechanical properties of dried-form DG/PVA hydrogel were studied as showed in Figure 35. Young's modulus and tensile strength of irradiated hydrogels at dose 15 and 25 kGy were significantly higher than non-irradiated hydrogel [$F(2,9) = 39.14$, $p = 0.000$ and $F(2,9) = 36.24$, $p = 0.000$], respectively. Percent of elongation at break were not different. From this result, gamma radiation affected on the properties of Young's modulus and tensile strength. Therefore, the dried-form hydrogels after gamma irradiation had more stiffness and strengthen than non-irradiated hydrogel.

4.5.2 Ethylene oxide gas sterilization

Table 11 Morphology of G-CSF loaded and unloaded dried-form hydrogel after ethylene oxide gas sterilization

Hydrogel	Appearance	Surface (x200)	Cross-section (x1000)
DG/PVA-F			
DG/PVA-F EO			
G-DG/PVA-F EO			

The morphology of G-CSF loaded and unloaded dried-form hydrogels sterilized by ethylene oxide gas sterilization were studied as showed in Table 11. The appearance and structure of the both G-CSF loaded and unloaded hydrogels were similar while G-CSF loaded hydrogel had more porosity at the surface.

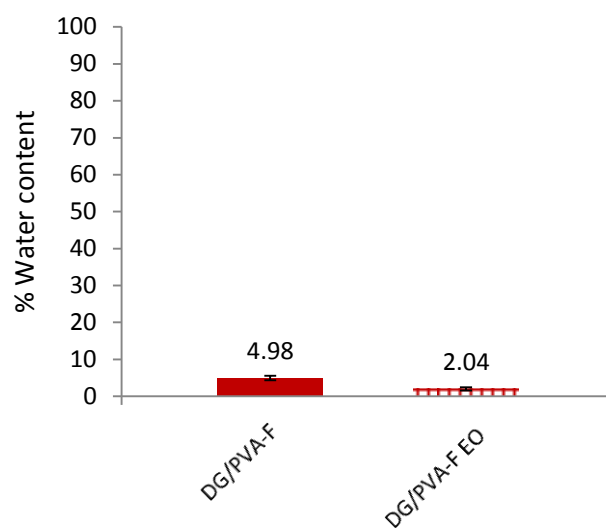


Figure 36 Water content of dried-form DG/PVA hydrogels after ethylene oxide gas sterilization

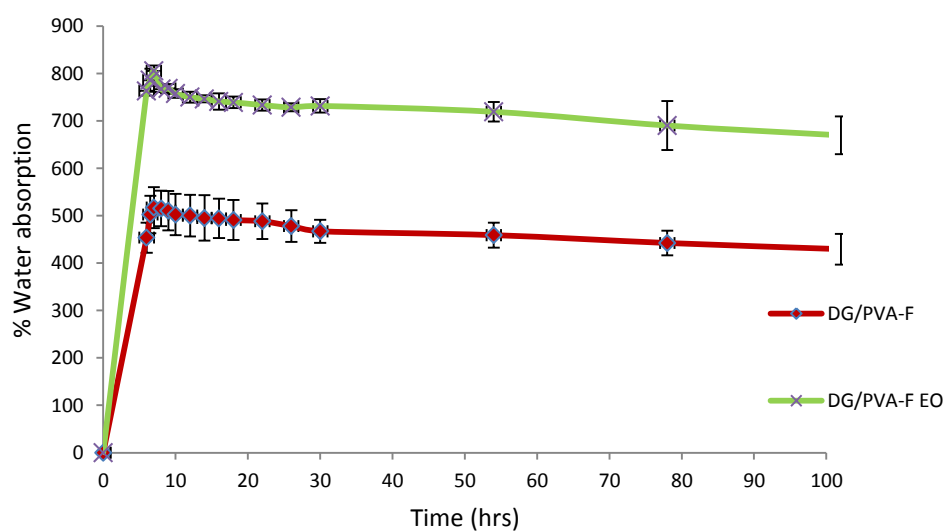


Figure 37 Water absorption capacity of dried-form DG/PVA hydrogels after ethylene oxide gas sterilization

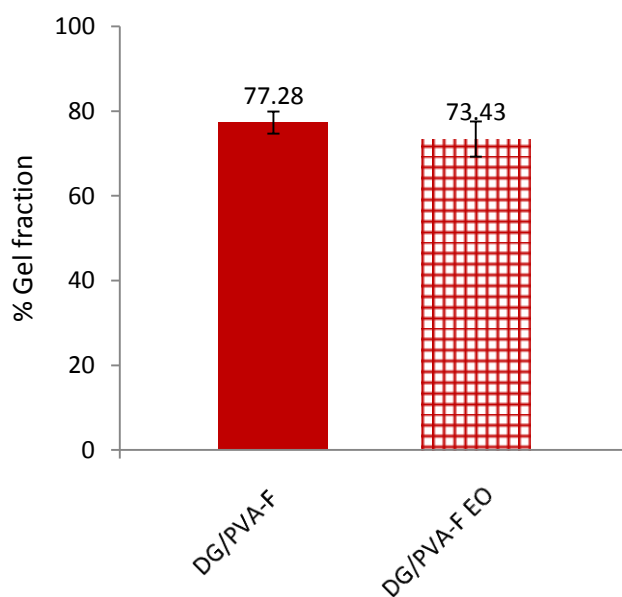


Figure 38 Gel fraction of dried-form DG/PVA hydrogels after ethylene oxide gas sterilization

The water content and gel fraction of dried-form DG/PVA hydrogels before and after EO gas sterilization were studied as showed in Figure 36 and 38. The water content and gel fraction were not changed after EO gas sterilization. The water absorption capacity were presented in Figure 37. It was found that hydrogel sterilized by ethylene oxide gas had water absorption capacity $805.30 \pm 11.29\%$ that significantly higher than $516.91 \pm 43.91\%$ of non-sterilized hydrogel [$t(3) = -8.81$, $p = 0.003$]. From the result, EO gas sterilization method enhanced water absorption capacity of dried-form DG/PVA hydrogel whereas water content and gel fraction were not changed.

Table 12 Mechanical properties of dried-form DG/PVA hydrogels after ethylene oxide gas sterilization

Hydrogel	Young's Modulus (N/mm ²)	% Elongation	Tensile strength (MPa)
DG/PVA-F	0.051±0.005	577.574±42.934	0.261±0.045
DG/PVA-F EO	0.055±0.007	626.196±48.290	0.318±0.055

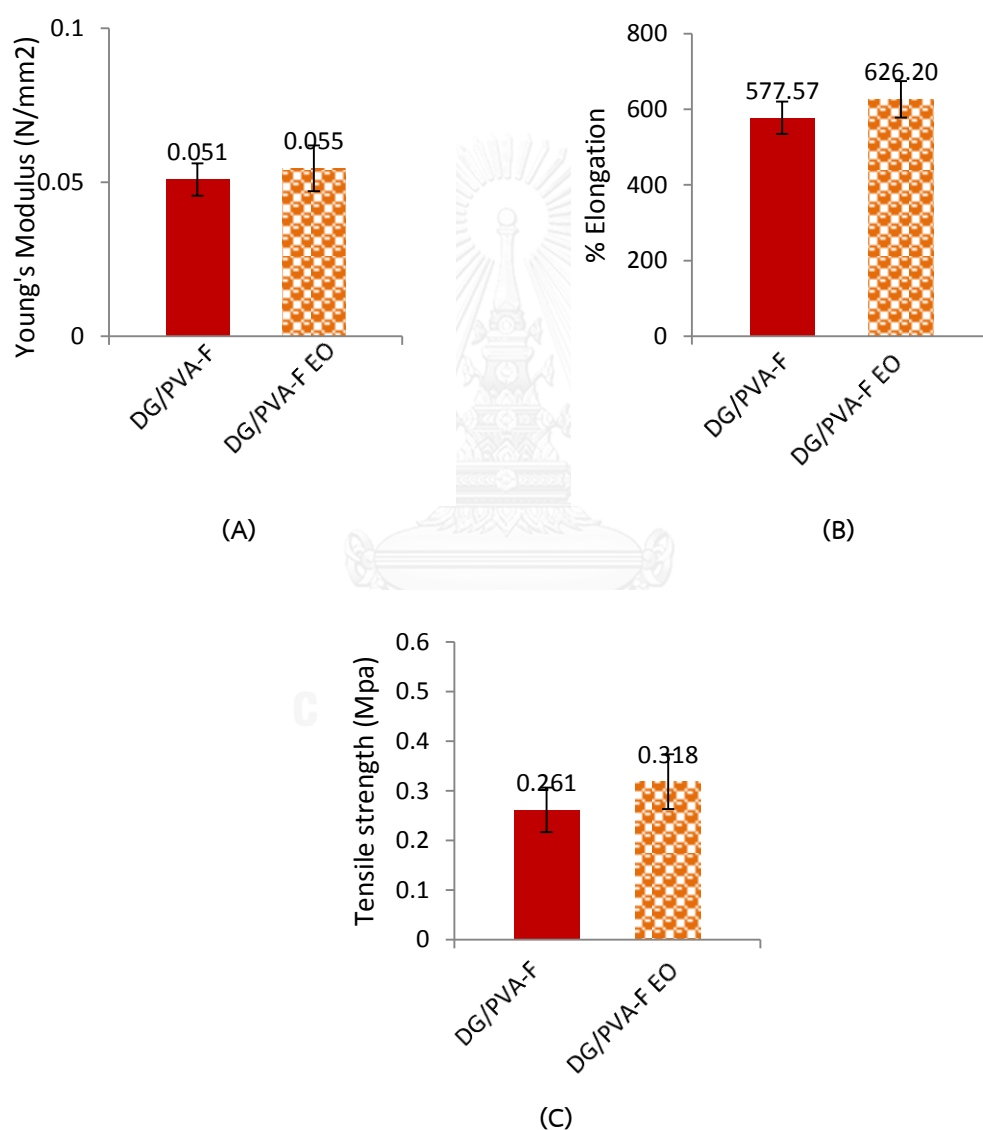


Figure 39 Mechanical properties of dried-form DG/PVA hydrogels after ethylene oxide gas sterilization (A) Young's Modulus (B) % Elongation (C) Tensile strength

The mechanical properties of dried-form DG/PVA hydrogels before and after ethylene oxide gas sterilization were studied as showed in Table 12 and Figure 39. Young's modulus, percentage of elongation and tensile strength of dried-form DG/PVA hydrogels after EO gas sterilization were unchanged. Therefore the EO gas sterilization method not affected the mechanical properties of dried-form hydrogel.

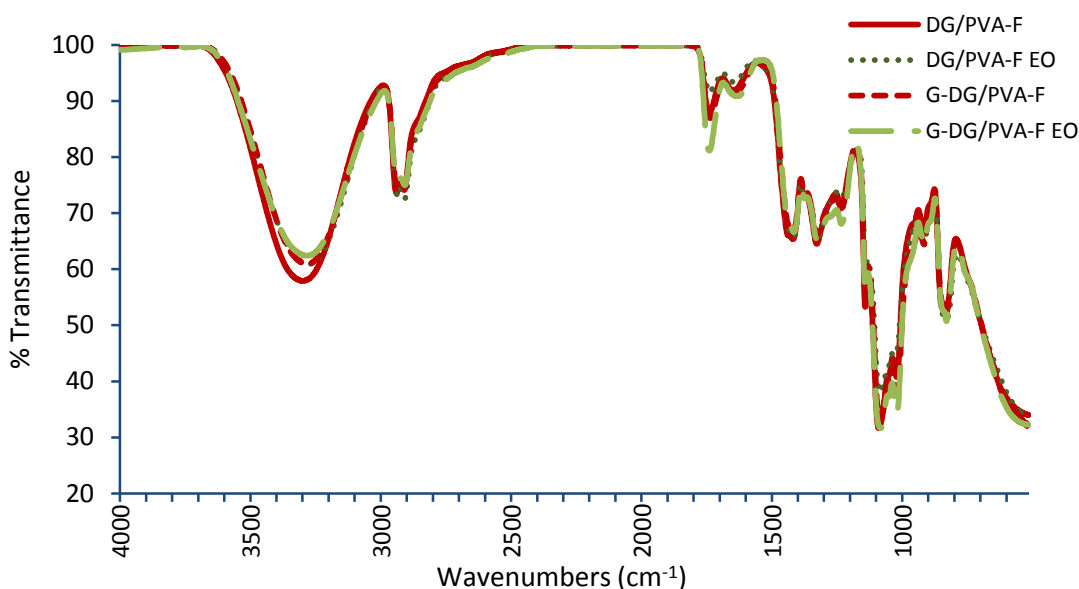
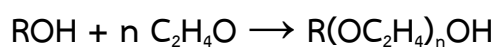



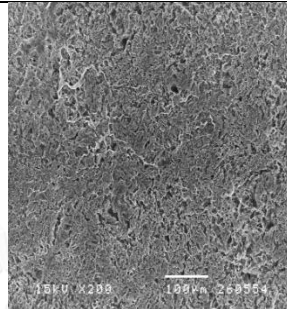
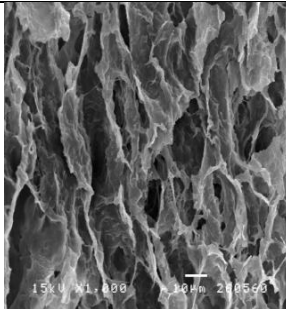

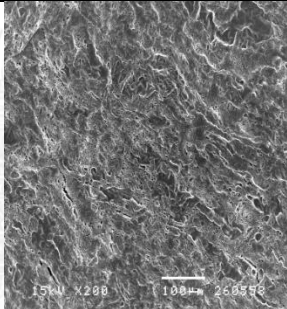
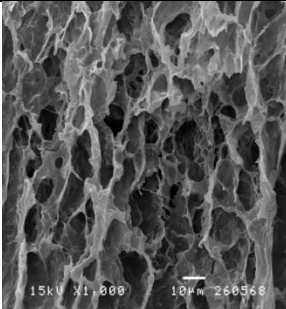

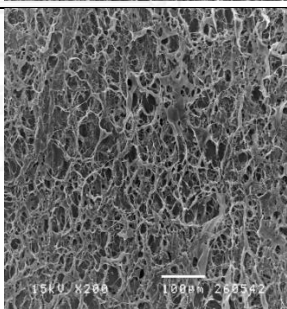
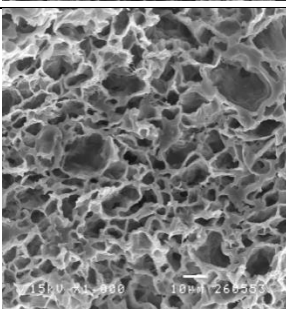
Figure 40 FTIR spectra of dried-form G-CSF loaded and unloaded DG/PVA hydrogels after ethylene oxide gas sterilization

From Figure 40, it was found that the intensity peak of carbonyl group at 1751 cm^{-1} in G-CSF loaded hydrogel after EO gas sterilization was increased. This might be the reaction of ethylene oxide with water to form ethylene glycol or with alcohol to form 2-ethoxyethanol especially in acidic catalyst condition. Hydroxyl group of PVA polymer could formed chemical reaction with ethylene oxide then decreasing in hemiacetal formation. Thus, the intensity peak of carbonyl group still higher than the peak of non-sterilized hydrogel. The proposed chemical reaction between ethylene oxide and alcohol was showed below (Brown and Eastham, 1960).



4.5.3 Hydrogen peroxide gas plasma

Table 13 Morphology of dried-form G-CSF loaded and unloaded DG/PVA hydrogels after hydrogen peroxide gas plasma sterilization

Hydrogel	Appearance	Surface (x200)	Cross-section (x1000)
DG/PVA-F			
DG/PVA-F HO			
G-DG/PVA-F HO			

The morphology of dried-form G-CSF loaded and unloaded DG/PVA hydrogels sterilized by hydrogen peroxide gas plasma were studied as showed in Table 13. The appearance of dried-form G-CSF loaded and unloaded DG/PVA hydrogels were similar. SEM photographs of G-CSF loaded hydrogel exhibited more porosity at the surface and its cross-section showed smaller pore sizes.

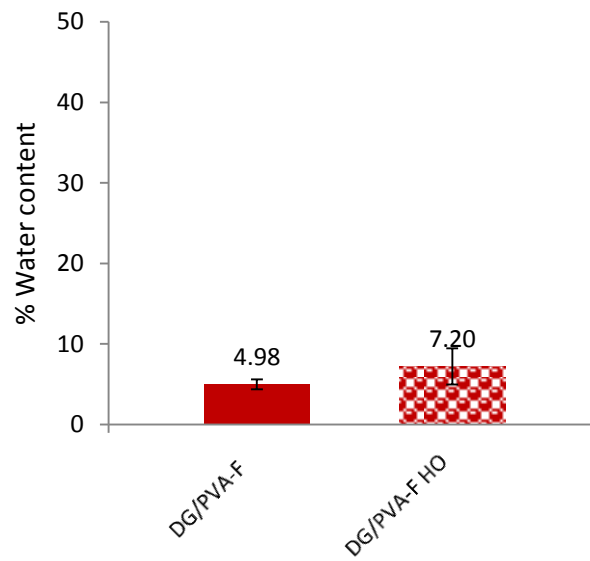


Figure 41 Water content of dried-form DG/PVA hydrogels after hydrogen peroxide gas plasma sterilization

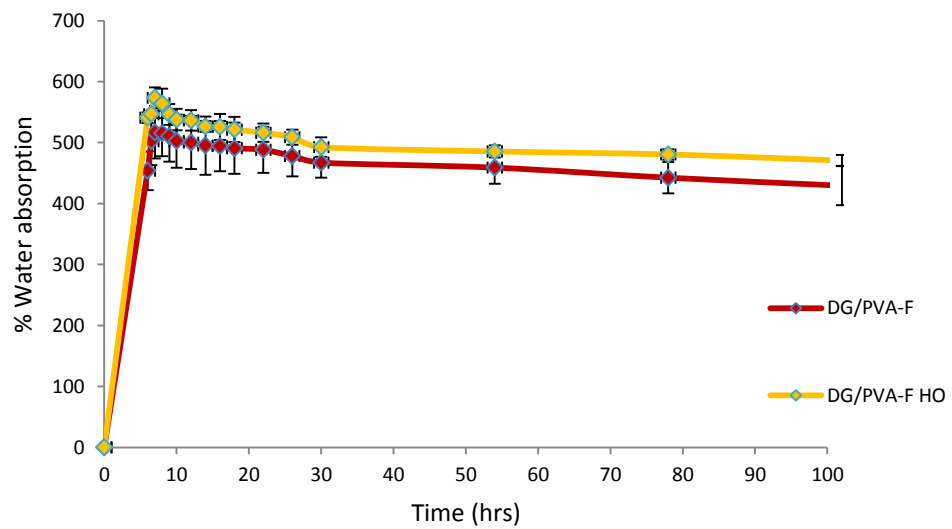


Figure 42 Water absorption capacity of dried-form DG/PVA hydrogels after hydrogen peroxide gas plasma sterilization

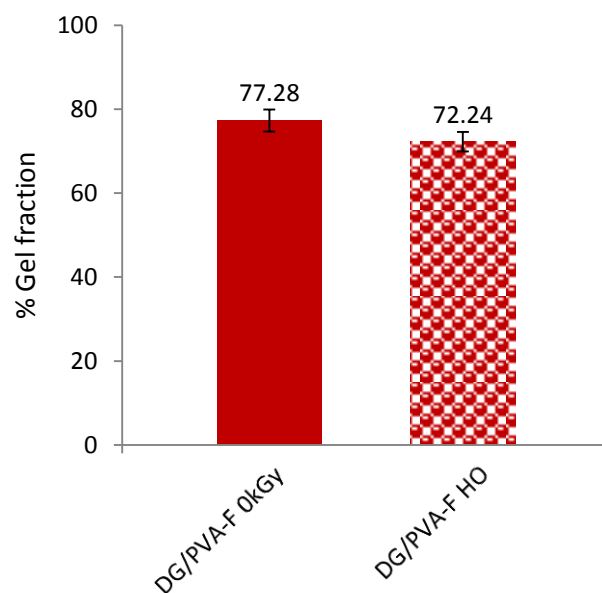


Figure 43 Gel fraction of dried-form DG/PVA hydrogels after hydrogen peroxide gas plasma sterilization

The water content, water absorption capacity and gel fraction of dried-form hydrogels after hydrogen peroxide gas plasma sterilization were studied as showed in Figure 41-43. It was found that the water content, water absorption capacity and gel fraction after hydrogen peroxide gas plasma sterilization were unchanged. From this result, the hydrogen peroxide gas plasma sterilization had not affected the water content, water absorption capacity and gel fraction of dried-form hydrogels.

Table 14 Mechanical properties of dried-form DG/PVA hydrogels after hydrogen peroxide gas plasma sterilization

Hydrogel	Young's Modulus (N/mm ²)	% Elongation	Tensile strength (MPa)
DG/PVA-F	0.051±0.005	577.574±42.934	0.261±0.045
DG/PVA-F HO	0.083±0.012	653.166±14.372	0.517±0.077

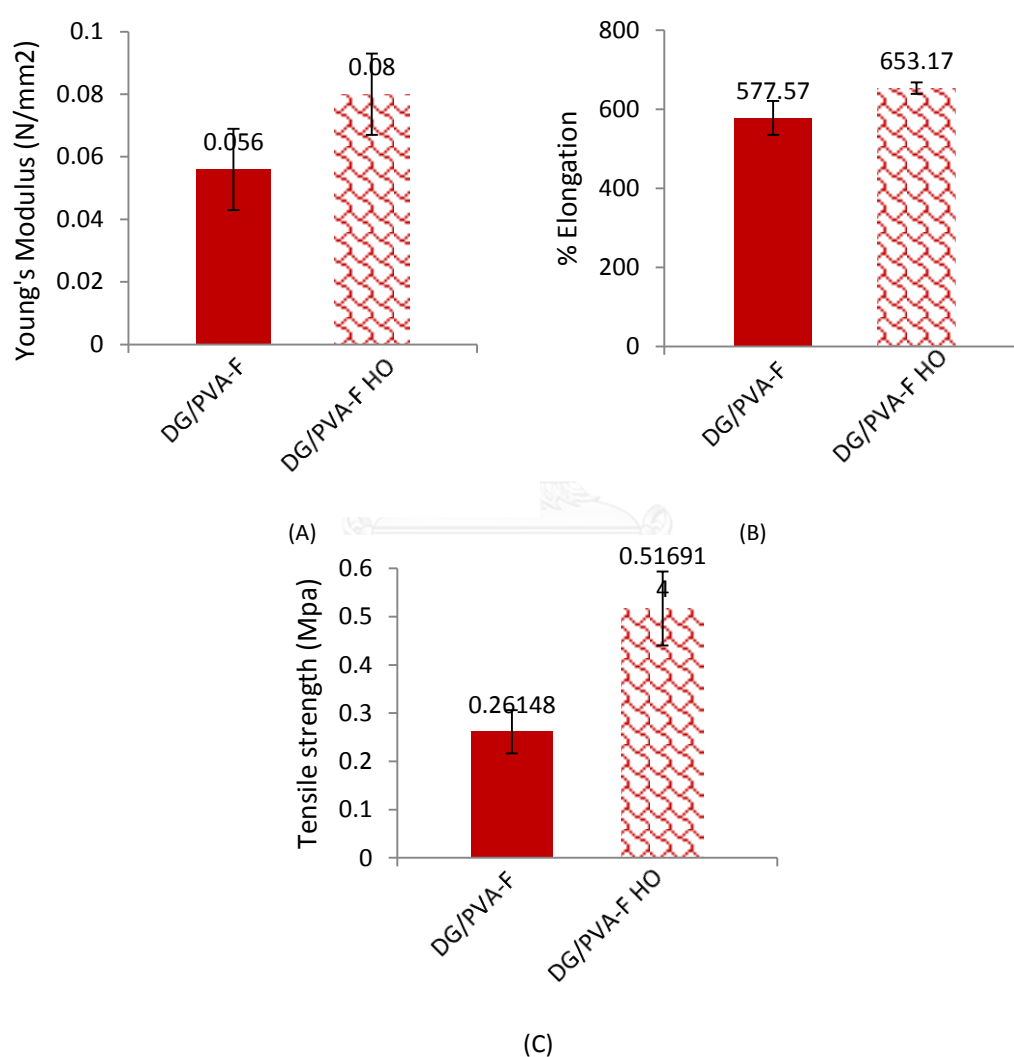


Figure 44 Mechanical properties of dried-form DG/PVA hydrogels after hydrogen peroxide gas plasma sterilization (A) Young's Modulus (B) % Elongation (C) Tensile strength

The mechanical properties of dried-form hydrogels after sterilized by hydrogen peroxide gas plasma were studied as showed in Table 14 and Figure 44. Young's modulus of hydrogen peroxide (HO) gas plasma sterilization was statistically higher than non-sterilized hydrogel [$t(12)=-3.25$, $p=0.007$] as well as tensile strength [$t(12)=-3.32$, $p=0.006$]. Percentage of elongation of the hydrogel was not changed after sterilization by HO gas plasma. From this result, HO gas plasma sterilization could affected Young's modulus and tensile strength of the dried-form hydrogels. Hydrogel sterilized by HO gas plasma had more rigidity and strengthen properties than the non-sterilized hydrogel.

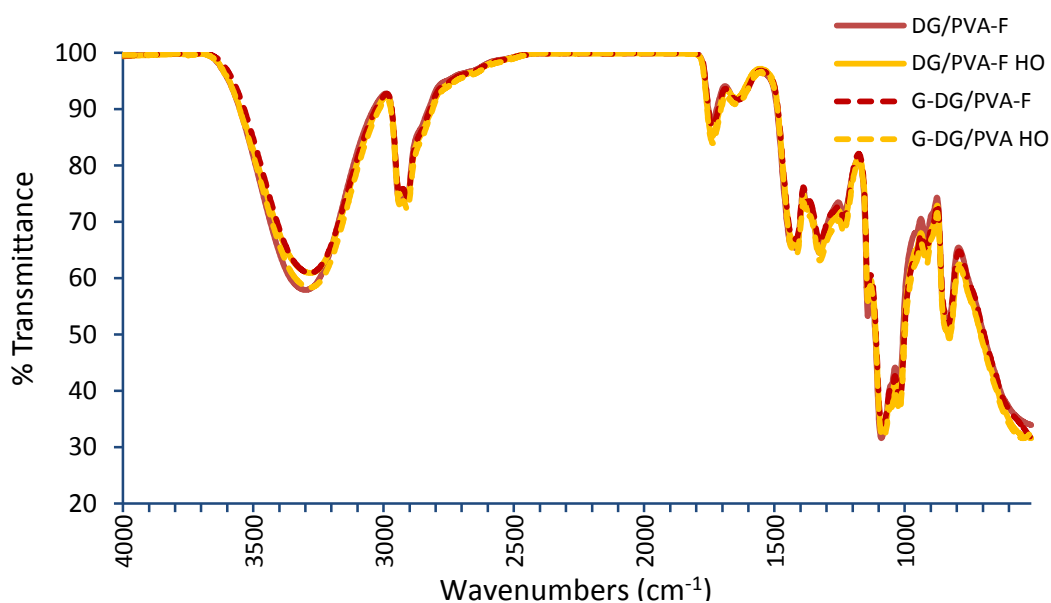


Figure 45 FTIR spectra of dried-form G-CSF loaded and unloaded DG/PVA hydrogels after hydrogen peroxide gas plasma sterilization

From Figure 45, there were no alteration on FTIR spectra of G-CSF loaded and unloaded dried-form DG/PVA hydrogels after sterilized by hydrogen peroxide gas plasma. As the result, hydrogen peroxide gas plasma affected only mechanical properties of hydrogel.

Table 15 Morphology of dried-form hydrogels after sterilization by gamma radiation 25 kGy, ethylene oxide and hydrogen peroxide gas plasma


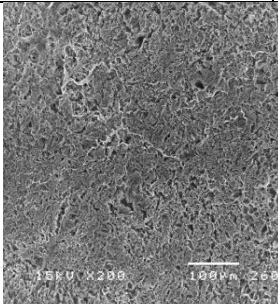
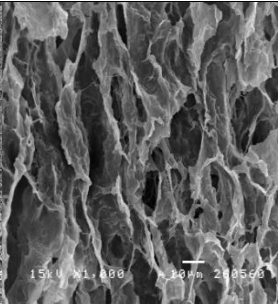

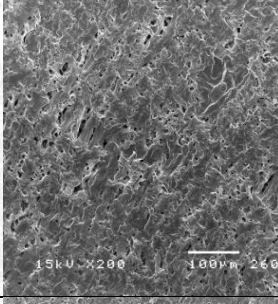
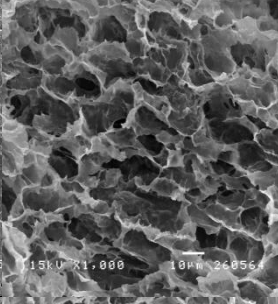

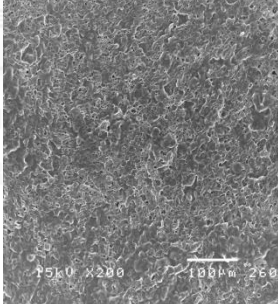
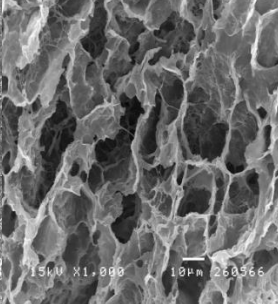

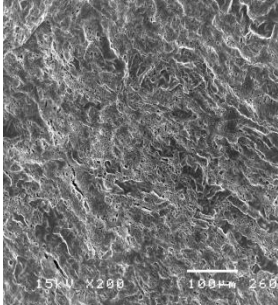
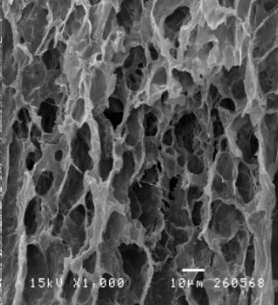

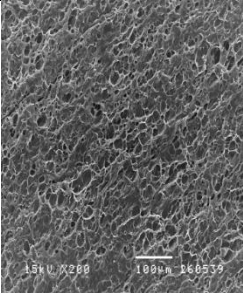
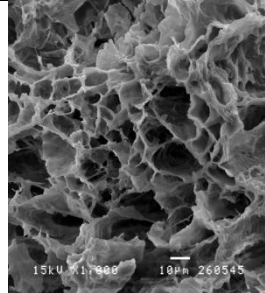

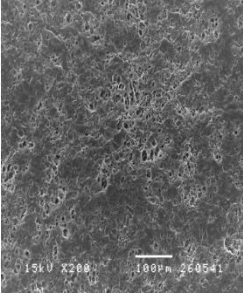
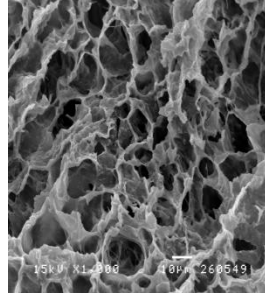

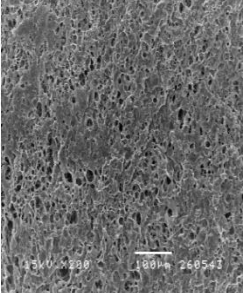
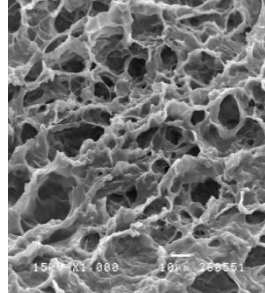

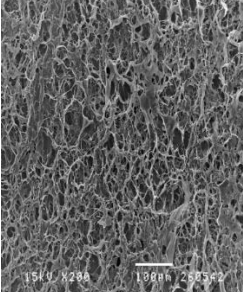
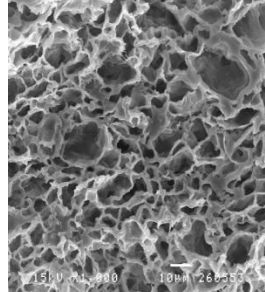
Hydrogel	Appearance	Surface (x200)	Cross-section (x1000)
DG/PVA-F			
DG/PVA-F 25kGy			
DG/PVA-F EO			
DG/PVA-F HO			

Table 16 Morphology of G-CSF loaded dried-form hydrogels after sterilization by gamma radiation 25 kGy, ethylene oxide and hydrogen peroxide gas plasma

Hydrogel	Appearance	Surface (x200)	Cross-section (x1000)
G-DG/PVA-F			
G-DG/PVA-F 25kGy			
G-DG/PVA-F EO			
G-DG/PVA-F HO			

The morphology of dried-form hydrogels with G-CSF loaded and unloaded sterilized by gamma irradiation 25 kGy, ethylene oxide and hydrogen peroxide gas plasma were studied as showed in table 15 and 16. Both dried-form hydrogels with G-CSF loaded and unloaded sterilized by gamma irradiation had darkened in color than

other sterilization methods. While SEM of the hydrogels from all sterilization methods had the same porosities.

Table 17 Mechanical properties of dried-form DG/PVA hydrogels after sterilization by gamma radiation 25 kGy, ethylene oxide and hydrogen peroxide gas plasma

Hydrogel	Young's Modulus (N/mm ²)	% Elongation	Tensile strength (MPa)
DG/PVA-F	0.051±0.005	577.574±42.934	0.261±0.045
DG/PVA-F 25kGy	0.095±0.012	651.613±43.045	0.590±0.072
DG/PVA-F EO	0.055±0.007	626.196±48.290	0.318±0.055
DG/PVA-F HO	0.083±0.012	653.166±14.372	0.517±0.077

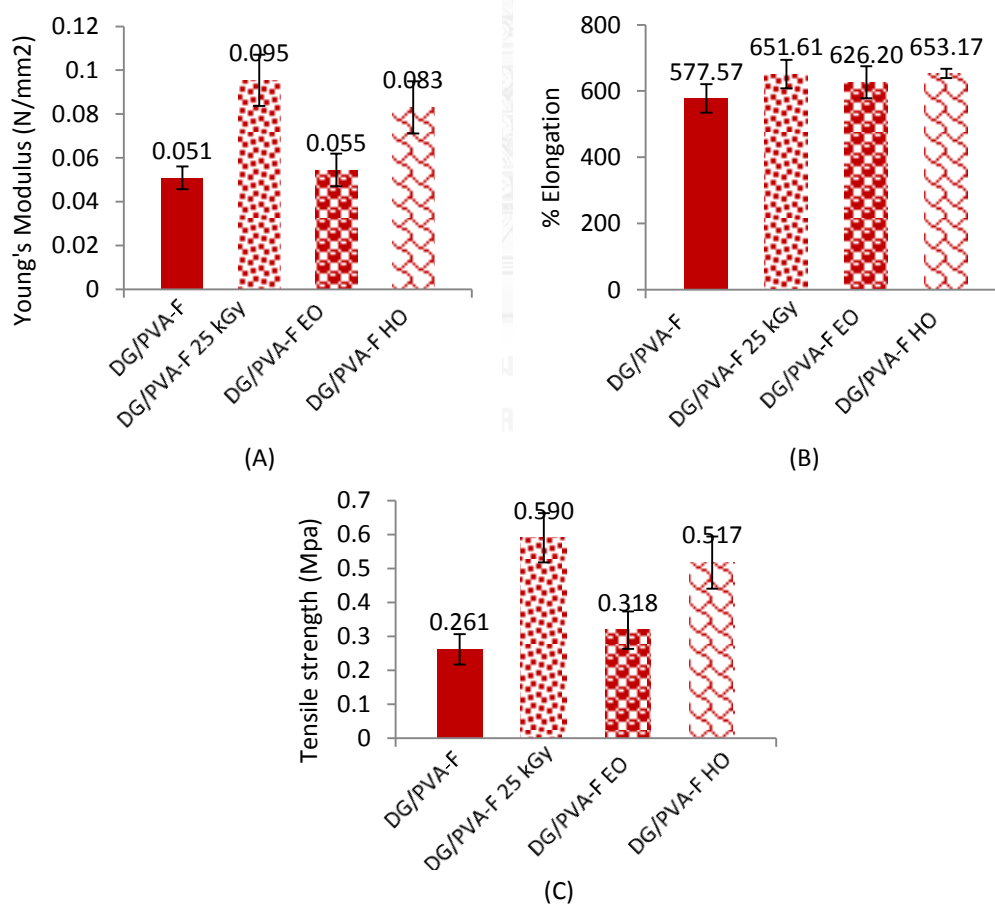


Figure 46 Mechanical properties of dried-form DG/PVA hydrogels after sterilization by gamma radiation 25 kGy, ethylene oxide and hydrogen peroxide gas plasma (A) Young's Modulus (B) % Elongation (C) Tensile strength

The mechanical properties of dried-form DG/PVA hydrogels sterilized by gamma irradiation 25 kGy, ethylene oxide and hydrogen peroxide gas plasma were studied as showed in Table 17 and Figure 46. Young's modulus and tensile strength of dried-form hydrogels sterilized by gamma irradiation 25 kGy and hydrogen peroxide gas plasma were statistically higher than non-sterilized hydrogel [$F(3,23)=12.99$, $p=0.00$] and [$F(4,19)=9.13$, $p=0.00$], respectively. However, there was unchanged on the percentage of elongation after sterilization. From the result, gamma irradiation 25 kGy and hydrogen peroxide gas plasma had effected on Young's modulus and tensile strength of dried-form hydrogels whereas ethylene oxide gas was not effected all mechanical properties.

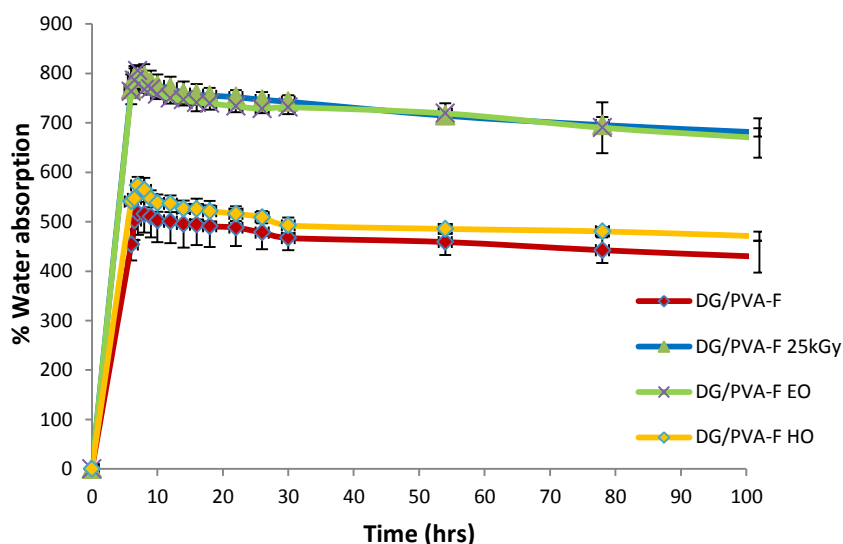


Figure 47 Water absorption capacity of dried-form DG/PVA hydrogels after sterilization by gamma radiation 25 kGy, ethylene oxide and hydrogen peroxide gas plasma

The water absorption capacity of dried-form DG/PVA hydrogels after sterilized by gamma irradiation 25 kGy, ethylene oxide and hydrogen peroxide gas plasma were studied as showed in Figure 47. The sterilization methods which affected water absorption capacity of the hydrogels were gamma irradiation and ethylene oxide gas sterilization [$F(4,10) = 10.20$, $p=0.001$]. However, the water absorption capacity of the hydrogel sterilized by hydrogen peroxide gas plasma was not differ from the non-sterilized dried-form hydrogels.

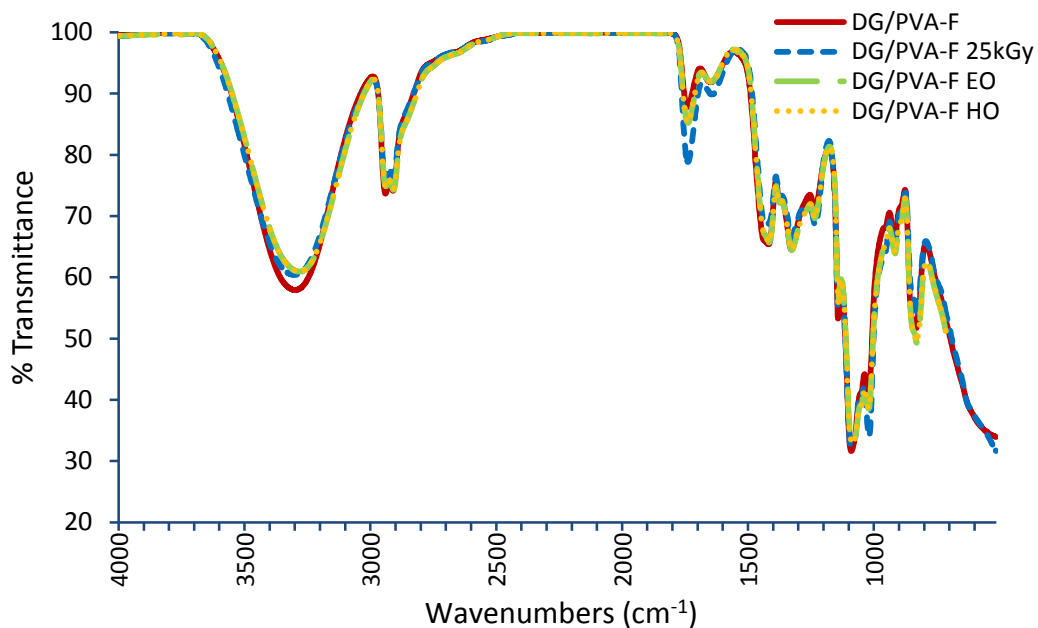


Figure 48 FTIR spectra of dried-form DG/PVA hydrogels after sterilization by gamma radiation 25 kGy, ethylene oxide and hydrogen peroxide gas plasma

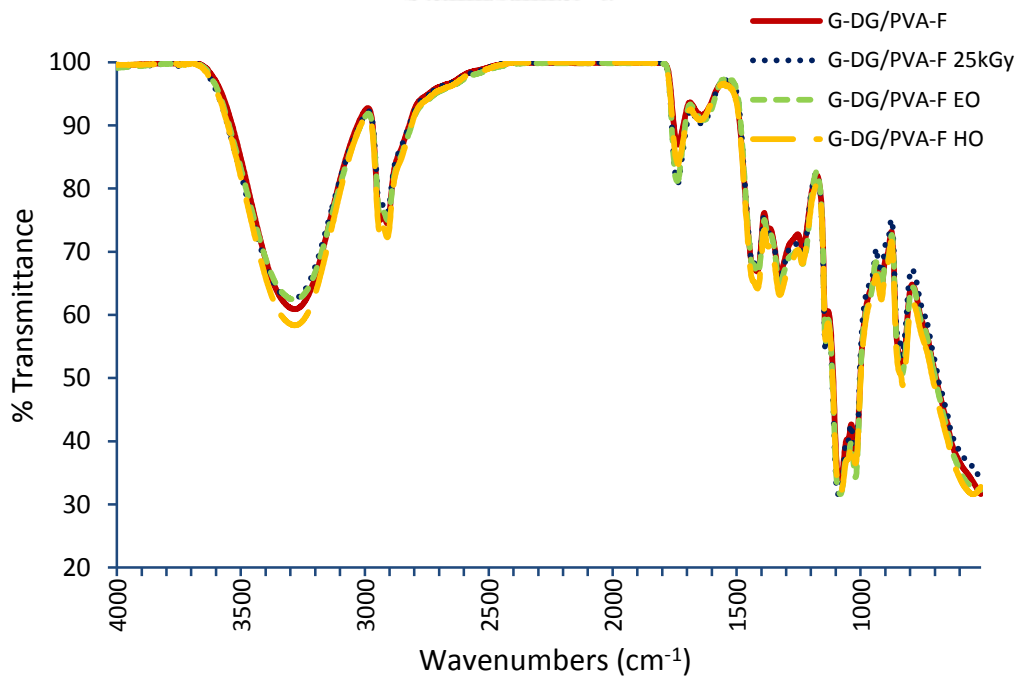


Figure 49 FTIR spectra of dried-form G-CSF loaded hydrogels after sterilization by gamma radiation 25 kGy, ethylene oxide and hydrogen peroxide gas plasma

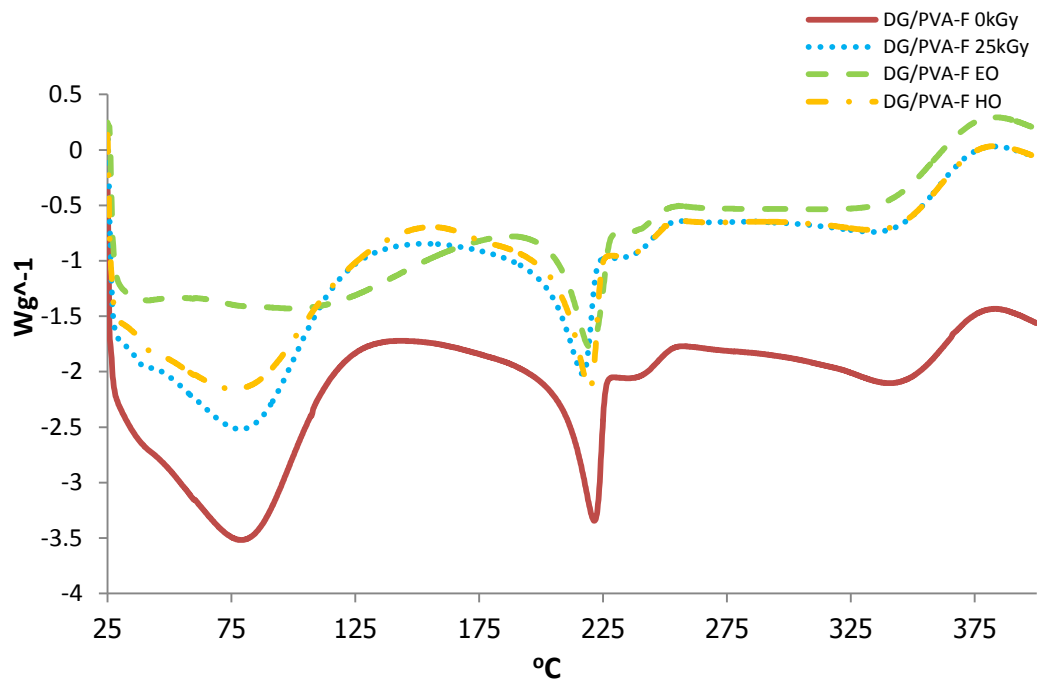


Figure 50 DSC thermograms of dried-form DG/PVA hydrogels after sterilization by gamma radiation 25 kGy, ethylene oxide and hydrogen peroxide gas plasma

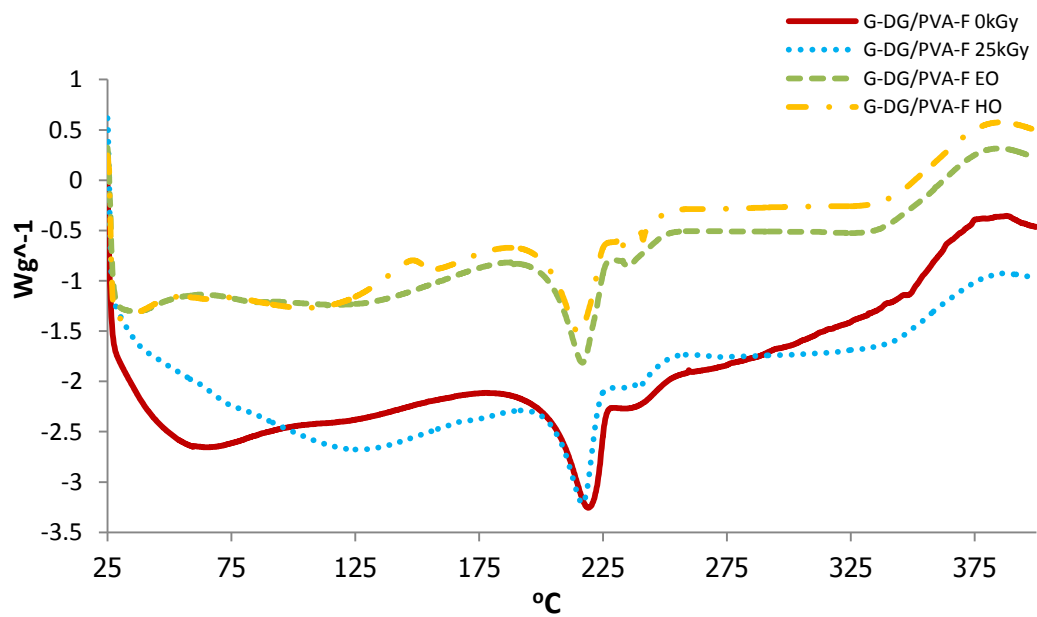


Figure 51 DSC thermograms of dried-form G-CSF loaded DG/PVA hydrogels after sterilization by gamma radiation 25 kGy, ethylene oxide and hydrogen peroxide gas plasma

The dried-form DG/PVA hydrogels and G-CSF loaded hydrogels which sterilized by gamma irradiation 25 kGy, ethylene oxide and hydrogen peroxide gas plasma were studied for FTIR as showed in Figure 48 and 49. There was slightly increased of peak intensity of C=O stretching associated to aldehyde at 1755 cm^{-1} of FTIR spectrum of the hydrogel sterilized by gamma irradiation (Figure 49) that could be the result of hemiacetal formation in hydrogel as described above. From Figure 49, found increasing peak intensity of carbonyl group at 1751 cm^{-1} in G-CSF loaded hydrogels after EO gas sterilization. It could be proposed that ethylene oxide can react with hydroxyl groups form PVA and OH containing amino acid residues in G-CSF to form 2-ethoxyethanol as described in Figure 40.

The thermal analysis of dried-form DG/PVA and G-CSF loaded hydrogels after sterilization by gamma irradiation 25 kGy, ethylene oxide and hydrogen peroxide gas plasma were studied as showed in Figure 50 and 51. The DSC thermograms of the hydrogels after sterilization had endothermic peak of PVA at the same region as non-sterilized hydrogel.

4.6 Effect of sterilization methods on G-CSF release from DG/PVA hydrogel

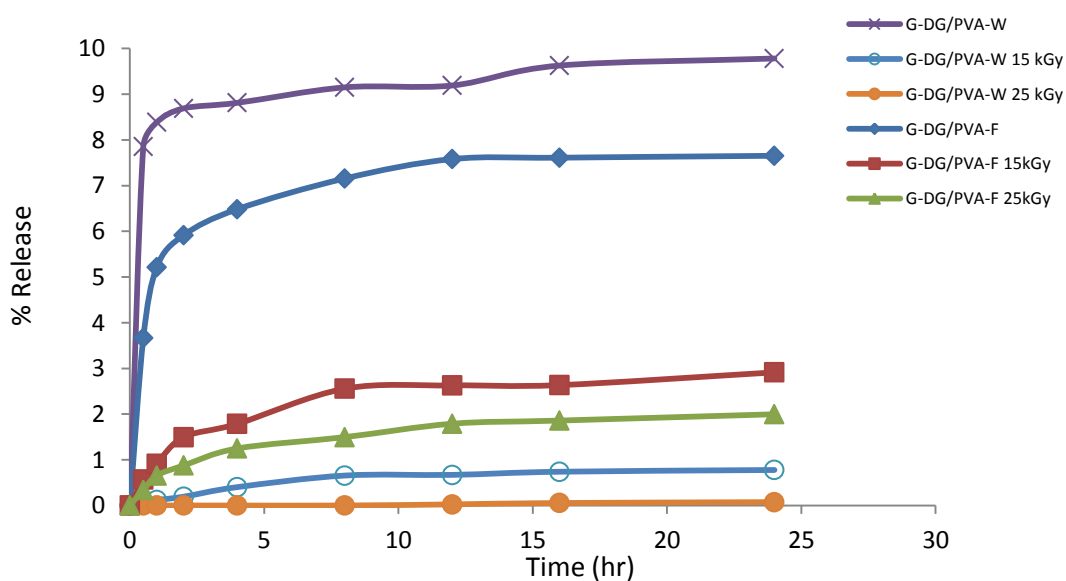


Figure 52 G-CSF release profile of wet and dried-form DG/PVA hydrogels after sterilization by gamma radiation 15 and 25 kGy

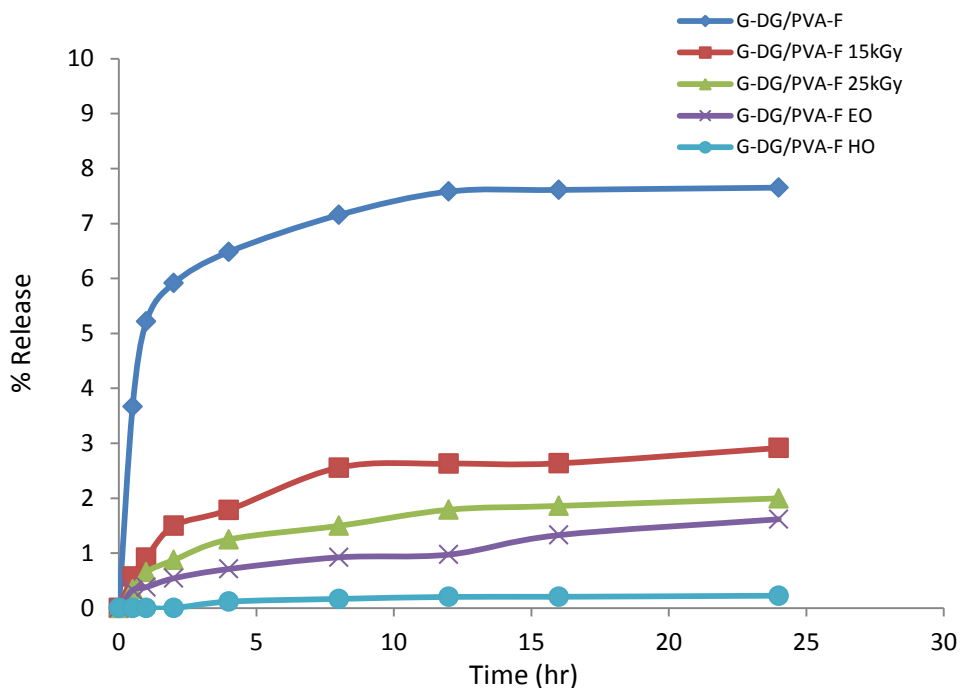


Figure 53 G-CSF release profile of dried-form G-CSF loaded hydrogels after sterilization by gamma radiation 15 and 25 kGy, ethylene oxide gas and hydrogen peroxide gas plasma

A preliminary study of G-CSF release from DG/PVA hydrogels were showed in Figure 52 and 53. G-CSF had highest released from non-sterilized DG/PVA hydrogel whereas irradiated DG/PVA hydrogel dose 25 kGy had lowest released. The release of G-CSF from DG/PVA hydrogel might be affected by gamma irradiation and increasing radiation dose could decreased the release. When compare the release with ethylene oxide gas and hydrogen peroxide gas plasma sterilization methods in Figure 53, found that G-CSF released greatest from non-sterilized hydrogels, hydrogel sterilized by gamma irradiation 15 and 25 kGy , ethylene oxide gas and hydrogen peroxide gas plasma, respectively.

CHAPTER V

CONCLUSION

Hydrogel composed of polysaccharide gel from durian fruit-hulls (DG) and polyvinyl alcohol (PVA) had better physical properties appropriated for used as wound dressing. The preparation of DG/PVA hydrogel in dried form improved the water absorption capacity properties of the hydrogel. The hydrogels can be sterilized by all sterilization methods; gamma irradiation, ethylene oxide and hydrogen peroxide gas plasma sterilization. The gamma irradiation could be processed with both wet- and dried-form hydrogels. Ethylene oxide gas and hydrogen peroxide gas plasma sterilization are suitable for hydrogels in dried form because ethylene oxide gas and hydrogen peroxide gas plasma had limitation of aqueous products. After gamma irradiation, the wet-form hydrogel had increased in gel fraction and tensile strength whereas decreased the water absorption capacity and water content. The dried-form hydrogel had increased in water absorption capacity and tensile strength but decreased in gel fraction. Gamma irradiation had increased tensile strength of both wet and dried-forms. Higher of radiation dose increased gel fraction resulted in the decrease of water content and water absorption capacity of wet-form hydrogels. Sterilization by gamma radiation, ethylene oxide gas or hydrogen peroxide gas plasma decreased gel fraction resulted in the increase of water absorption capacity of dried-form hydrogels. In addition, gamma irradiation or hydrogen peroxide gas plasma increased properties of Young's modulus and tensile strength. Preliminary study of G-CSF release from hydrogels implied that all three sterilization methods decreased the G-CSF release from hydrogels especially hydrogen peroxide gas plasma. However, hydrogen peroxide gas plasma sterilization method had less affected on the properties of hydrogel which might be suitable sterilization method for dried-form hydrogels without protein loaded. Ethylene oxide gas sterilization also less affected on the properties of hydrogels but have to consider the toxic residual in products. Gamma irradiation sterilization might be suitable and cost effective for large scale sterilization.

REFERENCES

- Ajji, Z., Othman, I., Rosiak, J.M. Production of hydrogel wound dressings using gamma radiation. Nuclear Instruments and Methods in Physics Research Section B: Beam Interactions with Materials and Atoms 229, 3–4 (2005):375-380.
- Al-Assaf, S., Phillips, G.O., Aoki, H. *et al.* Characterization and properties of Acacia senegal (L.) Willd. var. senegal with enhanced properties (Acacia (sen) SUPER GUM™): Part 1—Controlled maturation of Acacia senegal var. senegal to increase viscoelasticity, produce a hydrogel form and convert a poor into a good emulsifier. Food Hydrocolloids 21, 3 (2007):319-328.
- Azofra, L.M., Alkorta, I., Elguero, J. A theoretical study of hemiacetal formation from the reaction of methanol with derivatives of CX₃CHO (X = H, F, Cl, Br and I). Journal of Physical Organic Chemistry 25, 12 (2012):1286-1292.
- Bhat, N.V., Nate, M.M., Kurup, M.B. *et al.* Effect of γ -radiation on the structure and morphology of polyvinyl alcohol films. Nuclear Instruments and Methods in Physics Research Section B: Beam Interactions with Materials and Atoms 237, 3–4 (2005):585-592.
- Brown, R.K., Eastham, A.M. THE CHEMISTRY OF ETHYLENE OXIDE: VI. THE ACID-CATALYZED REACTION OF ETHYLENE OXIDE WITH ETHANOL–WATER MIXTURES. Canadian Journal of Chemistry 38, 11 (1960):2039-2041.
- Calvet, J.L., Grafahrend, D., Klee, D. *et al.* Sterilization effects on starPEG coated polymer surfaces: characterization and cell viability. Journal of materials science :Materials in medicine 19 4(2008):1631 -1636
- Chansiripornchai, P., Pramatwinai, C., Rungsipat, A. *et al.* THE EFFICIENCY OF POLYSACCHARIDE GEL EXTRACTED FROM FRUIT-HULLS OF DURIAN (DURIO ZIBETHINUS L.) FOR WOUND HEALING IN PIG SKIN. In: *ISHS Acta Horticulturae 679: III WOCMAP Congress on Medicinal and Aromatic Plants : Quality, Efficacy, Safety, Processing and Trade in Medicinal and Aromatic Plants 2005: Acta Hort; 2005: 37-43.*

- Chen, J., Liu, W., Liu, C.-M. *et al.* Pectin Modifications: A Review. Critical Reviews in Food Science and Nutrition 55, 12 (2014):1684-1698.
- Das, N. Preparation methods and properties of hydrogel : A reveiw. Int J Pharm Pharm Sci 5, 3 (2013):112-117.
- Dutta, J. Synthesis and Characterization of γ -irradiated PVA/PEG/CaCl₂ Hydrogel for Wound Dressing. American Journal of Chemistry 2, 2 (2012):6-11.
- Eakwaropas, P. Development of hydrogel wound dressing using mixtures of polyvinyl alcohol and polysaccharide extract from durian fruit-hulls.... Master's Thesis, Department of Pharmaceutics and Industrial Pharmacy, Faculty of Pharmaceutical Science, Chulalongkorn University, 2009.
- Fan, W., Yan, W., Xu, Z. *et al.* Formation mechanism of monodisperse, low molecular weight chitosan nanoparticles by ionic gelation technique. Colloids and Surfaces B: Biointerfaces 90, (2012):21-27.
- Francis, S., Mitra, D., Dhanawade, B.R. *et al.* Gamma radiation synthesis of rapid swelling superporous polyacrylamide hydrogels. Radiation Physics and Chemistry 78, 11 (2009):951-953.
- G, L., L, Y., C, Y. *et al.* Controlled release of epidermal growth factor from hydrogels accelerates wound healing in diabetic rats. J Am Podiatr Med Assoc 102, 2 (Mar-Apr 2012):89-98.
- Grazul-Bilska, A.T., Johnson, M.L., Bilski, J.J. *et al.* Wound healing: the role of growth factors. Drugs Today (Barc) 39, 10 (2003):787-800.
- Gulrez, S.K.H., Al-Assaf, S. Hydrogels: Methods of Preparation, Characterisation and Applications. Progress in Molecular and Environmental Bioengineering - From Analysis and Modeling to Technology Applications. 2011.
- Guo, S., DiPietro, L.A. Factors Affecting Wound Healing. J Dent Res 89, 3 (2010):219-229.
- Hassan, C.M., Peppas, N.A. Cellular PVA Hydrogels Produced by Freeze/Thawing. Journal of Applied Polymer Science 76, (2000):2075-2079.
- Hennink, W.E., Nostrum, C.F.v. Novel crosslinking methods to design hydrogels. Advanced Drug Delivery Reviews 54, (2002):13-36.

- Hokputsaa, S., Gerdditb, W., Pongsamartb, S. *et al.* Water-soluble polysaccharides with pharmaceutical importance from Durian rinds (*Durio zibethinus* Murr.): isolation, fractionation, characterisation and bioactivity. Carbohydrate Polymers 56, 4 (2004):471-481.
- Hu, X., Sun, H., Han, C. *et al.* Topically applied rhGM-CSF for the wound healing: A systematic review. Burns 37, 5 (2011):729-741.
- Huang, S., Miller, A.K., Wu, W. Substantial formation of hydrates and hemiacetals from pyridinium ketones. Tetrahedron Lett 50, 47 (2009):6584-6585.
- Jiang, S., Liu, S., Feng, W. PVA hydrogel properties for biomedical application. Journal of the Mechanical Behavior of Biomedical Materials 4, 7 (2011):1228-1233.
- Jones, V., Grey, J.E., Harding, K.G. Wound dressings. British Medical Journal 332, 7544 (2006):777-780.
- Kaplan, G., Walsh, G., Guido, L.S. *et al.* Novel responses of human skin to intradermal recombinant granulocyte/macrophage-colony-stimulating factor: Langerhans cell recruitment, keratinocyte growth, and enhanced wound healing. Journal of Experimental Medicine 175, 6 (June 1992):1717-1728.
- Kaplan, H., Güner, A. Characterization and determination of swelling and diffusion characteristics of poly(n-vinyl-2-pyrrolidone) hydrogels in water. Journal of Applied Polymer Science 78, 5 (2000):994-1000.
- Kharlampieva, E., Erel-Unal, I., Sukhishvili, S.A. Amphoteric Surface Hydrogels Derived from Hydrogen-Bonded Multilayers: Reversible Loading of Dyes and Macromolecules†. Langmuir 23, 1 (2007):175-181.
- Kickhöfen, B., Wokalek, H., Scheel, D. *et al.* Chemical and physical properties of a hydrogel wound dressing. Biomaterials 7, 1 (1986):67-72.
- Kim, S.H., Chu, C.C. Synthesis and characterization of dextran-methacrylate hydrogels and structural study by SEM. J Biomed Mater Res 49, 4 (2000):517-527.
- Kobayashi, M., Hyu, H.S. Development and Evaluation of Polyvinyl Alcohol-hydrogel as Artificial Articular Cartilage for Orthopedic Implants. Materials 3, (2010):2753-2771.
- Kondo, T., Ishida, Y. Molecular pathology of wound healing. Forensic Science International 203, (2010):93-98.

- Koria, P. Delivery of growth factors for tissue regeneration and wound healing. BioDrugs 26, 3 (2012):163-175.
- Li, B., Davidson, J.M., Guelcher, S.A. The effect of the local delivery of platelet-derived growth factor from reactive two-component polyurethane scaffolds on the healing in rat skin excisional wounds. Biomaterials 30, 20 (2009):3486-3494.
- Lieschke, G.J., Burgess, A.W. Granulocyte Colony-Stimulating Factor and Granulocyte-Macrophage Colony-Stimulating Factor. New England Journal of Medicine 327, 1 (1992):28-35.
- Lipipun, V., Nantawanit, N., Pongsamart, S. Antimicrobial activity (in vitro) of polysaccharide gel from durian fruit-hulls. Songklanakarin J Sci Technol 24, 1 (2002):31-38.
- Liu, Y., Cai, S., Shu, X. *et al.* Release of basic fibroblast growth factor from a crosslinked glycosaminoglycan hydrogel promotes wound healing. Wound Repair Regen 15, 2 (2007):245-251.
- Marreco, P.R., Moreira, P.d.L., Genari, S.C. *et al.* Effect of different sterilization method on the morphology, mechanical properties and cytotoxicity of chitosan membrane used as wound dressing. 2004. Wiley InterScience p. 268-277.
- Mathur, A.M., Scranton, A.B. Characterization of hydrogels using nuclear magnetic resonance spectroscopy. Biomaterials 17, 6 (1996):547-557.
- Mc Gann, M.J., Higginbotham, C.L., Geever, L.M. *et al.* The synthesis of novel pH-sensitive poly(vinyl alcohol) composite hydrogels using a freeze/thaw process for biomedical applications. International Journal of Pharmaceutics 372, 1-2 (2009):154-161.
- Mendes, G.C.C., Brandão, T.R.S., Silva, C.L.M. Ethylene oxide sterilization of medical devices: A review. American Journal of Infection Control 35, 9 (2007):574-581.
- Mishra, R.K., Datt, M., Banthia, A.K. Synthesis and Characterization of Pectin/PVP Hydrogel Membranes for Drug Delivery System. Aaps Pharmscitech 9, 2 (2008):395-403.

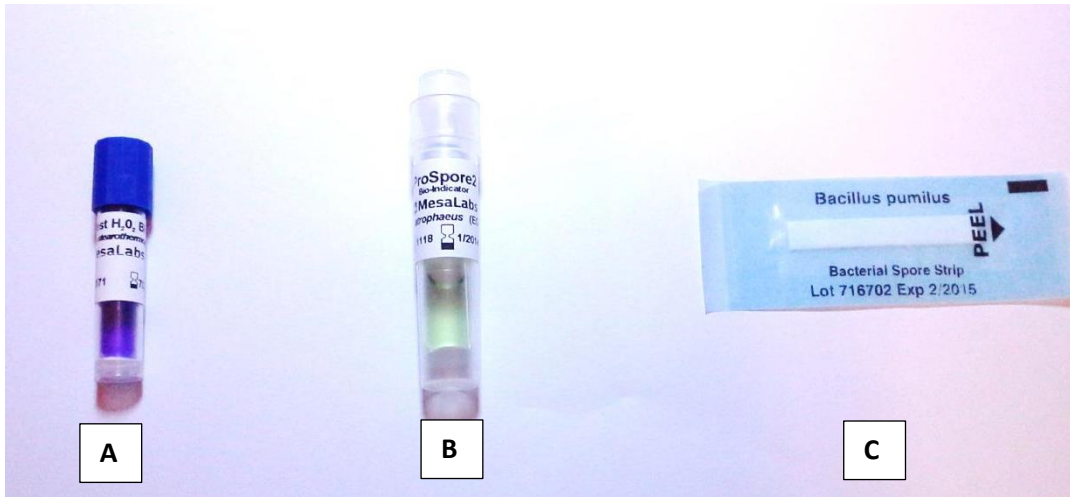
- Neri, R., Burillo, G., Castillo-Rojas, S. Gamma radiation synthesis of comb-type graft hydrogels based on poly(acrylic acid) and 4-vinylpyridine. Journal of Radioanalytical and Nuclear Chemistry 287, 3 (2011):787-793.
- Noda, S., Funami, T., Nakauma, M. *et al.* Molecular structures of gellan gum imaged with atomic force microscopy in relation to the rheological behavior in aqueous systems. 1. Gellan gum with various acyl contents in the presence and absence of potassium. Food Hydrocolloids 22, 6 (2008):1148-1159.
- Obara, K., Ishihara, M., Ishizuka, T. *et al.* Photocrosslinkable chitosan hydrogel containing fibroblast growth factor-2 stimulates wound healing in healing-impaired *db/db* mice. Biomaterials 24, 20 (2003):3437-3444.
- Oliveira, R.N., Rouzé, R., Quilty, B. *et al.* Mechanical properties and in vitro characterization of polyvinyl alcohol-nano-silver hydrogel wound dressings.4, 2014.
- Omidian, H., Park, K. Fundamentals and Application of Controlled Release Drug Delivery. Ined, pp.75-106. New York: Spinger, 2012.
- Peppas, N.A., Slaughter, B.V., Khurshid, S.S. *et al.* Hydrogel in Regenerative Medicine. ADVANCED MATERIALS 21 (2009):3307-3329.
- Pierce, G.F., Mustoe, T.A., Altrock, B.W. *et al.* Role of platelet-derived growth factor in wound healing. J Cell Biochem 45, 4 (1991):319-326.
- Pinho, E., Henriques, M., Soares, G. Cyclodextrin/cellulose hydrogel with gallic acid to prevent wound infection. Cellulose 21, 6 (2014):4519-4530.
- Pongsamart, S., Panmaung, T. Isolation of polysaccharides from fruit-hulls of durian (*Durio zibethinus* L.). Songklanakarin Journal of Science and Technology 20, 3 (1998):323-332.
- Pongsamart, S. Polysaccharide Product from Durian : Process for Isolation and Purification and Their Applications. Publication USPA, vol. US2003/0166608 A1.2003. Chulalongkorn University, Bangkok.
- Pongsamart, S., Nantawanit, N., Lertchaiporn, J. *et al.* Novel Water Soluble Antibacterial Dressing of Durian Polysaccharide Gel. In: *ISHS Acta Horticulturae 678 :III WOCMAP Congress on Medicinal and Aromatic Plants : Targeted*

- Screening of Medicinal and Aromatic Plants, Economics and Law: 2005: Acta Hort; 2005: 65-73.*
- PW, H., SP, S., DD, K. *et al.* Stromal-derived factor-1 delivered via hydrogel drug-delivery vehicle accelerates wound healing in vivo. Wound Repair Regen 19, 3 (2011):420-425.
- Reis, E.F.d., Campos, F.S., Lage, A.P. *et al.* Synthesis and Characterization of Poly(Vinyl Alcohol) hydrogels and hybrids for rMPB70 protein adsorption. Materials Research 9, 2 (2006):185-191.
- Rosiak, J.M. Gel/sol analysis of irradiated polymers. Radiation Physics and Chemistry 51, 1 (1998):13-17.
- Rubbia-Brandt, L., Sappino, A.-P., Gabbiani, G. Locally applied GM-CSF induces the accumulation of α -smooth muscle act in containing myofibroblasts. Virchows Archiv B 60, 1 (1991):73-82.
- Rusu, A.G., Popa, M.I., Lisa, G. *et al.* Thermal behavior of hydrophobically modified hydrogels using TGA/FTIR/MS analysis technique. Thermochimica Acta 613, (2015):28-40.
- RW, G., JA., S.-L. Recombinant human GM-CSF in the treatment of poorly healing wounds. Adv Skin Wound Care 13, 3 (2000):107-112.
- Siripokasupkul, R. Property of Polysaccharide Gel from Durian as Dressing Preparations and Its Effect on Wound Healing in Dog Skin. Master's Thesis, Department of Biomedical Chemistry, Faculty of Pharmaceutical Science, Chulalongkorn University, 2004.
- Sirousazar, M., Kokabi, M., Hassan, Z.M. *et al.* Dehydration kinetics of polyvinyl alcohol nanocomposite hydrogels containing Na-montmorillonite nanoclay. Scientia Iranica 18, 3 (2011):780-784.
- Smith, C.H., Allen, M.H., Groves, R.W. *et al.* Effect of granulocyte macrophage-colony stimulating factor on Langerhans cells in normal and healthy atopic subjects. British Journal of Dermatology 139, 2 (1998):239-246.
- Stasko, J., Kalnins, M., Dzene, A. *et al.* Poly(vinyl alcohol) hydrogels
In: *Proceeding of the Estonian Academy of Sciences: 2009; 2009: 63-66.*

- Tripathi, R., Mishra, B. “Development and Evaluation of Sodium Alginate–Polyacrylamide Graft–Co-polymer-Based Stomach Targeted Hydrogels of Famotidine”. Aaps Pharmscitech 13, 4 (2012):1091-1102.
- Varshney, L. Role of natural polysaccharides in radiation formation of PVA–hydrogel wound dressing. Nuclear Instruments and Methods in Physics Research Section B: Beam Interactions with Materials and Atoms 255, 2 (2007):343-349.
- Xu, J., Li, X., Sun, F. *et al.* PVA hydrogels containing beta-cyclodextrin for enhanced loading and sustained release of ocular therapeutics. J Biomater Sci Polym Ed 21, 8-9 (2010):1023-1038.
- Yang, X., Liu, Q., Chen, X. *et al.* Investigation on the formation mechanisms of hydrogels made by combination of γ -ray irradiation and freeze-thawing. Journal of Applied Polymer Science 108, 2 (2008):1365-1372.
- Yin, X., Stöver, H.D.H. Hydrogel Microspheres Formed by Complex Coacervation of Partially MPEG-Grafted Poly(styrene-alt-maleic anhydride) with PDADMAC and Cross-Linking with Polyamines. Macromolecules 36, 23 (2003):8773-8779.

APPENDIX

Appendix 1 Biological indicators



(A) *Geobacillus stearothermophilus* (B) *Bacillus atrophaeus* (C) *Bacillus pumilus*

Biological indicators (BIs)

(A) *Geobacillus stearothermophilus*

Biological indicator for hydrogen peroxide gas plasma (contained 3.0×10^6 CFU/7 mm borosilicate glass disc), $D_{H_2O_2}$ value 2.0 seconds (sterrad process at 50°C , 3 mg/L H_2O_2 concentration), Incubation at $60 \pm 2^\circ\text{C}$ for 24 hours

(B) *Bacillus atrophaeus*

Biological indicator for ethylene oxide gas sterilization (contained 3×10^6 CFU/9 mm paper disc), D_{EO} value 3.3 mins (600 mgEO/L, 54°C , 60% RH), Incubation at $30\text{--}35^\circ\text{C}$ for 48 hours

(C) *Bacillus pumilus*

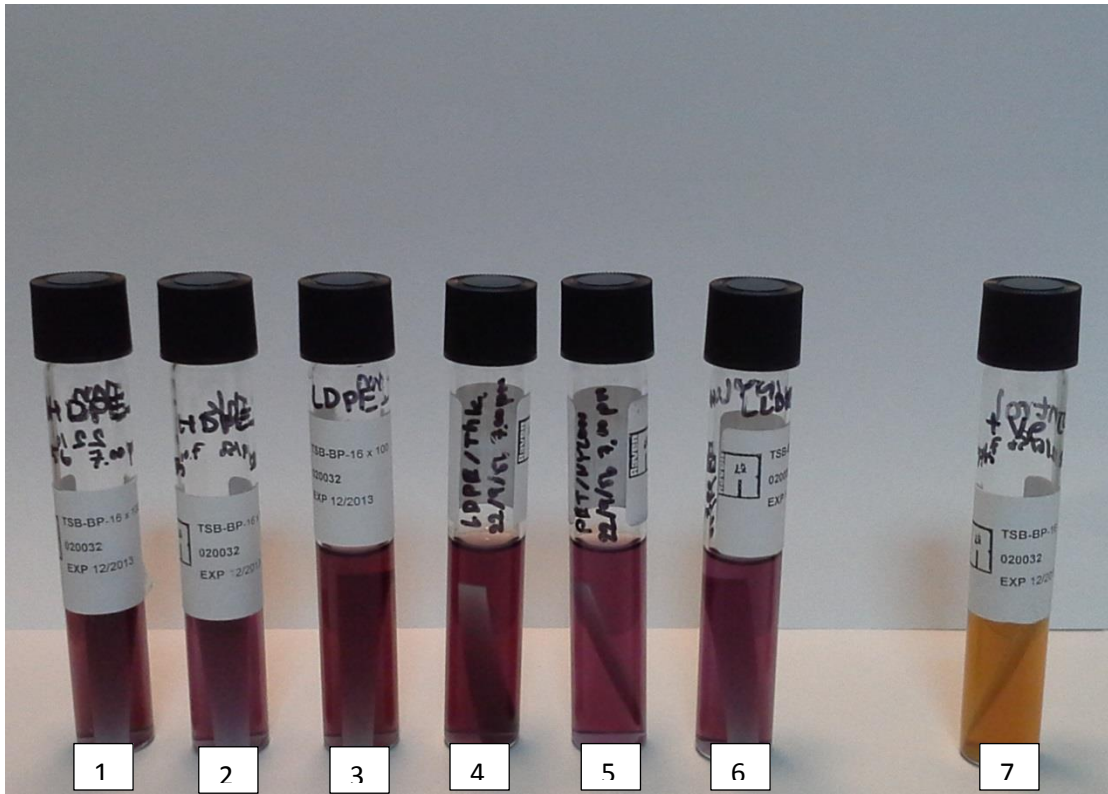
Biological indicator for gamma irradiation (contained 4×10^6 CFU / 1.5" x 0.25" strip), D_{Mrad} value 0.12 Mrads (1 Mrad = 10 kGy), Incubation in TSB at $30\text{--}35^\circ\text{C}$ for 7 days

Appendix 2 Packaging materials for hydrogel



Biological indicators for gamma irradiation in various packaging materials before sterilization

- (1) High density polyethylene-Thin type (HDPE-Thn)
- (2) High density polyethylene-Thick type (HDPE-Thk)
- (3) Low density polyethylene- Thin type (LDPE-Thn)
- (4) Low density polyethylene- Thick type (LDPE-Thk)
- (5) Linear low density polyethylene laminated Nylon (LLDPE/Nylon)
- (6) Polyethylene terephthalate laminated Nylon and Metallite (PET/Nylon/Metallite)



Biological indicators (BIs) from various packaging material after gamma irradiation at dose 25 kGy then immersed in TSB media and incubated at 30-35 °C for 7 days

- (1) High density polyethylene-Thin type (HDPE-Thn)
- (2) High density polyethylene-Thick type (HDPE-Thk)
- (3) Low density polyethylene- Thin type (LDPE-Thn)
- (4) Low density polyethylene- Thick type (LDPE-Thk)
- (5) Linear low density polyethylene laminated Nylon (LLDPE/Nylon)
- (6) Polyethylene terephthalate laminated Nylon and Metallite (PET/Nylon/Metallite)
- (7) Non-irradiated BIs for gamma radiation as Positive control



Biological indicators for ethylene oxide gas sterilization in various packaging materials before sterilization

- (1) Tyvek for ethylene oxide gas sterilization
- (2) Low density polyethylene- Thin type (LDPE-Thn)
- (3) Low density polyethylene- Thick type (LDPE-Thk)
- (4) High density polyethylene-Thin type (HDPE-Thn)
- (5) High density polyethylene-Thick type (HDPE-Thk)
- (6) Linear low density polyethylene laminated Nylon (LLDPE/Nylon)
- (7) Polyethylene terephthalate laminated Nylon and Metallite (PET/Nylon/Metallite)

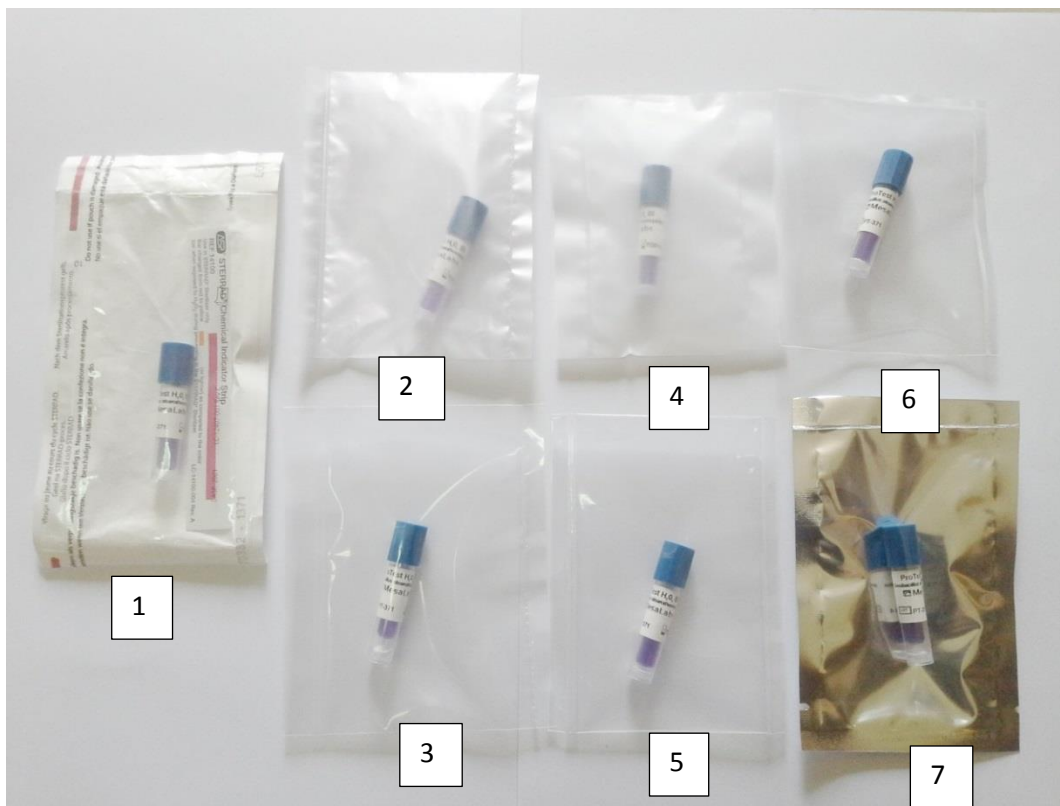


BIs in various packaging materials after EO gas sterilization and incubated at 30-35 °C for 48 hours

If the media color turn to yellow indicated EO gas could not permeated enough for sterilized BIs.

If the media color not changed after incubation indicated EO gas could permeated enough for sterilized BIs.

- (1) Tyvek for EO gas sterilization (6) LLDPE/Nylon
- (2) LDPE-Thn (7) PET/Nylon/Metallite
- (3) LDPE-Thk (8) Non-sterilized BIs as positive control
- (4) HDPE-Thn
- (5) HDPE-Thk



BIs for hydrogen peroxide gas plasma sterilization in various packaging materials before sterilization

- (1) Tyvek for hydrogen peroxide gas plasma sterilization
- (2) LDPE-Thn
- (3) LDPE-Thk
- (4) HDPE-Thn
- (5) HDPE-Thk
- (6) LLDPE/Nylon
- (7) PET/Nylon/Metallite



The BIs in various of packaging materials after HO gas sterilization and incubated at 60 °C 24 hours. Whereas the non-sterilized BIs was serve as positive control. The BIs no.1-7 are PET/Nylon/Metallite, LDPE-Thn, LDPE-Thk, HDPE-Thn, HDPE-Thk,

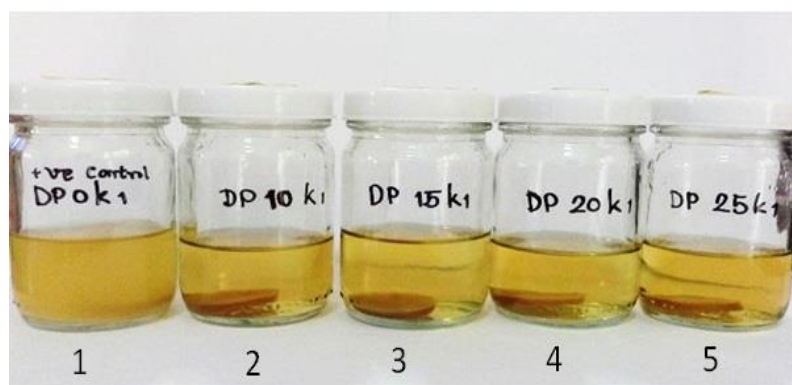
LDPE/Nylon and Tyvek for HO gas plasma sterilization, respectively. After incubation at 60 °C 24 hours, it was found that the media color of Tyvek, LLDPE/Nylon and HDPR-Thn were not changed, but the packaging material type of HDPE-Thn was be torn. Whereas other BIs media color turn to yellow. The studied was done again to confirm the result. There were changed in media color to yellow in every materials except Tyvek and LLDPE/Nylon. This result indicated that LLDPE/Nylon could be selected as the packaging material for HO gas plasma sterilization.



Retest for HDPE-Thn packaging material, the media turn to yellow after incubation.

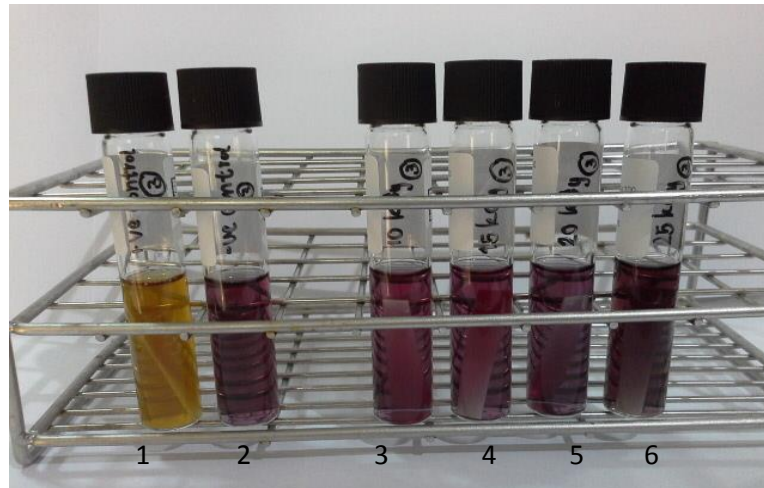
Appendix 3 Sterility testing

A 3.1 Sterility test of wet-form DG/PVA hydrogels after gamma irradiation



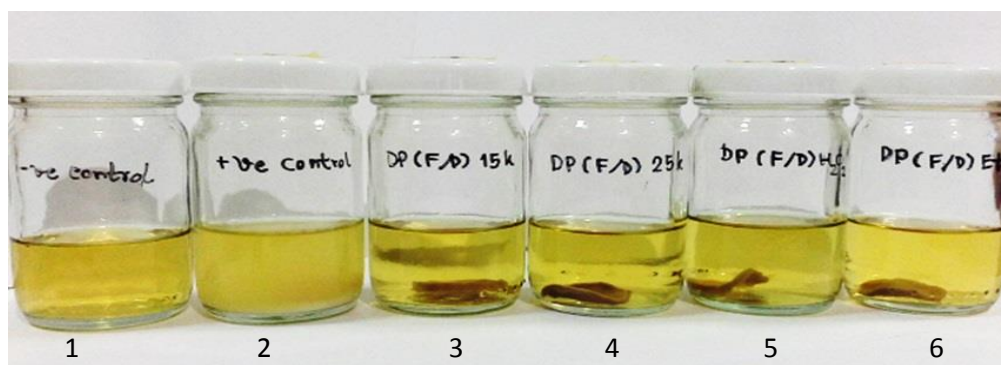
The wet-form of DG/PVA hydrogels after gamma irradiation at dose 10, 15, 20 and 25 kGy were inoculated in SCDB media and incubated at 37 °C for 7 days. From A 3.1 the DG/PVA-W hydrogel in bottle no.1 is non-sterilized hydrogel, no.2 is gamma irradiation 10 kGy, no.3 is gamma irradiation 15 kGy, no.4 is gamma irradiation 20 kGy and no.5 is gamma irradiation 25 kGy. After incubation for at 37 °C for 7 days the media of bottle no.1 was clouding indicated that the hydrogel was non-sterile and the media used in sterility test was allowing microbial growth. However, the media in bottle no.2-5 were clearness indicated that the hydrogel irradiated with gamma radiation dose 10 to 25 kGy were sterile.

A 3.2 Sterility test of biological indicators for gamma radiation after irradiated with gamma radiation at dose 10, 15, 20 and 25 kGy



From A 3.2 tube no.1 is non-irradiated Bls represent the positive control, no.2 is TSB media represent the negative control, no.3-6 are Bls irradiate with gamma ray 10, 15, 20 and 25 kGy, respectively. It was found that only the media in tube no.1 was turn to yellow that indicate the non-sterile of Bls. This studied was confirm the result from A 3.1 that gamma irradiation at dose 10 to 25 kGy could sterilized the hydrogels.

A 3.3 Sterility test of DG/PVA hydrogel sterilization by gamma radiation 15 and 25 kGy, ethylene oxide and hydrogen peroxide gas plasma.



The dried-form of DG/PVA hydrogel sterilization by gamma radiation 15 and 25 kGy, ethylene oxide and hydrogen peroxide gas plasma were inoculated in sterile SCDB media. From A 3.3, Bottle no.1 is sterile SCDB media serve as negative control, no.2. Is non-sterilized hydrogel serve as positive control, no.3-6 are DG/PVA-F sterilized by gamma irradiation 15 and 25 kGy, hydrogen peroxide gas plasma and ethylene oxide, respectively. After incubation for at 37 °C for 7 days the media of bottle no.2 was clouding indicated that the hydrogel was non-sterile and media was allowing the microbial growth. The media in bottle no.1 which was negative control still clear indicated that the media used in this studied was non-contaminate and sterile. The media in bottle of sterilized hydrogels were all clear. This result implied that the all three sterilization method were effective.



Appendix 4 ELISA assay

Standard preparations

1. Briefly spin the vial of G-CSF standard. Prepare the 10 ng/ml Stock standard by adding 800 μ l 1X Assay Diluent B into the vial
2. Ensure the powder is thoroughly dissolved by gentle mixing
3. Label tubes # 1-7
4. Prepare Standard #1 by adding 30 μ l of the 10 ng/ml Stock Standard, to 570 μ l of 1X Assay Diluent B into tube #1. Mix thoroughly and gently.
5. Pipette 400 μ l of 1X Assay Diluent B into remaining tubes.
6. Prepare Standard #2 by adding 200 μ l of Standard #1 to tube #2 and mix thoroughly.
7. Prepare Standard #3 by adding 200 μ l of Standard #2 to tube #3 and mix thoroughly.
8. Using the table below as a guide, prepare further serial dilutions.
9. 1X Assay Diluent B serves as the zero standard (0 pg/ml)

Standard dilution preparation table

Standard #	Volume to dilute (μ l)	Diluent (μ l)	Total volume (μ l)	Starting Conc. (pg/ml)	Final Conc. (pg/ml)
1	30	570	600	10,000	500
2	200	400	600	500	166.67
3	200	400	600	166.67	55.6
4	200	400	600	55.6	18.5
5	200	400	600	18.5	6.17
6	200	400	600	6.17	2.05
7	200	400	600	2.05	0.69
8	0	400	400	0	0

Assay procedure

1. Equilibrate all materials and prepared reagents to room temperature
2. Add 100 μl of each standard and sample into appropriate wells. Cover well and incubate for 2.5 hours at room temperature or overnight at 4 $^{\circ}\text{C}$ with gentle shaking.
3. Discard the solution and wash 4 times with 1X Wash solution. Wash by filling each well with 1X Wash solution 300 μl . Complete removal of liquid at each step. After the last wash, remove any remaining Wash buffer by aspirating or decanting. Invert the plate and blot it against clean paper towels.
4. Add 100 μl of 1X Biotinylated G-CSF Detection Antibody to each well. Incubate for 1 hour at room temperature with gentle shaking.
5. Discard the solution and repeat the wash as step 3.
6. Add 100 μl of 1X HRP-Streptavidin solution to each well. Incubate for 45 minutes at room temperature with gentle shaking.
7. Discard the solution and repeat the wash as step 3.
8. Add 100 μl of TMB One-Step Substrate reagent to each well. Incubate for 30 minutes at room temperature in the dark with gentle shaking.
9. Add 50 μl of Stop Solution to each well. Read at 450 nm (using microplate reader) immediately.

Calculations

Calculate the mean absorbance for each set of duplicate standards controls and samples, and subtract the average zero standard optical density. Plot the standard curve on log-log graph paper, with standard concentration on the x-axis and absorbance on the y-axis. Draw the best-fit straight line through the standard points.

VITA

Miss Chanthana Nainiran was born in Buriram, Thailand, on November 25th, 1980. She received her Bachelor of Science in Pharmacy degree in 2004 from the Faculty of Pharmacy, Silpakorn University, Thailand. After graduation, she has worked at Siriraj hospital, Bangkok, Thailand since 2004. She entered the Master's Program in Industrial Pharmacy at Chulalongkorn University in 2011.

